Self-Modulated Dynamics of Relativistic Charged Particle Beams in Plasmas

SUBMITTED AS PARTIAL FULFILLMENT OF THE
REQUIREMENTS FOR THE DEGREE OF
DOCTOR OF PHILOSOPHY
IN
FUNDAMENTAL AND APPLIED PHYSICS

Supervisor:
Professor Renato Fedele
Co-supervisors:
Dr. Sergio De Nicola
Professor Dusan Jovanović

Candidate:
Tahmina Akhter
XXVIII cycle

DIPARTIMENTO DI FISICA "ETTORE PANCINI"
UNIVERSITÀ DEGLI STUDI DI NAPOLI FEDERICO II

MARCH 31, 2016
NAPOLI, ITALY

UNIVERSITÀ DEGLI STUDI DI NAPOLI FEDERICO II
DIPARTIMENTO DI FISICA "ETTORE PANCINI"

The undersigned hereby certify that they have read and recommended to the Fundamental and Applied Physics for acceptance a thesis entitled "**Self-Modulated Dynamics of Relativistic Charged Particle Beams in Plasmas**" by **Tahmina Akhter** as partial fulfillment of the requirements for the degree of **Doctor of Philosophy**.

Dated: **March 31, 2016**

Research Supervisor: _____
Professor Renato Fedele

Co-Supervisors: _____
Dr. Sergio De Nicola

_____
Professor Dusan Jovanović

PhD Coordinator: _____
Professor Raffaele Velotta

Examiners: _____

_____

UNIVERSITÀ DEGLI STUDI DI NAPOLI FEDERICO II

Date: **March 31, 2016**

Author: **Tahmina Akhter**

Title: **Self-Modulated Dynamics of Relativistic Charged Particle Beams in Plasmas**

Department: **Dipartimento di Fisica "Ettore Pancini"**

Degree: **PhD**

Signature of Author

To my husband MD. ASHADUZZAMAN

Contents

List of Figures viii

List of Symbols xii

List of Acronyms xv

Acknowledgements xvi

Abstract xviii

Introduction 1

1 Models for plasmas 20
- 1.1 Preliminary considerations . . . 20
- 1.2 Fluid theory of a nonrelativistic plasma: the Lorentz-Maxwell system . . . 26
- 1.3 Kinetic description of a relativistic plasma . . . 30
- 1.4 Fluid description of a relativistic plasma . . . 32
- 1.5 Collisional plasmas . . . 33
- 1.6 Conclusions . . . 35

2 The theory of plasma wake field excitation: the Poisson-type equation 36
- 2.1 Introduction . . . 37
- 2.2 Definition of plasma wake field . . . 38
- 2.3 Lorentz-Maxwell system of equations for the beam-plasma system . . . 41
- 2.4 Poisson-type equation in overdense regime: collisionless nonrelativistic plasma 43
- 2.5 Ultrarelativistic driver in a cold plasma: longitudinal sharpness regimes . . 48
- 2.6 Ultrarelativistic driver in a cold plasma: transverse sharpness regimes . . . 50
- 2.7 Poisson-type equation for purely longitudinal case . . . 52
- 2.8 Poisson-type equation for purely transverse case . . . 53

2.9 Conclusions 54

3 Models for charged particle beams and its self-consistent interaction with the surrounding medium 55
3.1 Preliminary considerations 56
3.2 Relativistic Hamiltonian for a single-particle motion in the presence of EM fields 57
3.2.1 Slightly perturbed motion 58
3.2.2 Perturbed effective single particle Hamiltonian 58
3.3 The Vlasov equation for a relativistic charged-particle beam 61
3.4 The Vlasov-Poisson-type system of equations 61
3.5 Conclusions 62

4 Transverse self-modulated beam dynamics of a nonlaminar, ultra-relativistic beam in a non relativistic cold plasma 64
4.1 Introduction 65
4.2 The governing equations of the transverse beam dynamics 67
4.3 Beam envelope description 69
4.3.1 First virial equation 71
4.3.2 Second virial equation 73
4.3.3 Virial description and constants of motion 74
4.3.4 Constants of motion and envelope equations 75
4.3.5 Beam emittance 76
4.3.6 Cylindrical Symmetry 79
4.4 Self-modulated beam dynamics in purely local regime 79
4.4.1 Unmagnetized plasma 81
4.4.2 Magnetized plasma 83
4.4.3 Transverse beam emittance and equivalent Gaussian beam 84
4.5 Self modulation in strongly nonlocal regime 88
4.5.1 Aberration-less approximation 89
4.5.2 Self-modulation analysis by means of the Sagdeev potential 92
4.6 Qualitative stability analysis 95
4.7 Quantitative analysis of beam self-modulation in the arbitrary regime 98
4.7.1 General solution of U_w 98
4.7.2 Envelope equation and Sagdeev potential in the general case 101
4.7.3 Analysis of the envelope self-modulation in the general case 103
4.8 Conclusions 107

5 Longitudinal instability analysis of beam-plasma system **109**
5.1 Introduction 110
5.2 Dispersion relation 112
5.3 Monochromatic profile 113
5.4 Non-monochromatic case: weak Landau damping and instability 115
5.5 Conclusions 119

6 The coupling impedance concept for PWF self-interaction **120**
6.1 Introduction 120
6.2 Phenomenological platform of the beam-plasma interaction 123
6.3 Vlasov-Poisson-type pair of equations 124
6.4 Heuristic definition of coupling impedance 125
6.5 Stability analysis 125
6.5.1 Monochromatic beam 126
6.5.2 Non-monochromatic beam 127
6.6 Collisional beam-plasma system 128
6.7 Conclusions 131

Conclusions and Remarks **133**

A Virial descriptions **136**

B Envelope descriptions **143**

List of Publications/Communications **146**

Bibliography **150**

List of Figures

1 Scheme of the laser wakefield acceleration excited by a laser pulse. The driving laser pulse interacts with the active medium plasma and produces a driven system (charged particle beam) which leads to acceleration. 5

2 Plasma wake field acceleration scheme, excited by a relativistic electron beam, where the beam interacts with the surrounding plasma and thereby produces an wake field behind the beam itself. 7

4.1 Beam envelope surface that, at each τ, is described by $x^2 + y^2 = \sigma_\perp^2(\tau)$, for $\mathcal{A} > 0$ (self-defocusing of the beam for $B_0 = 0$). Here, $\sigma_0 = 1$, $\sigma_0^{'} = 0$, $\tau_0 = 0$ and $\mathcal{A} = 0.4$. 82

4.2 Beam envelope surface that, at each τ, is described by $x^2 + y^2 = \sigma_\perp^2(\tau)$, for $\mathcal{A} = 0$ (self-equilibrium of the beam for $B_0 = 0$). Here, $\sigma_0 = 1$, $\sigma_0^{'} = 0$ and $\tau_0 = 0$. 82

4.3 Beam envelope surface that, at each τ, is described by $x^2 + y^2 = \sigma_\perp^2(\tau)$, for $\mathcal{A} < 0$ (self-focusing of the beam for $B_0 = 0$). Here, $\sigma_0 = 1$, $\sigma_0^{'} = 0$, $\tau_0 = 0$ and $\mathcal{A} = -0.5$. 83

4.4 Beam envelope surface that, at each τ, is described by $x^2 + y^2 = \sigma_\perp^2(\tau)$, for $\mathcal{A} < 0$ and $0 \leq \mathcal{A} \leq \frac{1}{2}K\sigma_0^2$ (beam self-focusing leading to collapse for $B_0 \neq 0$). Here, $\sigma_0 = 2$, $\sigma_0^{'} = 0$, $K = 1$ and $\mathcal{A} = 1.5$. 84

4.5 Beam envelope surface that, at each τ, is described by $x^2 + y^2 = \sigma_\perp^2(\tau)$, $\sigma_0 = \sqrt{\mathcal{A}/K}$ (beam self-equilibrium for $B_0 \neq 0$). Here, $\sigma_0 = 2$, $\sigma_0^{'} = 0$, $K = 1$ and $\mathcal{A} = 4$. 85

4.6 Beam envelope surface that, at each τ, is described by $x^2 + y^2 = \sigma_\perp^2(\tau)$, for $\mathcal{A} > K\sigma_0^2/2$ (beam self-modulation, i.e., betatron-like oscillation, for $B_0 \neq 0$). Here, $\sigma_0 = 1$, $\sigma_0^{'} = 0$, $K = 1$ and $\mathcal{A} = 2.5$. 85
4.7 Sagdeev potential V_s (left) as defined by Eq. (4.5.23) and the corresponding numerical solution (right) of the Eq. (4.5.21) in absence of external magnetic field, where the plot of V_s is scaled by a factor 10^5. 93
4.8 Sagdeev potential V_s (left) as defined by Eq. (4.5.23) and the corresponding numerical solution (right) of the Eq. (4.5.21) in the presence of a strong external magnetic field, where the plot of V_s is scaled by a factor 10^5. . . . 93
4.9 Sagdeev potential V_s as defined by Eq. (4.5.23) and corresponding oscillations of spot sizes for the different values of the external magnetic field amplitude B_0, ranging from laboratory to astrophysical environments. Initial conditions defined by $\tilde{\sigma}_0$ sufficiently small and $\tilde{\sigma}_0' = 0$. Here, the plot of V_s is scaled by a factor 10^5 94
4.10 Qualitative plot of V_s over all the three different regimes. 96
4.11 Qualitative plot of V_s over all the regimes with a qualitative smoothing of the moderately non-local regime. 96
4.12 Plot of different initial profiles as function of $\tilde{r}$. 101
4.13 Plot of different Wake potential, U_w, for different density profiles. The plot is scaled here by a factor 10^6. 101
4.14 3D plot of plasma wake potential, $U_w(\tilde{r})$ for the parabola-square profile where $\tilde{r} = \sqrt{\tilde{x}^2 + \tilde{y}^2}$. The plot is scaled here by a factor 10^6. 102
4.15 V_s as function of $\tilde{\sigma}$ for the entire range of values and for a relatively small point of minimum, i.e., $\bar{\sigma} = 0.2$. 103
4.16 V_s as function of $\tilde{\sigma}$ ranging in the nonlocal region, for a very small point of minimum, i.e., $\bar{\sigma} = 0.09$. 104
4.17 Left: V_s as function of $\tilde{\sigma}$, for a very small point of minimum, i.e., $\bar{\sigma} = 0.09$. Right: envelope oscillations corresponding to initial conditions that fix $E < 0$ (see left) above the minimum, but below the plateau, i.e., $E = -0.19$. 104

4.18 Left: V_s as function of $\tilde{\sigma}$, for a relatively small point of minimum, i.e., $\bar{\sigma} = 0.394$. Right: envelope oscillations corresponding to initial conditions that fix $E < 0$ (see left) above the minimum, but below the plateau, i.e., $E = -0.06$. 105

4.19 Left: V_s as function of $\tilde{\sigma}$, for a relatively small point of minimum, i.e., $\bar{\sigma} = 0.394$. Right: envelope oscillations corresponding to initial conditions that fix $E < 0$ (see left) above the minimum, but below the plateau (i.e., $E = -0.004$), and therefore leading to an unstable evolution of the beam envelope, starting from of values of $\tilde{\sigma}_0$ sufficiently small between the asymptote around zero and $\bar{\sigma}$. 105

4.20 Left: V_s as function of $\tilde{\sigma}$, for a very small point of minimum, i.e., $\bar{\sigma} = 0.09$. Right: envelope oscillations corresponding to initial conditions that fix $E > 0$ (see left) above the plateau (i.e., $E = 0.021$), and therefore leading to an unstable evolution of the beam envelope, starting from of values of $\tilde{\sigma}_0$ sufficiently small between the asymptote around zero and $\bar{\sigma}$. 106

5.1 Variations of $\bar{\omega}_R$ with $\bar{k}$ for a monochromatic beam profile at fixed ratio n_{b0}/n_0. Here the solid lines indicate positive $\bar{\omega}_R$ and the dashed lines indicate negative $\bar{\omega}_R$ according to Eq. (5.3.4). 115

5.2 Variations of $\bar{\omega}_I$ with $\bar{k}$ for a monochromatic beam profile at fixed ratio n_{b0}/n_0. Here the solid lines indicate positive $\bar{\omega}_I$ and the dashed lines indicate negative $\bar{\omega}_I$ according to Eq. (5.3.5). 115

5.3 Variation of $\bar{\omega}_R$ with $\bar{k}$ for bell-like shaped non-monochromatic beams for different beam temperatures at fixed energy and ratio $n_{b0}/n_0 = 0.5$. 118

5.4 Variation of $\bar{\omega}_R$ with $\bar{k}$ for bell-like shaped non-monochromatic beams for different beam temperatures at fixed energy and ratio $n_{b0}/n_0 = 1.5$. 118

6.1 Stability analysis in the plane of the impedance for a monochromatic beam. 128

6.2 Qualitative plot of the contours in the plane (Z_R, Z_I), generated by the mapping (6.5.7) for different constant instability growth rates ω_I, for a thermal distribution given by (6.5.6). The stability region is surrounded by the curve $\omega_I = 0$. 129

6.3 Qualitative stability diagram in the plane of the impedance for a non-monochromatic beam whose thermal distribution is given by (6.5.6), as a result of the intersection between the contours of Figure 6.2 and the Z_I axis. 130

List of Symbols

e – absolute value of electron charge

Z_a – atomic number

n_b – beam number density

$\sigma_\perp$ – beam spot size

I_b – beam current

k_B – Boltzmann constant

q – charge of the particle

ρ_b – charge density

Z – coupling impedance

Γ_c – coupling parameter

ν_c – collision frequency

ξ – co-moving frame variable

I – current

J – current density

λ_D – Debye length

L – displacement

$\mathbf{vv}$ – dydadic product of $\mathbf{v}$

F – electric restoring force

ω_p – electron plasma frequency

ϕ – electric potential

$\mathbf{E}$ – electric field

F – external force

T_e – electron temperature

σ_z – effective length of the beam

ϵ – emittance

ω – frequency

$\langle F \rangle$ – General notation fo average of the the generic quantity F

∇ – gradient operator

$\nabla^{(6)}$ – gradient operator in $6-$ dimensional $\mu-$ space

$\nabla_{\mathbf{r}}$ – gradient operator in the configuration space

$\nabla_{\mathbf{v}}$ – gradient operator in the velocity space

$\nabla_{\mathbf{p}}$ – gradient operator in the momentum space

$\hat{\mathbf{I}}$ – identity tensor

i – integer; imaginary variable

L – inductance

m_i – ion mass

n_i – ion density

W_z – longitudinal componenet of wake field

E_{max} – maximum electric field

m – mass of the particle

$\mathbf{B}$ – magnetic field

$\sigma_{p\perp}$ – momentum spread

n – number density

n_1 – number density perturbation

E_M – oscillating electric field

n_e – plasma electron number density

s – plasma specie

T_p – plasma period

P – pressure; canonical variable

$\hat{\Pi}_e$ – pressure tensor of electron

U – potential energy

$\mathbf{r}$ – position vector

v – quiver velocity

m_{b0} – rest mass of charged particle

m_{e0} – rest mass of electron

γ – relativistic gamma factor

c – speed of light

x – space variable; configurational coordinate

τ – time-like variable

T – temperature

$\nabla_{\perp}$ – transverse gradient operator

$W_{\perp}$ – transverse componenet of wake field

y – transverse coordinate; space coordinate; configurational coordinate

ϵ_t – transverse emmittance

N – total number of particles in beam

t – time variable

y – transverse coordinate; space coordinate; configurational coordinate

γ_0 – unperturbed relativistic factor

n_{e0} – unperturbed plasma density

$\vec{\xi}$ – vector displacement

z – vertical position or perpendicular to the x and y axes

k – wavenumber

List of Acronyms

PWF	Plasma Wake Field
WFE	Wake Field Excitation
FEL	Free Electron Laser
EM	Electro-Magnetic
FELs	Free Electron Lasers
LWFE	Laser Wake Field Excitations
INFN	Intituto Nazionale di Fisica Nucleare
SL	Sparc Lab
PLASMONX	PLASma Acceleration and MONochromatic X-ray production
LPA	Laser Plasma Accelerators
HPL	High Power Laser
LWF	Laser Wake Field
AWAKE	Advanced Wakefield Experiment
COMB	Coherent plasma Oscillations excitation by Multiple electron Bunches
CPB	Charged Particle Beam
PE	Potential Equation
SMI	Self-Modulation Instability
LCI	Longitudinal Coupling Impedance
rms	root mean square
LM	Lorentz-Maxwell

Acknowledgements

Alhamdulillah, all the praises to Allah who has bestowed me by His uncountable blessings starting from the beginning of life until now.

I would like to express my deepest gratitude, thankful acknowledgment, and heartiest appreciations to my supervisor, *Prof. Renato Fedele*, for his constant guidance, encouragement, and un-tiring efforts during the course of my work. I thank him for his valuable suggestions and fruitful discussions. In fact, without his patient and kind help, this thesis would not even have been completed. I have been amazingly fortunate to have an advisor like him, who takes care of his students like his own children. He is the most honest, kind, humble, and sincere person I have ever seen in my life.

I offer my sincere thankfulness to my co-supervisors, *Prof. Dusan Jovanović* and *Dr. Sergio de Nicola*, who have been always there to listen and give me advices. I thank them for carefully reading and commenting on revisions of this thesis. Special thank goes to Dr. Sergio de Nicola for the discussions regarding the numerical problems of my work.

I am indebted to *Dr. Fatema Tanjia* for her kind helps starting from the very first day of my stay in Italy, to the end of my doctoral study. Whenever I faced any kind of problem, she was the one who I could imagine at first to go for suggestions. She was a source of inspiration and support that one usually gets from his/her elder sister. I further thank *Dr. Abdul Mannan* very much for his collaborations in this thesis and also for his friendly behaviour.

I acknowledge the efforts of my PhD coordinator *Prof. Raffaele Velotta* who was always available to help in any regard. It would be very difficult to get visa to come in Italy without his kind efforts. I also thank my internal referees *Prof. Salvatore Capozziello* and *Dr.ssa Maria Rosaria Masullo* for their valuable discussions and suggestions that helped me to improve my work.

I thank *Mr. Guido Celentano* for being so kind to all the foreign students. He is such a good soul who is ready to help any person in any situation. I further thank my honourable M.Sc supervisor, *Prof. Abdullah Al Mamun*, who inspires students to dream big and helps to open eyes. Without his help, it would not be possible to be here today.

Furthermore, I would like to thank all my lovely and genius friends in Napoli (specially, *Akif, Atanu, Nivya, Alan, Deborah, and Sara*) for their support and encouragements. I am really lucky to have friends like them.

My family has been a constant source of love, concern, support and strength all these years. I would like to express my heart-felt gratitude and love to my father, mother, siblings and their children. I also thank my mother-in-law and brother-in-law for their cordial supports and kind attitudes.

Md. Ashaduazzaman is certainly the main contributor of all the best in my life without whom it would be rather impossible even to stay abroad. I thank Allah for the extraordinary chance of having him as husband, friend, and companion.

Finally, I acknowledge the financial support from Intituto Nazionale di Fisica Nucleare and PhD school of Università degli studi di Napoli Federico II, which was helpful to participate international conferences and schools.

Tahmina Akhter
March 31, 2016
Napoli, Italy

Abstract

We carry out a theoretical investigation on the self-modulated dynamics of a relativistic, nonlaminar, charged particle beam travelling through a magnetized plasma due to the plasma wake field excitation mechanism. In this dynamics the beam plays the role of driver, but at the same time it experiences the feedback of the fields produced by the plasma. Driving beam and plasma are strongly coupled by means of the EM fields that they produce: the longer the beam (compared to the plasma wavelength), the stronger the self-consistent beam-plasma interaction. The sources of these EM fields are charges and currents of both plasma and driving beam. While travelling through the plasma, the beam experiences the electromechanical actions of the wake fields. They have a 3D character and affects sensitively the beam envelope. To provide a self-consistent description of the driving beam dynamics, we first start from the set of governing equations comprising the Lorentz-Maxwell fluid equations for the beam-plasma system. In the unperturbed particle system (i.e., beam comoving frame) and in quasi-static approximation, we reduce it to a 3D partial differential equation, called the Poisson-type equation. The latter relates the wake potential to the beam density which is coupled with the 3D Vlasov equation for the beam. Therefore, the Vlasov-Poisson-type pair of equations constitute our set of governing equation for the spatiotemporal evolution of the self-modulated beam dynamics. We divide the analysis in two different cases, purely transverse and purely longitudinal.

In the purely transverse dynamics, we investigate the envelope self-modulation of a cylindrically symmetric beam by implementing the Vlasov-Poisson-type system with the corresponding virial equations. This approach allows us to find some constant of motions and some ordinary differential equations, called the *envelope equations* that govern the time evolution of the beam spot size. They are easily integrable analytically and/or numerically and

therefore facilitate the analysis. Additionally, to approach our analysis also from the qualitative point of view, we make use of the so called *pseudo potential* or *Sagdeev potential*, widely used in nonlinear sciences, that is associated with the envelope equations. We first carry out an analysis in two different regimes, i.e., the local regime (where the beam spot size is much greater than the plasma wavelength) and the strongly nonlocal regime (where the beam spot size is much smaller than the plasma wavelength). In both cases, we find several types of self-modulation, such as focusing, defocusing and betatron-like oscillations, and criteria for instability, such as collapse and self-modulation instability. Then, the analysis is extended to the case where the beam spot size and the plasma wavelength are not necessarily constrained as in the local or strongly nonlocal cases. We carry out a full semi-analytical and numerical investigation for the envelope self-modulation. To this end, criteria for predicting stability and self-modulation instability are suitably provided.

In the purely longitudinal dynamics, we specialize the 3D Vlasov-Poisson-type equation to the 1D longitudinal case. Then, the analysis is carried out by perturbing the Vlasov-Poisson-type system up to the first order and taking the Fourier transformation to reduce the Vlasov-Poisson system to a set of algebraic equations in the frequency and wavenumber domain. This allows us to easily get a Landau-type dispersion relation for the beam modes, that is fully similar to the one holding for plasma modes. First, we consider the case of a monochromatic beam (i.e., cold beam) for which we find both a purely growing mode and a simple stability criterion. Moreover, by taking into account a non-monochromatic distribution function with finite small thermal correction, the Landau approach leads to obtain both the dispersion relation for the real and imaginary parts. The former shows all the possible beam modes in the diverse regions of the wave number and the latter shows the stable or unstable character of the beam modes, which suggests a simple stability criterion.

Finally, within the framework of the 1D longitudinal Vlasov-Poisson-type system of equations, we introduce the concept of coupling impedance in full analogy with the conventional accelerators. It is shown that also here the coupling impedance is a very useful tool for the Nyquist-type stability analysis.

Introduction

It is well known that a plasma can sustain large-amplitude electric and magnetic fields by means of suitable external actions that provide therein the creation of a charge separation between ions and electrons and the generation of an electric current. Typical external actions are provided by very intense electromagnetic pulses [1–3] or intense relativistic charged-particle beams [4–7], both called *drivers*, that are suitably launched into the plasma. The principal effect, predicted by the theory and even experimentally observed, is the generation of a plasma density perturbation behind the drivers at the same speed of the latter, as the water wake moves behind the boat. Very intense electric and magnetic fields, called *wake fields*, are associated with such a plasma perturbation. The mechanisms of the wake field excitation (WFE) can be artificially or naturally produced and, therefore, are relevant to the diverse environmental conditions ranging from laboratory to space and astrophysical plasmas.

Where do the WFE mechanisms take place?

In laboratory plasmas, the most relevant scientific and technological applications of the WFE are the realization of very compact schemes to provide very high gradients of accelerations. They can be efficiently used to accelerate bunches of charged-particles to ultra-high energy (f.i., up to 1 GeV in a few centimeters), or to provide the particle beam focusing (or other types of transverse beam manipulations) with ultra-strong strengths (f.i., 100 MGauss/cm) to be used in the final focusing stage of a linear collider. In addition, they can be used also to provide wiggling of particle beams with *plasma undulators* (or *plasma wigglers*) to be used in free electron laser (FEL) devices to produce coherent radiation of very small wavelengths

(f.i., X rays), by employing charged-particle beams of modest energies [1–12].

WFE-based acceleration of charged particle beams takes place also in space and astrophysical environments [13–16]. A mechanism for a *cosmic accelerator* has been proposed recently [17]. Even, Alfvén shocks can also excite large amplitude wake fields which, in turn, accelerate charged particles to high energy [17].

Why a plasma is necessary to sustain large amplitude wake fields?

The strong development of high-energy physics registered in the last three decades has required that particle accelerators have to work at the extreme conditions of luminosity, i.e., beyond 10^{34} cm^{-2} s^{-1} or brightness (high-intensity beams) and beam energy beyond several tens of TeV. To satisfy these requirements, but at the same time keeping very compact both the experimental set-up and the accelerating machines, very intense electromagnetic (EM) fields of about 100 GV m^{-1} are needed to manipulate the beams/bunches in suitable ways. Unfortunately, limitations in terms of costs and technology encountered in the use of the present generation of conventional accelerators fix the maximum fields at a few tens of MeV m^{-1}. On the other hand, the generation of coherent radiation in the X-ray regime using conventional magnetic undulators was accomplished long ago by using high energy electron beams. Many examples are found in the fields of free electron lasers (FELs) and synchrotron radiation sources [18–20]. However, this was done at very large and expensive accelerator facilities. New potentially inexpensive and compact FELs are needed to manipulate the charged particle beams in a more efficient way where the wiggler/undulator wavelength and the beam energy are effectively reduced.

To overcome such current technological limitations, plasma-based devices for efficient manipulation of charged particle beams seem to be feasible, manageable and flexible from the point of view of their insertion in a transport beam line.

It can been easily seen that the maximum electric field, E_{max}, expressed in V/cm, that can

be supported by a charge separation in a plasma of unperturbed density $n_0\left[\mathrm{cm}^{-3}\right]$, is given by

$$E_{max}\,[\mathrm{V/cm}] \approx \sqrt{n_0\,[\mathrm{cm}^{-3}]}\,. \tag{0.0.1}$$

This is the well known *Dawson limit* first introduced by John M. Dawson in 1959 [21, 22]. For a density $n_0 \sim 10^{18}\mathrm{cm}^{-3}$, $E_{max} \sim 1\mathrm{GV/cm}$, which is much greater than the one available in the conventional accelerating machines, i.e., $20 - 30$ MV/m (10^4 times larger than the ones employed in conventional accelerators!). This limit is sometimes also referred to as the *cold wave-breaking limit*. Recent valuable experimental results in this area have shown the absolute feasibility beyond $1cm$ acceleration with the record energy exceeding 1 GeV [23–29].

Compared to the conventional accelerators, the plasma-based acceleration is advantageous in terms of:

- compactness, because the size of the acceleration devices are reduced drastically of several order of magnitudes;
- costs, because less devices and the reduced dimensions drastically reduce the cost, as well;
- time, because the simpler arrangement implies reduced time of construction;
- technology, because simpler operations in delivering a charged-particle beam from the accelerator are required and no problems of electric insulation have to be solved. In fact, in the conventional accelerators the maximum electric fields must be suitably below the dielectric breakdown threshold. On the contrary, the plasma is the state of matter where a gas is fully ionized and, therefore, no problems of breakdown have to be solved!

Therefore, very compact accelerating and manipulating systems for charged particle beams, in principle capable to accelerate electrons to GeV in a few centimeters, or to focus particle or radiation beams with ultra-strong strengths (several orders more than the ones

provided by the conventional lenses), or to generate coherent radiation of very small wavelengths ranging from X- to γ-rays windows, seem to be feasible in the near future [30–36].

How does the wake field excitation work in a plasma and how do the wake fields provide very compact schemes?

As we have already mentioned above, there are two typical way to excite the wake fields in a plasma by using, as drivers, laser pulses and charged-particle beams, respectively. Let us briefly describe the related mechanisms.

Ultra-short and ultra-intense laser pulses as drivers

Recent studies of the EM pulse propagation in plasmas have witnessed the rapid growth of the frontiers of nonlinear optics. Thanks to this development, ultra-short and ultra-intense EM pulses are nowadays available. When such EM pulses are launched into the plasma, the gradient of the radiation intensity introduces a force on the plasma particles, the so-called ponderomotive force. It is independent of the charge sign, directly proportional to the opposite of the gradient of the radiation intensity, but inversely proportional to the particle mass. Therefore, it pushes the particles from the regions of greater intensities to the regions of lower intensities (ponderomotive effect), but it affects significantly the electron density compared to the ion one. On a time scale much less than the one of the carrier wave component of the laser pulse, the interplay by the ponderomotive effects and the restoring electric field between ions and electrons produces a net oscillating charge separation (plasma wave) behind the laser pulse. The plasma wave moves as a wake at the phase velocity that is almost equal to the group velocity of the laser pulse. This mechanism is usually referred to as the laser wake field excitation (LWFA) and it is expected to provide ultra-intense acceleration and strong focusing gradients [30, 37–39] at relatively lower cost compared to conventional accelerators. In general, the interaction between the ultra-short, ultra-intense laser pulse and the surrounding plasma consists of the number of electromechanical actions, which depend on the pulse

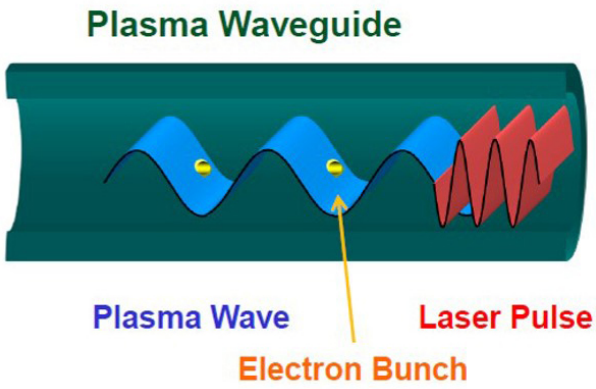

Figure 1: Scheme of the laser wakefield acceleration excited by a laser pulse. The driving laser pulse interacts with the active medium plasma and produces a driven system (charged particle beam) which leads to acceleration.

intensity. In turn, these actions affect the collective pulse dynamics which is nonlinear, as well. Consequently, the plasma and the pulses are strongly coupled. The electromechanical actions can be longitudinal (self-compression/expansion, self-modulation, bunch lengthening/shortening, etc.) or transverse (self-focusing/defocusing, beam widening, etc.), but they have a three dimensional (3D) character, in general. Usually, these effects provide the physical mechanisms that may enhance an initially small perturbation in the beam amplitude, leading to the large variety of instabilities, such as the modulational instability, filamentation and collapse (in the broadest sense, they belong to the family of coherent instabilities). An efficient plasma acceleration has been already tested in preliminary experiments devoted to the diverse aspects of very high energy gain, very intense focusing and production of radiation of very small wavelengths. A great effort in this direction is ongoing also at Intituto Nazionale di Fisica Nucleare (INFN) within the project Sparc Lab (SL), devoted to the R&D of plasma-based new acceleration techniques that has been originated by the former project PLASma acceleration and MONochromatic X-ray production (PLASMONX). SL collects a number of synergic experiments, all coming from the former multidisciplinary project PLASMONX. The INFN effort is based on the use of the FLAME laser, which provides one of the most powerful femtosecond pulsed laser with 10 Hz repetition rate presently available

with a maximum power of 220 TW and the maximum intensities of the order of or exceeding 10^{21} W/cm^2.

In summary, in the laser-plasma accelerators (LPA) schemes, high power laser (HPL) pulses produce a very strong ponderomotive effect (macroscopic Compton effect) capable of inducing very strong charge separations between ions and electrons. The latter create very strong electric fields (whose character is three-dimensional due to the three-dimensional profile of the HPL). The longitudinal component of such a field can be used to accelerate externally-injected charged particle beams. It has been demonstrated that suitable physical conditions, in terms of plasma density and HPL intensity, allow also to efficiently accelerate the electrons of the plasma to very high energy (*self injection scheme*) that are comparable to the ones achievable in the *external injection scheme*. In both schemes, the accelerated charged-particle beams are driven by the laser pulse. To reach these goals, ultra-strong (powers and intensities of the order of 10^2 TW and 10^{20} W/cm^2, respectively) and ultra-short femto-second HPL pulses have to be employed.

Intense relativistic beams as drivers

The interest, and therefore the study, of the relativistic charged-particle beam dynamics in plasmas has increased gradually in connection with the richness of nonlinear and collective effects induced by the propagation of very intense charged-particle bunches, even earlier than the growth of interest for the LWF acceleration [4]. The typical charged particle beam-driven plasma wave excitation is the well-known plasma wake field (PWF) excitation [4, 40, 41]. In the PWF excitation, a relativistic charged particle beam/bunch (i.e., driver, also called *driving beam/bunch*) is launched into a neutral plasma. This way, due to the violation of the local charge neutrality, the beam induces both charge and current perturbations of the plasma. In general, the spatial particle distribution of the driver has a 3D character, as in the case of the LWF excitation. Then, the driver carries charge and current that are spatially distributed and therefore they are, together with the charge and the current perturbations of the plasma, the sources of the total electromagnetic field of the system *driver* + *plasma*. The

resulting plasma perturbation manifests as a wake behind the driver. It corresponds to the generation of a plasma wave moving behind the driver with a phase velocity almost equal to the driver velocity. Electromagnetic fields, i.e., *plasma wake fields* (PWFs), are associated with such a wave. As in the driving laser case, the plasma wave has a 3D character (due to the 3D density profile of the driving bunch) and it oscillates at the electron plasma frequency [4]. Consequently, the electromagnetic field associated with the wake has both transverse and longitudinal components. The stronger the gradient of both longitudinal and transverse driver profiles, the stronger the amplitude of the longitudinal and transverse PWF components, respectively. Thus, a test particle experiences the effects of both the transverse (focusing/defocusing) and the longitudinal (acceleration/deceleration) components of the wake field. Depending on the regimes, the test particle can be the one of a secondary beam, called *driven beam*, externally injected in phase locking with the wake or belonging to the driver. In general, as in the case of LWF excitation, the transverse fields can be usable to manipulate the driven beam while accelerated by the longitudinal electric field. Drivers

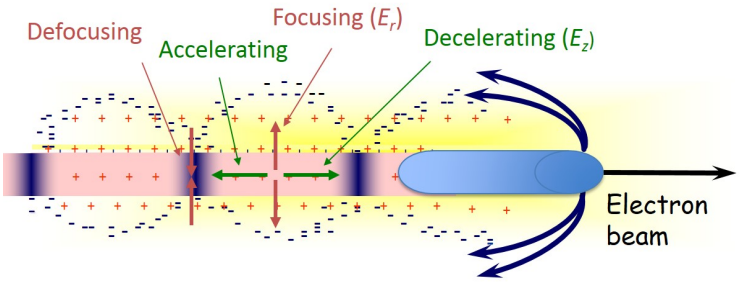

Figure 2: Plasma wake field acceleration scheme, excited by a relativistic electron beam, where the beam interacts with the surrounding plasma and thereby produces an wake field behind the beam itself.

sufficiently short compared to the plasma wavelength generate wakes that are completely located behind them. However, as the driver length gradually increases, the PWF generation takes place also partially inside the driver (especially within its tail), due to the head of the driver. Then, sufficiently long drivers compared to the plasma wavelength generate PWFs

mostly inside themselves. Therefore, the driver experiences the effects of the PWF that itself has produced (self interaction). This is a sort of collective self-consistent effect of the beam-plasma interaction that leads to the self-modulation of the driver. Physically, when a charged particle beam enters the plasma, the violation of the local charge neutrality is shielded by the plasma. The shielding of the beam is provided by an excess of plasma particles with opposite charge. Therefore, the longer beam the longer time of the shielding. This implies that for sufficiently long beams, the plasma has the time to shield adiabatically the driver in such a way that the drivers' dynamics is fully governed by the collective self-consistent PWF excitation.

There are many remarkable experimental and theoretical projects devoted to the PWF excitation. A plasma-based acceleration project planned at CERN (Geneva, Switzerland) jointly with Max Planck Institute for Physics (Munich, Germany), i.e., the Advanced Wake-field Experiment (AWAKE) [42, 43] which deals with proton-driven PWF excitation. Since long time, SLAC laboratory is dealing with many projects relating PWF acceleration mech-anism. One of the recent activities is the one where FACET facilities are used in an ex-periment to employ short electron bunch to generate high gradient field which accelerates a second trailing beam to high energies [44]. Theoretical and numerical studies seem to show that this technique has the capability to produce a high brightness beam. Moreover, within the Italian SPARC LAB collaboration COMB (Coherent plasma Oscillations excitation by Multiple electron Bunches) is a PWF-based experiment which is in progress at the National Laboratories of INFN in Frascati (Rome, Italy). The generation of sub-picosecond, high brightness electron bunch trains is achieved by means of velocity bunching technique (the so called *comb beam*). Such bunch trains (with a charge ranging from 200 pC to 400 pC at energies greater than 100 MeV) can be used to drive tunable and narrow band THz sources, FELs and PWF accelerators [45].

What is the goal of this thesis?

In this thesis we deal with the self modulated dynamics of a relativistic, nonlaminar, charged particle beam while travelling in a plasma. This is done in the context of PWF excitation mechanism. During the self interaction, the driving beam experiences a number of electromechanical effects in both longitudinal and transverse directions which are fully similar to the ones mentioned above for the case of LWF excitation. A large spectrum of longitudinal and transverse phenomena involving the beam density modulation, such as self-compression/decompression, self-focusing/defocusing, beam widening/squeeezing, beam lengthening/shortening, envelope oscillations are generated in the diverse conditions of:

- plasma motion (i.e., nonrelativistic or relativistic);
- plasma temperature (i.e., cold or warm plasma);
- beam motion (i.e., nonrelativistic or relativistic beam);
- beam temperature (i.e., cold or warm beam);
- beam-plasma collisions (i.e., collisionless or collisional beam-plasma system);
- ambient conditions (i.e., unmagnetized or magnetized plasma).

We first elaborate the appropriate models to describe self-consistently the modulated beam-plasma dynamics. The description of the dynamics of the *beam-plasma* system is provided by the kinetic theory by means of the Vlasov-Maxwell system of equations which, under suitable assumptions, can be reduced to the fluid Lorentz-Maxwell system of equations or to an hybrid system of equations comprising the Vlasov-Maxwell system for the driving beam and the Lorentz-Maxwell system for the plasma, respectively.

Going to the beams' co-moving frame and expressing the electromagnetic fields in terms of the four-potential, the Maxwell's equations can be conveniently reduced to a Poisson-like equation for a scalar function, called *plasma wake potential*, whose gradient gives the PWF.

Therefore, the Vlasov-Maxwell (or Lorentz-Maxwell) system of equations is reduced to the Vlasov-Poisson-type (or Lorentz-Poisson-like) pair of equations.

A further level of description of the beam modulation is given in terms of averaged quantities (such as, beam length, beam spot-size, longitudinal and transverse beam momentum spreads, etc.) by determining the virial equations (virial description) associated with the Vlasov-Poisson-type pair of equations. The virial description provides a very useful approach to the analysis of the envelope modulation which includes the formulation of the stability criteria.

Basic concepts of plasma and beam physics

In order to facilitate the description given in the next chapters, here we put forward some basic and tutorial concepts concerning both plasmas and beams. To this end, we privilege the physical aspects compared to the mathematical ones.

Plasma concept and plasma parameters

A plasma is a globally neutral system which is basically constituted of ionized matter and eventually of a minor part of neutral matter. In this thesis, for simplicity, we consider plasma constituted by a fully ionized matter. Under this assumption, the plasma is a system of ions (in general of several species) and electrons. In principle, all these charged particles are free to move with the random thermal motion, under the internal mutual electromagnetic forces, and eventually under the action of external forces that include external electromagnetic forces. Due to the long range character of the internal mutual electric and magnetic forces, the plasma motion (i.e., the motion of its particle) exhibit a collective behaviour. It is characterized by regimes of high temperature and low density, commonly found in laboratory as well as in space and astrophysical environments.

Due to the difference of three orders of magnitude between ions and electron mass (note that the proton mass is almost 1.8×10^3 times the electron mass), the mobility of the ions is

much reduced compared to the one of electrons. This means that, under the actions of oscillating electric fields, the electrons may respond with vibrations while ions remain practically at rest, provided that the oscillation frequency is sufficiently high. This physical circumstance, allows to separate electrons from ions. On the other hand, oscillating fields with much lower frequency can solicit the ions to vibrate, but the small mass of the electrons allows them the respond almost instantaneously by means of the electric restoring force and therefore ions and electrons are dragged along by the oscillating field and do not separate significantly.

When a portion of plasma is depleted of some electrons (thus creating a net positive charge), the resulting Coulomb force tends to pull back the electrons towards the excess of positive charge. Due to their inertia, the electrons will not simply replenish the positive region, but travel further away thus re-creating an excess of positive charge. In the absence of collisions, this effect gives rise to undamped electron oscillations at a frequency, i.e., ω_p, called the *electron plasma frequency* (or simply *plasma frequency*).

To provide a simple mathematical description of plasma frequency, let us assume a cold, collision-less electron plasma with ions constituting uniform background. We consider a rigid layer of electrons that are displaced along the x direction, lead by the vector displacement $\vec{\xi}$ (with respect to ions). In the case of a capacitor plate, the electric field produced by the capacitor is $\mathbf{E} = 4\pi e n_e \vec{\xi}$, where n_e is the plasma electron number density and e being the absolute value of electron charge, respectively. Then, the electric restoring force on an electron is $\mathbf{F} = -e\mathbf{E} = -4\pi e^2 n_e \vec{\xi}$. From these relation, we can find that the electron motion equation yields as,

$$\frac{d^2\xi}{dt^2} + \omega_p^2 \xi = 0, \tag{0.0.2}$$

where $\omega_p = \left(4\pi e^2 n_e / m_{e0}\right)^{1/2}$ and m_{e0} is the rest mass of electron. Equation (0.0.2) is the equation for simple harmonic motion describing the oscillation frequency of the fluctuating plasma electrons around the equilibrium position.

Let us consider a plasma initially with a uniform density of n_0 for both protons and

electrons. There is no net charge density, so that we can assume that there is initially no electric field. Now, let us suppose that the proton density is changed from n_0 to $(1-\delta)n_0$ in the region $-L < x < L$. If L is sufficiently small, the electric field due to this change will be so small that the electrons will suffer negligible disturbance. On the other hand, if L is sufficiently large, the change will have a drastic effect on the electron distribution. We are going to estimate the range of L at which transition takes place.

If there were no change in electron density, the Poisson's equation would lead to the following equation for the electric potential

$$\frac{d^2\phi}{dx^2} = 4\pi\delta n_0. \tag{0.0.3}$$

Assuming that the plasma as a whole is maintained at potential $\phi = 0$, the appropriate solution of Eq. (0.0.3) is $\phi = 2\pi\delta n_0(x^2 - L)$ for $|x| < L$ and $\phi = 0$ for $|x| > L$, which in particular becomes, $\phi(0) = -2\pi\delta n_0 L^2$.

Now suppose that the plasma has a temperature T, so that each particle has mean kinetic energy $k_B T/2$ in each degree of freedom (k_B is the Boltzmann constant). If $\phi(0)$ is so small that an electron of average thermal energy can easily reach $x = 0$, there will be only a small change in the state of plasma. On the other hand, if $\phi(0)$ is so large that a very few electrons can reach $x = 0$, there will be a drastic change in the state of the plasma. Hence the requirement that the plasma remain 'quasi-neutral' is that $\frac{1}{2}k_B T > 2\pi\delta n_0^2 L^2$, which can be rewritten in the form $\delta < \left(\frac{\lambda_D}{L}\right)^2$, where we have introduced the quantity called the the 'Debye length':

$$\lambda_D = \left(\frac{k_B T}{4\pi n_0^2}\right)^{1/2}.$$

The Debye length describes the important phenomenon of electrostatic screening, i.e., if an excess of positive charge is introduced in the plasma, it will be rapidly surrounded by a cloud of electrons (which are more mobile and thus react quickly). As a result, the positive charge will be partially screened and will be virtually 'invisible' to other particles situated at a large enough distance. The Debye screening is at the origin of one of the most crucial of all plasma properties, namely quasi-neutrality.

A dimensionless parameter using the above quantities (m_{e0}, e, n_0, and T) exists, and it reads as, coupling parameter i.e.,

$$\Gamma_c = \frac{4\pi e^2 n_0^{1/3}}{k_B T} . \tag{0.0.4}$$

Γ_c can be written as the ratio of the potential energy to the average kinetic energy. When Γ_c is small, the plasma is dominated by thermal effects. This is known as the weakly coupled plasma. On the contrary, when $\Gamma_c \gtrsim 1$, the plasma is said to be strongly coupled.

A violation of the local charge neutrality induces an electrostatic oscillation of the electric field in the plasma with frequency ω_p. This means that the quantity $T_p = \omega_p/2\pi$, called the *plasma period*, estimates the *characteristic time of charge separation*.

Plasma can support ultra-high electric field which depends on the number density perturbations according to the Poisson equation, $\nabla \cdot \mathbf{E} = -4\pi e n_1$, where n_1 is the number density perturbation. However, the maximum value of the field amplitude corresponds to a density perturbation numerically equal to the unperturbed plasma density (i.e., $n_1 \sim n_0$). It easily leads to the Dawson limit given by Eq. (0.0.1).

However, plasmas can become relativistic when the temperature is very large ($T > mc^2$) [46] or in the presence of large amplitude waves [47]. The case of large amplitude wave for cold plasma has been investigated by Akhiezer *et al.* [48]. In this case, relativistic corrections to plasma particle's mass and velocity are important.

Under the action of an oscillating field with large amplitude E_M at frequency ω, the plasma particle motion can be described in terms a parameter, called *quiver velocity*, i.e., $\nu = qE_M/m\omega c$, where q and m are the charge and mass of the particle. If $\nu \ll 1$, the plasma particle motion is non relativistic. With the gradual increase of amplitude, plasma particle velocity gradually become a significant fraction of light velocity, c. The condition $\nu \approx 1$, corresponds to radiation intensity of the order of $10^{13} - 10^{16}$ W/cm^2. Larger intensities ($\gtrsim 10^{17}$ W/cm^2) lead the plasma particles to be fully relativistic.

Particle beam concept and beam parameters

There is no univocal definition of beam. Typically, a charged particle beam stands for a collection of particles that have almost same same velocity and hence same kinetic energy and, therefore, move in almost same direction. The charged particle beams we are dealing with in this thesis are *paraxial systems*. In such a system the particle velocities are almost oriented along a privileged direction, say z, called the *propagation direction* or *longitudinal direction*. Let us denote by x and y a pair of orthogonal axis that are orthogonal to z, as well. This way, x, y and z, consitute a Cartesian reference frame. In such a frame, the trajectory of each beam particle can be represented by equation of the type:

$$z \;=\; z(x, y)\,. \tag{0.0.5}$$

Then, the paraxial character of our beam is established by the conditions

$$\frac{dx}{dz} \ll 1\,, \quad \textit{and} \;\; \frac{dx}{dz} \ll 1\,, \tag{0.0.6}$$

which state that the slopes of the particle trajectories in the beam must be very small.

At normal temperature, the kinetic energies of the particles are higher than the thermal energies. Charged particle beams can be categorized into two branches i.e., laminar beams and nonlaminar beams. In a laminar beam, the particles follow fixed layers of trajectories that never intersect. All the particles have identical transverse velocities and while flowing they make a small angle with the propagation axis (paraxial motion). The area of the phase space, that is occupied by a laminar beam, is a straight line of zero thickness. When the beam crosses the ideal lens is transformed in a converging laminar beam. It is easy to transform a diverging (or converging) beam to a parallel beam by using a lens of the proper focal length. On the other hand, the particles of a nonlaminar beam have random transverse velocities. Therefore, it is impossible to focus all particles from a location in the beam toward a common point. Lenses can influence only the average motion of particles. The phase space plot of a non-laminar beam is not a straight line.

A charged particle beam can be released from a material source and propagated through a medium (like plasma) or in a vacuum. When a charged particle beam has pulsed motion in the longitudinal direction, it is called *bunched beam*. The unbunched (*coasting*) beam has no pulses in the longitudinal direction. The bunched beams are the ones that are mostly used in modern accelerators. Charged particle beams can be described by various properties viz., particle species, energy, current, beam size, beam emittance (a measure of thermal spreading in the particle trajectories), brightness, etc.

The beam-plasma interaction ruled by the PWF mechanism can be described in various situations those depend on the relative density of beam and plasma, the velocity, temperature, collective or single particle behavior, etc. For instance, if the beam density is much smaller than the plasma density i.e., $n_b \ll n_0$, the system is in the overdense regime. When the beam density is nearly equal or a little above the plasma density i.e., $n_b \gtrsim n_0$ the PWF interaction is in underdense regime [4–8].

Brief summary of all the chapters We report here the synthetic descriptions of the chapters' contents. To help the reader, they are also reported as abstracts at the beginnings of each chapter.

Chapter 1: Models for plasmas

We present the basic concept of the kinetic theory for plasmas that are relevant for the self-consistent plasma wake field excitation. We start from the Vlasov-Maxwell system of equations for a plasma. From the kinetic model of each plasma specie, we find the hierarchy of moment equations of the distribution function that we truncate, with suitable closure conditions, to the level of fluid theory. This way, the set of fluid Lorentz-Maxwell equations is also presented in view of the construction of plasma wake field theory in Chapter 2. Finally, a simple extension of both kinetic and fluid models to include collisional effects is presented.

Chapter 2: The theory of plasma wake field excitation: the Poisson-type equation

We present the general theory of plasma wake field excitation in a magnetoactive, nonrelativistic, warm and collisionless plasma. This is done by using the 3D Lorentz-Maxwell system of equation for the 'beam-plasma' system that has been presented in Chapter 1. The driving beam is assumed to be ultra-relativistic in overdense regime. We first give a simple concept of plasma wake field and plasma wake potential by starting from the expression of the Lorentz force experienced by a test particle in its co-moving frame, in the presence of the self-consistent EM field of the 'beam-plasma' system. Then, in the quasi-static approximation, we reduce the Lorentz-Maxwell system of equations to a novel 3D partial differential equation, i.e., the generalized Poisson-type equation, that relates the beam density to the wake potential. Such an equation extends the PWF theory to the case of warm plasmas and accounts for the presence of an ambient magnetic field, the longitudinal and transverse plasma pressure terms, and the generalized conditions of beam energy and sharpness of the beam profile. The generalized Poisson-type equation found here is then specialized to several limiting cases in order to recover the particular equations that have been used in the literature.

Chapter 3: Models for charged particle beams and its self-consistent interaction with the surrounding medium

We formulate the kinetic description of an ultra-relativistic driving beam while self-consistently interacting with the plasma wake field excited in a warm, magnetized, collisionless plasma in overdense regime. The driver is supposed to be in the arbitrary conditions of sharpness of its density profile. Such a general formulation is provided by starting from the relativistic single-particle 3D Hamiltonian in the presence of an ambient magnetic field. In the reference frame of the *unperturbed particle*, we express the Hamiltonian of the *perturbed particle* in terms of a slight variation from the one of the unperturbed particle that is associated with the relativistic unperturbed beam state. After expanding the four potential to the first-order and performing the non-relativistic expansion with respect to the unperturbed state, we get the effective single-particle Hamiltonian. The latter is used to construct the 3D Vlasov equation

for the beam motion in the reference frame of the unperturbed particle. This way, by coupling the Vlasov equation with the generalized Poisson-type equation obtained in Chapter 2, we provide the self-consistent 3D kinetic description to be used in the next chapters to study the self-modulated dynamics of the driver while interacting with the surrounding plasma.

Chapter 4: Transverse self-modulated beam dynamics of a nonlaminar, ultra-relativistic beam in a non relativistic cold plasma

An analysis of the self-modulated transverse dynamics of a cylindrically symmetric nonlaminar driving beam is carried out. To this end, we disregard the longitudinal dynamics. Therefore, the general 3D Vlasov-Poisson-type system of equation constructed in Chapter 3 is reduced to a 2D pair of equations governing the spatiotemporal evolution of the purely transverse dynamics of the driving beam, which is supposed to be very long compared to the plasma wavelength and travelling through a cold, magnetized and overdense plasma. Due to the conditions of very long beam, the self-consistent PWF mechanism is very efficient and it sensitively characterizes the self-modulated dynamics.

The analysis is carried out by using the pair of Vlasov-Poisson-type equations in cylindrical symmetry that are implemented by the virial equations to provide the analysis of the self-modulated dynamics of the driver envelope. We show the important role played by the constants of motions that are involved in such a description. We first carry out an analysis in two different limiting cases, i.e., the local case (the beam spot size is much greater than the plasma wavelength) and the strongly nonlocal case (the beam spot size is much smaller than the plasma wavelength) where several types of self-modulation, in terms of focusing, defocusing and betatron-like oscillations, are obtained and the criteria for instability, such as collapse and self-modulation instability, are formulated. To this ends, within the context of the envelope description, we find suitable envelope equations, i.e., ordinary differential equations for the beam spot size, that are easily integrated analytically and that provide also suitable physical explanations in terms of the method of the pseudo potential or Sagdeev potential.

Then, the analysis is extended to the case where the beam spot size and the plasma wavelength are not necessarily constrained as in the local or strongly nonlocal cases. The analysis of the system can be still carried out with the virial equations and with the same methods used in the above limiting cases (envelope equations, Sagdeev potential) to provide a full semi-analytical and numerical investigation for the envelope self-modulation. To this end, criteria for predicting stability and self-modulation instability are suitably provided.

Chapter 5: Instability analysis of beam-plasma system

We carry out an analysis of the beam modes that are originated by perturbing the 'beam-plasma system' in the purely longitudinal case. This is done by considering the pair of 3D Vlasov-Poisson-type equation, presented in Chapter 3 that are specialized to the case in which the transverse driving beam dynamics is disregarded and only the longitudinal dynamics becomes effective. To this end, we perturb the Vlasov-Poisson-type system up to the first order, then take the Fourier transform to reduce the Vlasov-Poisson system to a set of algebraic equations in the frequency and wavenumber domain, from which we easily get a Landau-type dispersion relation for the beam modes, that is fully similar to the one holding for plasma modes. First, we consider the case of a monochromatic beam (i.e., cold beam, that is described by a distribution function in the form of delta-function in p space) for which the existence of a purely growing mode is shown and a simple stability criterion formulated. Then, by taking into account a unperturbed distribution function with finite, relatively small width (small thermal correction), the Landau approach, widely used in other physics area, leads to obtain both the dispersion relation for the real part (showing all the possible beam modes in the diverse regions of the wavenumber) and an expression for the imaginary part of the frequency (showing the stable or unstable character of the beam modes), which suggests a simple stability criterion.

Chapter 6: The coupling impedance concept for PWF self-interaction

Starting from the collisionless Vlasov-Poisson-type system of equation for longitudinal beam dynamics, that has been presented in Chapter 5, we formulate a novel approach in which

we put forward the concept of longitudinal coupling impedance associated with the beam-plasma interaction, in a way fully similar to the one in use in conventional particle accelerator physics. As in the conventional theory, the concept of coupling impedance seems to be very fruitful in a plasma-based accelerator to schematize the self-interaction of the relativistic driving beam with the surrounding plasma. In particular, it allows us to develop a simple instability analysis in the plane of the real and imaginary parts of the impedance that is based on the Nyquist approach widely used in the control system theory. Furthermore, we extend the Vlasov-Poisson-type system to the collision context with a simple model of collisions between the plasma particles (actually plasma electrons) and the beam particles. Under these assumptions, the role and the features of the coupling impedance defined here are compared to then ones of the coupling impedance in conventional theory. Examples of specific physical situations are finally illustrated.

Chapter 1

Models for plasmas

We present the basic concept of the kinetic theory for plasmas that are relevant for the self-consistent plasma wake field excitation. We start from the Vlasov-Maxwell system of equations for a plasma. From the kinetic model of each plasma specie, we find the hierarchy of moment equations of the distribution function that we truncate, with suitable closure conditions, to the level of fluid theory. This way, the set of fluid Lorentz-Maxwell equations is also presented in view of the construction of plasma wake field theory in Chapter 2. Finally, a simple extension of both kinetic and fluid models to include collisional effects is presented.

1.1 Preliminary considerations

We refer here to the notions of plasmas and charged particle beams (CPBs) given in the Introduction. In both systems, the (charged) particles are free to move and their collective dynamics is governed by the electromagnetic interactions. The most important difference between plasmas and CPBs is that the former are globally neutral whilst the latter carry a nonzero total electric charge. Since in this thesis we are interested in describing the self-modulated dynamics of a beam, we consider the plasma as the environment which the beam moves through and interacts with. Therefore, in the collective beam dynamics the role of the plasma is taken into account through the wake fields produced therein. The wake fields can be derived from a potential, i.e., the *wake potential*, which is a function of the Eulerian space

coordinates. The wake potential is related to the beam density by means of the Poisson-like equation. This means that the beam interacts with the plasma through a macroscopic quantity which can be indifferently provided by a kinetic or a fluid description. In this thesis, we provide the Poisson-like equation within the context of the fluid plasma theory.

In the next section, in view of the presentation of the self-modulated dynamics of a relativistic beam travelling in a plasma (see Chapters 4-6), we will first present the simple kinetic description of a nonrelativistic plasma, within the context of the Vlasov-Maxwell theory, and derive the fluid limit and the corresponding set of plasma fluid equations (Lorentz-Maxwell system). Then, we generalize the latter to the fluid theory of a relativistic plasma.

Plasma models depend on the adopted length scale. On a scale much less than λ_D, the dynamics is governed by equations which take into account the collisions among the single plasma particles (*short range interaction*). At this scale, the most appropriate description of plasma is the microscopic one, which focuses on the single collision processes and on the single-particle dynamics in the presence of microscopic electromagnetic fields. At length scales of the order of λ_D, the short range interaction are almost negligible, whilst the system dynamics is dominated by the longer range interactions. The latter are due to mean macroscopic electric and magnetic fields. At such scales, the most appropriate description of plasma is the one provided by the Boltzmann's kinetic theory, but with the inclusions of the collective effects due to the collective nature of the macroscopic fields. At length scales much greater than λ_D, the plasma description reduces to the one of a set of fluids: a single fluid for each ion specie and one for electrons. In this limiting case, the system dynamics is governed by a set of fluid dynamics equations with the inclusion of the collective effects introduced by the macroscopic fields.

The kinetic model for plasma has been first introduced by Vlasov [49]. The plasma is thought to be as a system of macroparticles whose dimensions are of the order of λ_D. They are assumed to be the effective particles of the system. Vlasov's model is based on the *Hartree's mean field theory* [50] which allows to simplify the interaction among many particles, by assuming that each particle moves in a field (mean field) generated by all the

other particles of the plasma. Note that the mean field depends on the instantaneous particle distribution and it is defined in any point of the space. The kinetic model can be introduced by means of the notion of *single-particle Boltzmann's phase space*, also called *reduced phase space* or simply *μ-space* [51]. A point P of this space represents a single-particle dynamical state, i.e., the pair of single-particle position and velocity (or momentum). Therefore, P has six coordinates: $(\mathbf{r}, \mathbf{v}) = (x, y, z, v_x, v_y, v_z)$, where $\mathbf{r} = (x, y, z)$ is the position of the generic particle in configuration space and $\mathbf{v} = (v_x, v_y, v_z)$ is the related velocity.

Let us now suppose to have a system of charged particles constituted by a so large number of identical particles that, at the length scales of the order of the Debye length, the dynamical states are distributed with continuity in μ-space. We define the *Boltzmann's distribution function* of such a system as the function $f = f(\mathbf{r}, \mathbf{v}, t)$ such that the mean number, say dN, of dynamical states within an elementary volume $d^3r\, d^3v$ of the μ-space $dN = f(\mathbf{r}, \mathbf{v}, t)\, d^3r\, d^3v$. Given the uniqueness of the solutions of the single-particle motion equations (provided that the initial conditions are imposed), the above system is a set of identical but distinguishable particles. Consequently, the dynamical states (i.e., points of the μ-space) are in a one-to-one correspondence with the particle of the system. Then, at each instant of time t, the total number of dynamical state concides with the total number, N, of system particles, i.e.,

$$N = \int f(\mathbf{r}, \mathbf{v}, t)\, d^3r\, d^3v\,. \tag{1.1.1}$$

Note that, if the particles keep their own identity during the evolution of the system (f.i., absence of ionization/recombination processes, decays, etc.), N remains unchanged in time. It follows that $f(\mathbf{r}, \mathbf{v}, t)$ is normalizable. Then, under this assumption, if we normalize f, i.e., $\int f(\mathbf{r}, \mathbf{v}, t)\, d^3r\, d^3v = 1$, it can be regarded as a probability density in μ-space. Adopting the kinetic model, at the scale comparable to λ_D, it is then possible to describe any system constituted by a large number of interacting charged particles, such as charged-particle beams (usually produced and/or employed in an accelerating machine or naturally generated in space and astrophysical environments) and plasmas (usually produced in and/or employed in laboratory for a number of scientific and technological applications or already present in

space and astrophysical environments in the most diversified conditions of density and temperatures). In particular, in a plasma we can attribute a distribution function, say $f_s(\mathbf{r}, \mathbf{v}, t)$, to each species s, i.e., each subsystem of identical particles (called *plasma components*, such as electrons and various species of ions). Let us assume that there are no processes capable to change the identity of the particles of each specie and that the short-range collisions are negligible (*collisionless plasma*). Then, given the one-to-one correspondence between particles and dynamical states, during the evolution of the system, the number of dynamical state of a given specie that enter per unitary time an arbitrary volume of μ-space equals the number of dynamical states of the same species that leave per unitary time the same volume. This corresponds to assume an equation of continuity in μ-space for a continuous system of dynamical states of each species with density $f_s(\mathbf{r}, \mathbf{v}, t)$ and velocity field $\mathbf{U}^{(6)} = (\dot{\mathbf{r}}, \dot{\mathbf{v}}) = (\mathbf{v}, \mathbf{a})$, where $\mathbf{a}$ is the instantaneous acceleration of the generic volume element of such a continuous system. Then, we can write

$$\frac{\partial f_s}{\partial t} + \nabla^{(6)} \cdot \left(f_s \mathbf{U}^{(6)} \right) = 0 \,, \tag{1.1.2}$$

where $\nabla^{(6)} = (\partial_x, \partial_y, \partial_z, \partial_{v_x}, \partial_{v_y}, \partial_{v_z})$ is the six-dimensional gradient in the μ.

By taking into account that: (i) $\mathbf{r}$ and $\mathbf{v}$ are indipendent variables; (ii) given the force field acting on the specie s, i.e., $\mathbf{F}_s = \mathbf{F}_s(\mathbf{r}, \mathbf{v}, t)$, from the motion of the single particle (of mass m_s) it follows $\mathbf{a} = \mathbf{F}_s(\mathbf{r}, \mathbf{v}, t)/m_s$; continuity equation (1.1.2) becomes

$$\frac{\partial f_s}{\partial t} + \mathbf{v} \cdot \nabla_{\mathbf{r}} f_s + \frac{\mathbf{F}_s}{m_s} \cdot \nabla_{\mathbf{v}} f_s + \frac{f_s}{m_s} \left(\nabla_{\mathbf{v}} \cdot \mathbf{F}_s \right) = 0 \,, \tag{1.1.3}$$

where $\nabla_{\mathbf{r}} = (\partial_x, \partial_y, \partial_z)$ and $\nabla_{\mathbf{v}} = (\partial_{v_x}, \partial_{v_y}, \partial_{v_z})$ are the gradients in the configuration space and in the velocity space, respectively. The force field $\mathbf{F}_s(\mathbf{r}, \mathbf{v}, t)$ can be in general the sum of the external fields and the ones that are generated by the particles of the system (self-consistent fields). For the time being, we confine our attention to the self-consistent fields and put: $\mathbf{F}_s = q_s[\mathbf{E} + \mathbf{v} \times \mathbf{B}]$, where the fields $\mathbf{E} = \mathbf{E}(\mathbf{r}, t)$ and $\mathbf{B} = \mathbf{B}(\mathbf{r}, t)$ satisfy suitable Maxwell's equations, whose sources are given by both the charge and current distributions ranging over all the species. To calculate these source terms, we introduce the following macroscopic

quantities

$$n_s(\mathbf{r},t) = \int f_s(\mathbf{r},\mathbf{v},t)d^3v\,, \tag{1.1.4}$$

$$\mathbf{V}_s(\mathbf{r},t) = \frac{\int \mathbf{v} f_s(\mathbf{r},\mathbf{v},t)d^3v}{n_s}\,, \tag{1.1.5}$$

corresponding to the *density* and the *mean velocity* (also called *current velocity* or *velocity field*) of the specie s, respectively. Then, the total charge and the total current of the specie s are respectively given by

$$\rho = \sum_s q_s n_s(\mathbf{r},t)\,, \tag{1.1.6}$$

and

$$\mathbf{j} = \sum_s q_s n_s(\mathbf{r},t)\mathbf{V}_s(\mathbf{r},t)\,, \tag{1.1.7}$$

where q_s is the charge of the single particle of the species s.

According to to above arguments and assumptions and observing that the electromagnetic Lorentz force $\mathbf{F}_s$ satisfies the condition $\nabla_{\mathbf{v}}\cdot\mathbf{F}_s = 0$, from Eq. (1.1.3) and the above equations, we obtain the following set of Vlasov-Maxwell system of equations, viz. (in cgs units),

$$\frac{\partial f_s}{\partial t} + \mathbf{v}\cdot\nabla_{\mathbf{r}} f_s + \frac{q_s}{m_s}[\mathbf{E} + q\mathbf{v}\times\mathbf{B}]\cdot\nabla_{\mathbf{v}} f_s = 0\,, \tag{1.1.8}$$

$$\nabla\cdot\mathbf{E} = 4\pi q_s \sum_s \int f_s(\mathbf{r},\mathbf{v},t)d^3v\,, \tag{1.1.9}$$

$$\nabla\cdot\mathbf{B} = 0\,, \tag{1.1.10}$$

$$\nabla\times\mathbf{B} = \frac{4\pi q_s}{c}\sum_s \int \mathbf{v} f_s(\mathbf{r},\mathbf{v},t)d^3v + \frac{1}{c}\frac{\partial\mathbf{E}}{\partial t}\,, \tag{1.1.11}$$

$$\nabla\times\mathbf{E} = -\frac{1}{c}\frac{\partial\,\mathbf{B}}{\partial t}\,, \tag{1.1.12}$$

where s ranges over all particle species, which means all ions species and electrons and we have used Eqs. (1.1.4) - (1.1.7). It describes the self-consistent spatiotemporal phase space evolution of the plasma within the kinetic theory. It is worthy to outline some important aspects of this system of equations.

1. For any s, Eq. (1.1.8) is called *kinetic Vlasov equation* for the specie s. It can be thought as a Boltzmann equation in which the collisions are negligible. Actually, the

presence of long-range interaction through the Lorentz force term involves the self-consistent collective effects and therefore makes this equation deeply different from Boltzmann equation. For nstance, an important aspect of this diversity is the development of *non-dissipative damping* of collective oscillations with reversible character, usually referred to as the *Landau damping*. In the Vlasov's kinetic theory, these processes can be described as a statistical result of a large number of resonant interactions between the collective modes and the individual particles of the plasma [52].

2. For any s, the left-hand side of Eq. (1.1.8) can be thought as the total derivative of f_s. In fact, we observe that:

$$\frac{\partial f_s}{\partial t} + \mathbf{v} \cdot \nabla_{\mathbf{r}} f_s + \frac{\mathbf{F}_s}{m_s} \cdot \nabla_{\mathbf{v}} f_s = \frac{\partial f_s}{\partial t} + \dot{\mathbf{r}} \cdot \nabla_{\mathbf{r}} f_s + \dot{\mathbf{v}} \cdot \nabla_{\mathbf{v}} f_s = \frac{df_s}{dt} \,.$$

   Consequently, by virtu of Eq. (1.1.8), it follows that $df_s/dt = 0$. Hence, the distribution function f_s is conserved along the characteristics $\mathbf{r} = \mathbf{r}(t)$, $\mathbf{v} = \mathbf{v}(t)$. This result has the following simple physical interpretation. Since each f_s represents the density of dynamical states in μ-space, the set of these states constitutes an incompressible fluid. Consequently, by virtu of the conservation of the number of dynamical states in an arbitrary volume of μ-space (continuity equation), the volume of the phase space associated with any subsystem of particles of the specie s conserves (*Liouville theorem* in μ-space). It is easy to show that the same property holds for the volume associated to any subsystem containing particles of all species.

3. The mathematical coupling among the equations of the system (1.1.8) - (1.1.12) corresponds to the following representation of the self-consistency. In principle, given both the initial conditions and the boundary conditions, we can formally integrate Vlasov equation for each specie with respect to f_s. Then we can compute both charge and current distributions which, in turn, allow us to integrate the Maxwell equations for $\mathbf{E}$ and $\mathbf{B}$, once both initial and boundary conditions are imposed. However, to determine explicitly f_s for any s from Eq. (1.1.8), it is necessary to know already explicitly the

fields **E** and **B**; but, nevertheless, to determine the latter from the Maxwell equations it is necessary to know explicitly the distributions of the sources (charges and currents) and, therefore, f_s for any s.

4. System of equations (1.1.8) - (1.1.12) is a system of nonlinear partial differential equations. The *sources of nonlinearity* lie in the third term at the left-hand side of Eq. (1.1.8) for any s. The nonlinearity of system (1.1.8) - (1.1.12) makes impossible the application of the superposition principle. Then, a linear combination of solutions of system (1.1.8) - (1.1.12) is not, in turn, a solution of this system.

For simplicity, we will consider plasmas constituted by electrons and only one ion specie, whose electric charge is e (i.e., atomic number $Z_a = 1$) which is the absolute value of the electron charge (the generalization to an arbitrary numbers of ion species with arbitrary atomic number Z_a is not difficult), viz.,

$$\frac{\partial f_e}{\partial t} + \mathbf{v}\cdot\nabla_{\mathbf{r}} f_e - \frac{e}{m_e}[\mathbf{E} + q\mathbf{v}\times\mathbf{B}]\cdot\nabla_{\mathbf{v}} f_e = 0\,, \tag{1.1.13}$$

$$\frac{\partial f_i}{\partial t} + \mathbf{v}\cdot\nabla_{\mathbf{r}} f_i + \frac{e}{m_i}[\mathbf{E} + q\mathbf{v}\times\mathbf{B}]\cdot\nabla_{\mathbf{v}} f_i = 0\,, \tag{1.1.14}$$

$$\nabla\cdot\mathbf{E} = 4\pi e\left[\int f_i(\mathbf{r},\mathbf{v},t) - \int f_e(\mathbf{r},\mathbf{v},t)\right], \tag{1.1.15}$$

$$\nabla\cdot\mathbf{B} = 0\,, \tag{1.1.16}$$

$$\nabla\times\mathbf{B} = \frac{4\pi e}{c}\left[\int \mathbf{v} f_i(\mathbf{r},\mathbf{v},t)d^3v - \int \mathbf{v} f_e(\mathbf{r},\mathbf{v},t)d^3v\right] + \frac{1}{c}\frac{\partial\mathbf{E}}{\partial t}\,, \tag{1.1.17}$$

$$\nabla\times\mathbf{E} = -\frac{1}{c}\frac{\partial\,\mathbf{B}}{\partial t}\,, \tag{1.1.18}$$

where e and i stand for electrons and ions, respectively, and we have used Eqs. (1.1.4) - (1.1.7).

1.2 Fluid theory of a nonrelativistic plasma: the Lorentz-Maxwell system

It is possible to derive a set of equations for fluid plasma species at scales much larger than the Debye length for a certain species constituting the plasma. The set of Vlasov-Maxwell

equations can be cast into a set of fluid equations, called Lorentz-Maxwell (LM) system. This can be done by reducing the system in μ- space to the configuration space. To do this, we integrate Vlasov equation upon multiplying by appropriate monomial or polynomials of velocity.

We first consider a plasma which is free from any external field. The plasma is constituted by electrons and ions. Then, let us introduce the following differential operator in the μ-space:

$$\hat{D}_s = \frac{\partial}{\partial t} + \mathbf{v}\cdot\nabla_{\mathbf{r}} + \frac{q_s}{m_s}\left[\mathbf{E}(\mathbf{r},t) + \frac{\mathbf{v}}{c}\times\mathbf{B}(\mathbf{r},t)\right]\cdot\nabla_{\mathbf{v}}\,.$$

In terms of this operator, Vlasov equation (1.1.8) can be written as,

$$\hat{D}_s f_s = 0\,. \tag{1.2.1}$$

Now we multiply Eq. (1.2.1) by a monomial of v, such as 1 (scalar), $\mathbf{v}$ (vector), $\mathbf{vv}$ (tensor), ..., and integrate over velocity space. Then, we perform the following integrals:

$$\int \hat{D}_s\, f_s\, d^3v = 0\,, \tag{1.2.2}$$

$$\int \mathbf{v}\hat{D}_s\, f_s\, d^3v = 0\,, \tag{1.2.3}$$

$$\ldots\ldots\ldots\ldots\ldots\ldots\,, \tag{1.2.4}$$

by obtaining

$$\frac{\partial I_s^{(0)}}{\partial t} + \nabla_r\cdot\mathbf{I}_s^{(1)} = 0\,, \tag{1.2.5}$$

$$\frac{\partial I_s^{(1)}}{\partial t} + \nabla_r\cdot\hat{\mathbf{I}}_s^{(2)} - \frac{q_s}{m_s} I_s^{(0)}\left[\mathbf{E} + \frac{\mathbf{I}_s^{(1)}}{c}\times\mathbf{B}\right] = 0\,, \tag{1.2.6}$$

$$\ldots\ldots\ldots\ldots\ldots\ldots\,, \tag{1.2.7}$$

where we have introduced the following quantities: *Moment of zero order of f_s* (scalar quantity),

$$I_s^{(0)} = \int f_s(\mathbf{r},\mathbf{v},t)\, d^3v = n_s(\mathbf{r},t)\,. \tag{1.2.8}$$

First order moment of f_s (vector quantity, also called as current density of species s),

$$\mathbf{I}_s^{(1)} = \int \mathbf{v} f_s(\mathbf{r},\mathbf{v},t)\, d^3v = n_s(\mathbf{r},t)\mathbf{V}_s(\mathbf{r},t)\,. \tag{1.2.9}$$

Second order moment of f_s (tensor quantity),

$$\hat{\mathbf{I}}_s^{(2)} = \int \mathbf{v}\mathbf{v} f_s(\mathbf{r}, \mathbf{v}, t)\, d^3v = \frac{\hat{\mathbf{P}}_s}{m_s} = n_s \langle \mathbf{v}\mathbf{v} \rangle_s \,, \tag{1.2.10}$$

$$\text{.........................} \,. \tag{1.2.11}$$

In Eqs. (1.2.8) - (1.2.11), the integration is done over all the entire velocity space. In addition, flux momentum density tensor of the species s is,

$$\hat{\mathbf{P}}_s \equiv m_s \hat{\mathbf{I}}_s^{(2)}(\mathbf{r}, t) = m_s \int \mathbf{v}\mathbf{v} f_s(\mathbf{v})\, d^3v = m_s n_s \frac{\int \mathbf{v}\mathbf{v} f_s(\mathbf{r}, \mathbf{v}, t)\, d^3v}{\int f_s(\mathbf{r}, \mathbf{v}, t)\, d^3v} \,. \tag{1.2.12}$$

From Eq. (1.2.5), we can observe that to know the zero-order moment, $I_s^{(0)}$, we need to know the first order moment $\mathbf{I}_s^{(1)}$. Furthermore, from Eq. (1.2.6), we can observe that to know the first-order moment, $\mathbf{I}_s^{(1)}$, we need to know the second-order moment $\mathbf{I}_s^{(2)}$. Similarly, we can obtain an equation for second-order moment, which will contain third-order moment as well. In fact, an evolution equation for the moment of order n would contain the moments of order $n + 1$.

To obtain fluid equations up to the first order of moment equation, we need to truncate the hierarchy by expressing $\hat{\mathbf{I}}_s^{(2)}$ in terms of moments of lower order (*closure reports)*. This can be done by taking averages of physical quantities on scales much greater than λ_D which represents a sort of *smoothing* operation. If λ is the characteristic length of the spatial variation of the physical quantities involved in our description, then the condition of validity of a fluid model is expressed by $\lambda_D \ll \lambda$. For each specie s, we express velocity $\mathbf{v}$ as the sum of a part corresponding to its average and another part which has a random character, i.e.,

$$\mathbf{v} = \mathbf{V}_s + \mathbf{u} \,, \tag{1.2.13}$$

where $\mathbf{V}_s = \langle \mathbf{v} \rangle_s$ and $\langle \mathbf{u} \rangle_s = 0$. Here, $\mathbf{u}$ is the *random velocity* of the particle that takes into account their thermal motion. Using Eqs. (1.1.4) and (1.1.5), into Eqs. (1.2.8) - (1.2.11) and (1.2.13), Eqs. (1.2.5) and (1.2.6) become,

$$\frac{\partial n_s}{\partial t} + \nabla_r \cdot (n_s \mathbf{V}_s) = 0 \,, \tag{1.2.14}$$

$$\frac{\partial \mathbf{V}_s}{\partial t} + (\mathbf{V}_s \cdot \nabla_r)\mathbf{V}_s = \frac{q_s}{m_s}\left(\mathbf{E} + \frac{\mathbf{V}_s}{c} \times \mathbf{B}\right) - \frac{\nabla_r \cdot \hat{\mathbf{p}}_s}{m_s n_s} \,, \tag{1.2.15}$$

where $\hat{\mathbf{p}}_s$ is the *pressure tensor* on the species s, defined as

$$\hat{\mathbf{p}}_s = m_s n_s \langle \mathbf{uu} \rangle_s = m_s \int f_s \, \mathbf{uu} \, d^3u \,. \tag{1.2.16}$$

Since the short ranged collisions are considered negligible and if no other form of dissipations are important, then we can assume the following isotropic form for the pressure tensor

$$\hat{\mathbf{p}}_s = p_s \hat{\mathbf{I}} \,, \tag{1.2.17}$$

where $\hat{\mathbf{I}}$ is the identity tensor and p_s is the scalar pressure of the species s. It is also assumed to be $p_s = n_s k_B T_s$ for temperatures T_s and Boltzmann constant k_B. The most recurrent forms of closure of the system are the following one corresponds to the *adiabatic hypothesis*, i.e., $T_s / n_s^{\gamma_{sr}-1}$ = constant, where γ_{sr} is the ratio of specific heat at constant pressure to the specific heat at constant volume of species s. In this case, Eq. (1.2.15) becomes:

$$\left(\frac{\partial}{\partial t} + \mathbf{V}_s \cdot \nabla_r \right) \mathbf{V}_s = \frac{q_s}{m_s} \left(\mathbf{E} + \frac{\mathbf{V}_s}{c} \times \mathbf{B} \right) - \gamma_{sr} \frac{k_B T_s}{m_s} \frac{\nabla_r n_s}{n_s} \,. \tag{1.2.18}$$

The other hypothesis is called *isothermal*, i.e., $\nabla_r T_s = 0$, for which case Eq. (1.2.15) can be written as

$$\left(\frac{\partial}{\partial t} + \mathbf{V}_s \cdot \nabla_r \right) \mathbf{V}_s = \frac{q_s}{m_s} \left(\mathbf{E} + \frac{\mathbf{V}_s}{c} \times \mathbf{B} \right) - \frac{k_B T_s}{m_s} \frac{\nabla_r n}{n_s} \,. \tag{1.2.19}$$

Equations (1.2.18) and (1.2.14) or (1.2.19) and (1.2.14) have to be coupled with the Maxwells equations given in the following form:

$$\nabla \cdot \mathbf{E} = 4\pi \sum_s q_s n_s \,, \tag{1.2.20}$$

$$\nabla \cdot \mathbf{B} = 0 \,, \tag{1.2.21}$$

$$\nabla \times \mathbf{B} = \frac{4\pi}{c} \sum_s q_s n_s \mathbf{V}_s + \frac{1}{c} \frac{\partial \mathbf{E}}{\partial t} \,, \tag{1.2.22}$$

$$\nabla \times \mathbf{E} = -\frac{1}{c} \frac{\partial \mathbf{B}}{\partial t} \,. \tag{1.2.23}$$

The system of equations consisting of (1.2.20) - (1.2.23), (1.2.14) and (1.2.18) is known as the *Lorentz-Maxwell system in the adiabatic approximation*, whilst the system of equations

(1.2.20) - (1.2.23), (1.2.14) and (1.2.19) is known as *Lorentz-Maxwell system in the isothermal approximation*, respectively. Note that these systems of equations contain the following sources of nonlinearity:

1. the product $n_s\mathbf{V}_s$ in continuity equation and equation for $\nabla \times \mathbf{B}$;

2. the products $(\mathbf{V}_s \cdot \nabla)\,\mathbf{V_s}$ and $\mathbf{V}_s \times \mathbf{B}$, and the term $T_s \nabla n_s/n_s$ in motion equation.

1.3 Kinetic description of a relativistic plasma

The Vlasov-Maxwell system of Eqs. (1.1.8) - (1.1.12) can be easily generalized to a relativistic case [53, 54].

Let us consider a collisionless plasma with an arbitrary different species of particles, where a particle of species s has rest mass m_{so}. The plasma is assumed to be *relativistic*, i.e., its particles may move at relativistic speed. This implies that, in principle, particle masses depend on the speed (note that the relativistic mass is $m_s = m_{so}\gamma$, $\gamma = 1/(1 - v^2/c^2)^{1/2}$ being the relativistic factor) and, therefore, the Boltzmann μ-space, presented above for the non-relativistic case, has to be redefined. In fact, the pair $(\mathbf{r}, \mathbf{v})$ cannot be used to denote a dynamical state. If $\mathbf{p}$ is the instantaneous single-particle linear momentum, the μ-space is now defined as the six-dimensional space of all the pairs $(\mathbf{r}, \mathbf{p})$. Each pair $(\mathbf{r}, \mathbf{p})$ represents a dynamical state of the single particle. Given the uniqueness of the relativistic motion equations, the set of dynamical states associated to each species is in a one-to-one correspondence with the particles of the same specie. Therefore, each species is described by a particle density $f_s = f_s(\mathbf{r}, \mathbf{v}, t)$. As in the non-relativistic case, the particles interact by the electromagnetic forces they create themselves so that the density functions f_s together with the self consistent electromagnetic fields $\mathbf{E}(\mathbf{r}, t)$ and $\mathbf{B}(\mathbf{r}, t)$ evolve according to the following

relativistic Vlasov-Maxwell system, viz.,

$$\frac{\partial f_s}{\partial t} + \mathbf{v}\cdot\nabla_r f_s + q_s\left(\mathbf{E} + \frac{\mathbf{v}}{c}\times\mathbf{B}\right)\cdot\nabla_p f_s = 0\,, \tag{1.3.1}$$

$$\nabla\cdot\mathbf{E} = 4\pi\sum_s q_s\int f_s(\mathbf{r},\mathbf{p},t)d^3p\,, \tag{1.3.2}$$

$$\nabla\cdot\mathbf{B} = 0\,, \tag{1.3.3}$$

$$\nabla\times\mathbf{B} = \frac{4\pi}{c}\sum_s q_s\int \mathbf{v} f_s(\mathbf{r},\mathbf{p},t)d^3p + \frac{1}{c}\frac{\partial\mathbf{E}}{\partial t}\,, \tag{1.3.4}$$

$$\nabla\times\mathbf{E} = -\frac{1}{c}\frac{\partial\,\mathbf{B}}{\partial t}\,, \tag{1.3.5}$$

where s ranges over all the species and the particle velocity is given by

$$\mathbf{v} = \frac{\mathbf{p}}{m_{s0}\gamma} = \frac{\mathbf{p}}{m_{s0}\left(1 + p^2/m_{s0}^2c^2\right)^{1/2}}\,. \tag{1.3.6}$$

Note that the number density n_s, the current velocity $\mathbf{V}_s$, the total charge density ρ and the total current densities $\mathbf{j}$ are here defined, respectively, as

$$n_s(\mathbf{r},t) = \int f_s(\mathbf{r},\mathbf{p},t)d^3p\,, \tag{1.3.7}$$

$$\mathbf{V}_s(\mathbf{r},t) = \frac{\int \mathbf{v} f_s(\mathbf{r},\mathbf{p},t)d^3p}{n_s}\,, \tag{1.3.8}$$

$$\rho(\mathbf{r},t) = \sum_s q_s n_s(\mathbf{r},t) = \sum_s q_s\int f_s(\mathbf{r},\mathbf{p},t)d^3p\,, \tag{1.3.9}$$

$$\mathbf{j}(\mathbf{r},t) = \sum_s q_s n_s(\mathbf{r},t)\mathbf{V}_s(\mathbf{r},t) = \sum_s q_s\int \mathbf{v} f_s(\mathbf{r},\mathbf{p},t)d^3p\,. \tag{1.3.10}$$

It is easy to see that the relativistic extension of the Vlasov-Maxwell system (1.1.13) - (1.1.18) is the following

$$\frac{\partial f_e}{\partial t} + \mathbf{v}\cdot\nabla_r f_e - e\left(\mathbf{E} + \frac{\mathbf{v}}{c}\times\mathbf{B}\right)\cdot\nabla_p f_e = 0\,, \tag{1.3.11}$$

$$\frac{\partial f_i}{\partial t} + \mathbf{v}\cdot\nabla_r f_i + e\left(\mathbf{E} + \frac{\mathbf{v}}{c}\times\mathbf{B}\right)\cdot\nabla_p f_i = 0\,, \tag{1.3.12}$$

$$\nabla \cdot \mathbf{E} = 4\pi e \left[\int f_i(\mathbf{r}, \mathbf{p}, t) d^3p - \int f_e(\mathbf{r}, \mathbf{p}, t) d^3p \right], \tag{1.3.13}$$

$$\nabla \cdot \mathbf{B} = 0\,, \tag{1.3.14}$$

$$\nabla \times \mathbf{B} = \frac{4\pi e}{c} \left[\int \mathbf{v} f_i(\mathbf{r}, \mathbf{p}, t) d^3p - \int \mathbf{v} f_e(\mathbf{r}, \mathbf{p}, t) d^3p \right] + \frac{1}{c} \frac{\partial \mathbf{E}}{\partial t}\,, \tag{1.3.15}$$

$$\nabla \times \mathbf{E} = -\frac{1}{c} \frac{\partial \mathbf{B}}{\partial t}\,, \tag{1.3.16}$$

where $s = e$ (electrons), i (ions).

1.4 Fluid description of a relativistic plasma

The procedure of constructing the hierarchy of moment equations, starting from the Vlasov-Maxwell system (1.1.8) - (1.1.12), can be easily extended to the relativistic case to obtain the Lorentz-Maxwell system of equation for a relativistic plasma [52, 53]. We easily arrive to the following relativistic Lorentz-Maxwell fluid equations

$$\frac{\partial n_s}{\partial t} + \nabla \cdot (n_s \mathbf{V_s}) = 0\,, \tag{1.4.1}$$

$$\left(\frac{\partial}{\partial t} + \mathbf{V}_s \cdot \nabla \right) \mathbf{P}_s = q_s \left(\mathbf{E} + \frac{\mathbf{V}_s}{c} \times \mathbf{B} \right) - \nabla \cdot \hat{\Pi}_s\,, \tag{1.4.2}$$

$$\nabla \times \mathbf{E} = -\frac{1}{c} \frac{\partial \mathbf{B}}{\partial t}\,, \tag{1.4.3}$$

$$\nabla \times \mathbf{B} = -\frac{4\pi}{c} \sum_s q_s n_s \mathbf{V}_s + \frac{1}{c} \frac{\partial \mathbf{E}}{\partial t}\,, \tag{1.4.4}$$

$$\nabla \cdot \mathbf{E} = 4\pi \sum_s q_s n_s\,, \tag{1.4.5}$$

$$\nabla \cdot \mathbf{B} = 0\,, \tag{1.4.6}$$

where $n_s = n_s(\mathbf{r}, t)$ and $\mathbf{V}_s = \mathbf{V}_s(\mathbf{r}, t)$ are the number density and the fluid velocity of the s-th specie and still defined by Eqs. (1.3.7) and (1.3.8), $\hat{\Pi}_s(\mathbf{r}, t)$ is a stress tensor accounting for the thermal effects of the s-th specie, $\hat{\Pi}_s$ is the pressure tensor and

$$\mathbf{P}_s(\mathbf{r}, t) = m_{s0} \gamma_s(\mathbf{r}, t) \mathbf{V}_s(\mathbf{r}, t) \tag{1.4.7}$$

is the *relativistic fluid linear momentum of the s-th specie*, $\gamma_s(\mathbf{r}, t)$ being the *fluid relativistic factor of the s-th specie*, i.e.,

$$\gamma_s(\mathbf{r}, t) = \frac{1}{\sqrt{1 - V_s^2(\mathbf{r}, t)/c^2}} \,. \tag{1.4.8}$$

The stress tensor term, under the assumptions of adiabatic or isothermal conditions, can be cast in forms that are similar to the corresponding non relativistic cases, respectively.
Note that the relativistic Lorentz-Maxwell system contains all the sources of nonlinearity that are contained in the corresponding non-relativistic system, but in addition it contains the one due to the relativistic mass variation through the term $m_{s0}\mathbf{V}_s/\sqrt{1 - V_s^2(\mathbf{r}, t)/c^2}$ in motion equation.

1.5 Collisional plasmas

The descriptions provided in the previous sections has regarded collisionless plasmas. This is a physical circumstance compatible with the Vlasov equation, which can be basically thought as a sort of collisionless Boltzmann equation. Although the presence of collective effects in Vlasov equations make this equation quite different from Boltzmann equation, actually one can introduce collision effects in the plasma by assuming that the right-hand side of Vlasov equation is no longer zero, but equal to a source of collisions, as it is done with Boltzmann equation in the case of a neutral gas [51]. Therefore, the existence of non negligible collisional effects of the specie s makes non zero the total derivative of the distribution function f_s along the characteristics. This, in turn, implies the non conservation of the volume in the μ-space (i.e., Liouville theorem for the s-th specie is no longer valid). It is worthy noting that, if we include the collision source terms in the Vlasov-Maxwell system, the corresponding fluid model will contain collisional terms, as well. Then, in both kinetic and fluid models, they lead to the inclusion of the dissipative effects as well as the macroscopic irreversibility of the system.

We assume here that: (i) the rate of collisions among particles belonging to the same

specie is much less than the characteristic parameter of time variation of the plasma quantities; (ii) the rate of binary collisions between particles of different species is comparable to the characteristic parameter of time variation of the plasma quantities. Then, a possible estimate of the variation rate of f_s due to binary collisions of the particles of s-th specie with the ones of the s'-th specie is given by

$$\left(\frac{\partial f_s}{\partial t}\right)_{coll,ss'} = \frac{f_{s'} - f_s}{\tau_{ss'}}\,, \tag{1.5.1}$$

where $\tau_{ss'}$ is the characteristic time of the momentum transfer from the specie s-th to the specie s'. Consequently, the total rate that accounts for all the collisional contributions is obtained by summing over all the species $s' \neq s$. Therefore, the total derivative is no longer zero, as in the collisionless case, but

$$\frac{df_s}{dt} = \sum_{s'} \left(\frac{\partial f_s}{\partial t}\right)_{coll,ss'} = \sum_{s'} \frac{f_{s'} - f_s}{\tau_{ss'}}\,. \tag{1.5.2}$$

Hence, the inclusion of the collisions in Eq. (1.3.1) finally gives

$$\frac{\partial f_s}{\partial t} + \mathbf{v}\cdot\nabla_r f_s + q_s\left(\mathbf{E} + \frac{\mathbf{v}}{c}\times\mathbf{B}\right)\cdot\nabla_p f_s = \sum_{s'} \frac{f_{s'} - f_s}{\tau_{ss'}}\,. \tag{1.5.3}$$

For any s, Eq. (1.5.3) has to be coupled with Eqs. (1.3.2) - (1.3.5).

To get the corresponding fluid description, we have to calculate the moments of Eq. (1.5.3). We easily see that the zero-th order moment equation gives still the continuity Eq. (1.4.1), because the integral of the collision term at the right-hand side of Eq. (1.5.3) over all the momentum space vanishes in the absence of production or losses of particles of each specie. Moreover, the first-order moment equation gives the motion equation of the s-th specie that in principle differs from Eq. (1.4.2) due to the presence of the variation of the momentum of the specie s per unit time due to the collisions with all the other species. Under the assumption that the current velocities of two different species, say s and s', are different, a net momentum transfer between them takes place. It turns out that such a momentum transfer is proportional to the difference of current velocities of the two different species. Therefore, the total net momentum transfer of the s-th specie results from the sum over all

the species s' which appears as a new term at the right-hand side of the motion equation, i.e.,

$$\left(\frac{\partial}{\partial t} + \mathbf{V}_s \cdot \nabla\right)\mathbf{P}_s = q_s\left(\mathbf{E} - \frac{\mathbf{V}_s}{c} \times \mathbf{B}\right) - \nabla \cdot \hat{\Pi}_s = \sum_{s'} \frac{V_{s'} - V_s}{\tau_{ss'}} \,. \tag{1.5.4}$$

1.6 Conclusions

The basic concept of the kinetic theory for plasmas that are relevant for the self-consistent plasma wake field excitation have been presented. Starting from the Vlasov-Maxwell system of equations for the single plasma specie, we have provided the kinetic description of the plasma. Furthermore, we have found the hierarchy of moment equations of the single-specie distribution function that we have truncated, with suitable closure conditions, to the level of fluid theory. In view of the construction of plasma wake field theory in Chapter 2, this has allowed to provide the fluid description of the plasma in terms of the set of fluid Lorentz-Maxwell system of equations. Finally, both kinetic and fluid models have been also extended in order to include simple collisional effects.

Chapter 2

The theory of plasma wake field excitation: the Poisson-type equation

We present the general theory of plasma wake field excitation in a magnetoactive, nonrelativistic, warm and collisionless plasma. This is done by using the 3D Lorentz-Maxwell system of equation for the 'beam-plasma' system, where the sources of the EM fields include charges and currents of both plasma and beam. The driving beam is assumed to be relativistic in overdense regime. We first give a simple concept of plasma wake field and plasma wake potential by starting from the expression of the Lorentz force experienced by a test particle in its co-moving frame, in the presence of the self-consistent EM field of the 'beam-plasma' system. Then, in the quasi-static approximation, we reduce the Lorentz-Maxwell system of equations to a novel 3D partial differential equation, i.e., the generalized Poisson-type equation, that relates the beam density to the wake potential. Such an equation extends the PWF theory to the case of warm plasmas and accounts for the presence of an ambient magnetic field, the longitudinal and transverse plasma pressure terms, and the generalized conditions of beam energy and sharpness of the beam profile. The generalized Poisson-type equation found here is then specialized to several limiting cases in order to recover the particular equations that have been used in the literature.

2.1 Introduction

The basic concept of PWF can be suitably provided by determining the force experienced by a relativistic particle of charge q, which has a relative motion with respect to an electromagnetic field, i.e., the pair $(\mathbf{E}(\mathbf{r},t),\mathbf{B}(\mathbf{r},t))$ of electric and magnetic field that has been created by some source.

Let us denote the test particle velocity by $\mathbf{v}$ and assume that it has the relativistic motion along z, i.e., $\mathbf{v} = \beta c\hat{z} + \mathbf{v}_\perp$, where $\beta \sim 1$ and $\mathbf{v}_\perp$ is the transverse component of $\mathbf{v}$ such that $\mathbf{v}_\perp \ll c$. Then, the Lorentz force experienced by the particle is:

$$\mathbf{F} = \frac{d\mathbf{p}}{dt} = q\left[\mathbf{E} + \frac{\mathbf{v}}{c}\times\mathbf{B}\right] , \tag{2.1.1}$$

where $\mathbf{p}$ is the linear momentum of the particle, i.e.,

$$\mathbf{p} = m_0\gamma\,\mathbf{v} , \tag{2.1.2}$$

where m_0 and γ are the rest mass and relativistic factor, respectively. We now introduce the four-potential $(\mathbf{A}(\mathbf{r},t),\phi(\mathbf{r},t))$, such that:

$$\mathbf{E} = -\nabla\phi - \frac{1}{c}\frac{\partial\mathbf{A}}{\partial t} , \tag{2.1.3}$$

$$\mathbf{B} = \nabla\times\mathbf{A} . \tag{2.1.4}$$

Then, Eq. (2.1.1) can be easily cast as:

$$\mathbf{F} = q\left[\nabla\left(\mathbf{A}\cdot\frac{\mathbf{v}}{c} - \phi\right) - \frac{1}{c}\left(\frac{\partial}{\partial t} + \mathbf{v}\cdot\nabla\right)\mathbf{A}\right] . \tag{2.1.5}$$

Note that vector and scalar potentials, i.e., $\mathbf{A}$ and ϕ, depend on the Eulerian coordinates $\mathbf{r}$ and t, whilst $\mathbf{F}$ depends on $\mathbf{r}$, $\mathbf{v}$ and t, $\mathbf{v}$ being independent of $\mathbf{r}$. We split $\mathbf{r}$, gradient operator, and $\mathbf{A}$ into longitudinal and transverse components, i.e.,

$$\mathbf{r} = \hat{z}z + \mathbf{r}_\perp , \tag{2.1.6}$$

$$\nabla = \hat{z}\frac{\partial}{\partial z} + \nabla_\perp , \tag{2.1.7}$$

$$\mathbf{A} = \hat{z}A_z + \mathbf{A}_\perp . \tag{2.1.8}$$

Then, Eq. (2.1.5) becomes:

$$\mathbf{F} = q\nabla\left(\beta A_z - \phi\right) + q\nabla\left(\mathbf{A}_\perp \cdot \frac{\mathbf{v}_\perp}{c}\right) - \frac{q}{c}\left(\frac{\partial}{\partial t} + \beta c\frac{\partial}{\partial z}\right)\mathbf{A} - \frac{q}{c}\left(\mathbf{v}_\perp \cdot \nabla_\perp\right)\mathbf{A}\,, \tag{2.1.9}$$

which under the following coordinate transformation

$$\xi(\mathbf{r}_\perp, z, t) = z - \beta' ct\,, \tag{2.1.10}$$

$$\mathbf{R}_\perp(\mathbf{r}_\perp, z, t) = \mathbf{r}_\perp\,, \tag{2.1.11}$$

$$\tau(\mathbf{r}_\perp, z, t) = t\,, \tag{2.1.12}$$

where $\beta' \sim 1$, becomes:

$$\mathbf{F}' = q\nabla'\Omega + q(\beta' - \beta)\frac{\partial \mathbf{A}'}{\partial \xi} - \frac{q}{c}\frac{\partial \mathbf{A}'}{\partial \tau} + q\nabla'\left(\mathbf{A}'_\perp \cdot \frac{\mathbf{v}'_\perp}{c}\right) - q\left(\frac{\mathbf{v}'_\perp}{c} \cdot \nabla'_\perp\right)\mathbf{A}'\,. \tag{2.1.13}$$

Here we have denoted the transformed quantities by primes and also defined the quantity $\Omega(\mathbf{R}_\perp, \xi, \tau) = \beta A'_z(\mathbf{R}_\perp, \xi, \tau) - \phi'(\mathbf{R}_\perp, \xi, \tau)$. We assume that the test particle and the fields are moving at the same speed, i.e., $\beta' = \beta$ (rigidity condition). Furthermore, since $\mathbf{v}'_\perp \ll c$, we neglect the higher-order terms coming from the last two terms at right hand side of Eq. (2.1.13). Then, we finally obtain:

$$\mathbf{F}'(\mathbf{R}_\perp, \xi, \tau) = q\nabla'\Omega(\mathbf{R}_\perp, \xi, \tau) - \frac{q}{c}\frac{\partial \mathbf{A}'(\mathbf{R}_\perp, \xi, \tau)}{\partial \tau}\,, \tag{2.1.14}$$

where $\nabla' = \partial/\partial\mathbf{R}_\perp + \hat{z}\partial/\partial\xi$.

2.2 Definition of plasma wake field

Let us now consider a relativistic charged particle beam moving through a plasma along the z-direction. We assume that the beam has a finite temperature. Therefore, we assume that the beam particles experience the effect of the thermal spreading while moving in the plasma along z in such a way that the beam performs a *nonlaminar motion*. In these physical conditions, the velocity of each beam particle can be thought as the sum of a deterministic part corresponding to the relativistic motion along z whose average is not zero (mean

velocity), plus a random instantaneous part along an arbitrary direction whose average is zero corresponding to the thermal spreading. In addition, we assume that the beam temperature corresponds to a non-relativistic random motion, so that the instantaneous slope of the single-particle trajectory can be considered sufficiently small to fulfill the conditions:

$$\frac{dx}{dz} \ll 1 \ , \quad \frac{dy}{dz} \ll 1 \, , \tag{2.2.1}$$

where x and y are the transverse space coordinates assumed by the single particles. Condition (2.2.1) is equivalent to assume that the beam is *paraxial*.

The excess of charge that is introduced by the beam while moving through the plasma is responsible for the violation of the local charge neutrality, which in turn, creates a local electric field in the system. On the other hand, the motion of the beam corresponds to a current injected in the plasma which generates a local magnetic field. We can conclude that the propagation of a relativistic charged particle beam through the plasma perturbs the initial stationary conditions of the plasma itself. Therefore, the *beam-plasma* system excites therein the local electromagnetic field. This is a macroscopic field, whose sources are the charges and the currents of both plasma and beam, that it is called plasma wake field (PWF). The corresponding mechanism is usually referred to as *PWF excitation*. Since the PWF is excited the propagation of the relativistic beam through the plasma, it is evident that it moves through the plasma with almost the same velocity of the beam itself.

Note that, in principle, the PWF can act on any test particle which is instantaneously in the plasma region where it has been excited. We want here to emphasize the causality aspects of the beam-plasma interaction: (i) starting from the initial stationary condition, the charged particle beam propagates through the plasma and introduces therein an excess of charge and an external current; (ii) the latter generates plasma perturbations that, in turn, excite the PWF. Then, we can conclude that the relativistic beam has actually driven the PWF excitation by means of the an *active medium*, i.e., the plasma. We call this beam the *driving beam* or simply the *driver* of the PWF excitation. In other words, the mechanism of the PWF excitation is obtained by the external action of the driver into the active medium which, in

turn, can sustain such an excitation. Although the causality works as described here, the connection between the *external action* of the driver and the *response* of the active medium manifests so rapidly that they should be considered contextually, i.e., on same timescale.

If the driver is actually a bunch, i.e., it carries a very sharp particle distribution in configuration space (number density), the PWF acts on test particles those are behind the bunch travelling at almost its same speed. If the driver density profile has a 3D character it is expected that the PWF has a 3D character as well. Therefore, a test particle can be accelerated or decelerated by the instantaneous longitudinal component of the PWF, depending on the synchronism conditions of the test particles with respect to the phase of the PWF. On the other hand, meanwhile, the transverse component of the PWF may affect the test particle motion by providing a transverse manipulation of its trajectory, such as focusing, defocusing, etc.

If the driver is a sufficiently long beam, the PWF will act also on the particle of the driver itself, providing this way a sort of self-interaction of the beam: *the driver is affected by the PWF that itself has generated*.

According to the above assumptions, the force produced by the PWF, that is experienced by a test charged particle located in the position $(\mathbf{R}_\perp, \xi)$ at time τ, is given by Eq. (2.1.14). However, since the external action of the driver and the plasma-response manifest on the same timescale, we can assume that $\partial/\partial\tau \simeq 0$ (quasi-static approximation). Consequently, the force per unitary charge, at the location $(\mathbf{r}_\perp, \xi)$ that is generated by the PWF mechanism is given by:

$$\mathbf{W}(\mathbf{r}_\perp, \xi) = \nabla\Omega(\mathbf{r}_\perp, \xi)\,, \tag{2.2.2}$$

where $\nabla = \partial/\partial\mathbf{r}_\perp + \hat{z}\partial/\partial\xi$ and $\Omega(\mathbf{r}_\perp, \xi) = \beta A_z(\mathbf{r}_\perp, \xi) - \phi(\mathbf{r}_\perp, \xi)$, $A_z(\mathbf{r}_\perp, \xi)$ and $\phi(\mathbf{r}_\perp, \xi)$ being the z-component of the vector potential and scalar potential, respectively, of the *beam-plasma* system at location $(\mathbf{r}_\perp, \xi)$. Here, $\mathbf{W}$ is the PWF excited by the driving beam and Ω is the related *plasma wake potential*. It can be easily proven that

$$\nabla_\perp W_z = \frac{\partial \mathbf{W}_\perp}{\partial \xi}\,, \tag{2.2.3}$$

which is the Panofsky-Wenzel theorem [55]. Here W_z and $\mathbf{W}_\perp$ are longitudinal and transverse components of W, respectively. Therefore, in the quasi-static approximation, $\mathbf{W}$ has the feature of an electrostatic field which can be derived by an effective potential Ω. In the subsequence sections, we show that the Lorentz-Maxwell system that governs, at the diverse physical conditions, the spatiotemporal evolution of the plasma in the presence of both *internal* sources (charge and current provided by the plasma) and *external* sources (charge and current provided by the beam), can be reduced to a Poisson-type equation which relates the PWF potential to the beam density.

All the Poisson-type equation that we will obtain at the diverse physical assumptions, can be cast in the following generic form:

$$\hat{\mathcal{P}}\Omega = \hat{\mathcal{Q}}\, n_b\,, \tag{2.2.4}$$

where $n_b = n_b(\mathbf{r}_\perp, \xi)$ is the local number density of the beam; $\hat{\mathcal{P}}$ and $\hat{\mathcal{Q}}$ are two generic partial differential operators whose explicit form depends on the physical assumptions we take for the beam-plasma system. Their role will be crucial in Chapter 4 and subsequent chapters, where we couple Eq. (2.2.4) with appropriate equations for the beam dynamics to describe the self-consistent spatio-temporal beam evolution (beam self-modulation).

2.3 Lorentz-Maxwell system of equations for the beam-plasma system

Let us consider a plasma where a relativistic charged particle beam is travelling through, along the z axis, as the driver of the PWF. We also assume, for simplicity, that the plasma consists of electrons and a single specie of ions with $Z_a = 1$. The latter are also supposed to be infinitely massive forming a uniform background of positive charge with unperturbed number density n_0. Let us finally assume that the plasma electrons have in general a relativistic motion. Then, according to the section 1.4 and 1.5, and in order to take into account the presence of an external uniform magnetic field and collisions between plasma particles and the beam particles, our system is described by the following set of coupled relativistic

fluid equations ($s = e$):

$$\frac{\partial n_e}{\partial t} + \nabla \cdot (n_e \mathbf{V_e}) = 0\,, \tag{2.3.1}$$

$$\left(\frac{\partial}{\partial t} + \mathbf{V}_e \cdot \nabla\right)\mathbf{P}_e = -e\left[\mathbf{E} + \frac{\mathbf{V}_e}{c} \times \mathbf{B}\right] - \nabla \cdot \hat{\Pi}_e - \frac{(\mathbf{V}_e - \mathbf{V}_b)}{\tau_{eb}}\,, \tag{2.3.2}$$

$$\nabla \times \mathbf{E} = -\frac{1}{c}\frac{\partial \mathbf{B}}{\partial t}\,, \tag{2.3.3}$$

$$\nabla \times \mathbf{B} = -\frac{4\pi}{c} e n_e \mathbf{V}_e + \frac{4\pi}{c} q n_b \mathbf{V}_b + \frac{1}{c}\frac{\partial \mathbf{E}}{\partial t}\,, \tag{2.3.4}$$

$$\nabla \cdot \mathbf{E} = 4\pi e\,(n_0 - n_e) + 4\pi q n_b\,, \tag{2.3.5}$$

$$\nabla \cdot \mathbf{B} = 0\,, \tag{2.3.6}$$

where $\mathbf{V}_e = \mathbf{V}_e(\mathbf{r}, t)$ is the electron plasma current velocity, $\mathbf{P}_e = \mathbf{P}_e(\mathbf{r}, t)$ is the electron plasma fluid linear momentum, i.e.,

$$\mathbf{P}_e(\mathbf{r}, t) = m_{e0}\gamma_e(\mathbf{r}, t)\mathbf{V}_e(\mathbf{r}, t) \tag{2.3.7}$$

(m_{e0} being the plasma electron rest mass), $\hat{\Pi}_e = \hat{\Pi}_e(\mathbf{r}, t)$ is the pressure tensor of the electron plasma fluid, $\mathbf{V}_b = \mathbf{V}_b(\mathbf{r}, t)$ is the beam fluid velocity, $n_e = n_e(\mathbf{r}, t)$ and $n_b = n_b(\mathbf{r}, t)$ are the electron plasma number density and the beam number density, respectively, and q is the charge of the single particle of the beam. In addition, within the adiabatic approximation, we assume that the pressure tensor has the form:

$$\hat{\Pi}_e = \begin{pmatrix} p_{e\perp} & 0 & 0 \\ 0 & p_{e\perp} & 0 \\ 0 & 0 & p_{ez} \end{pmatrix}, \tag{2.3.8}$$

where $p_{e\perp} = n_e k_B T_{e\perp}$, and $p_{ez} = n_e k_B T_{ez}$, $T_{e\perp}$ and T_{ez} being transverse and longitudinal temperatures, respectively. Here, $p_{e\perp}$ and p_{ez} are transverse and longitudinal pressures, respectively. The adiabatic approximation implies that the following conditions:

$$p_{e\perp} n_e^{-\Gamma_{e\perp}} = \text{constant} \tag{2.3.9}$$

and

$$p_{ez} n_e^{-\Gamma_{ez}} = \text{constant} \tag{2.3.10}$$

has to be satisfied. Here $\Gamma_{e\perp} = D + 2/D = 2$ and $\Gamma_{ez} = D + 2/D = 3$ are the adiabatic exponents in transverse and longitudinal directions, respectively, where D is the number of degrees of freedom. Note that, in the above set of fluid equations, the driving charged-particle beam is involved through its charge density, i.e., $\rho_b(\mathbf{r}, t) \equiv qn_b(\mathbf{r}, t)$, its current density, i.e., $\mathbf{J}_b(\mathbf{r}, t) \equiv qn_b(\mathbf{r}, t)\mathbf{V}_b(\mathbf{r}, t)$, and the collision term accounting for the collisions between plasma electrons and beam particles, i.e., $-(\mathbf{V}_e - \mathbf{V}_b)/\tau_{eb}$, τ_{eb} being the corresponding characteristic collision time.

In the next sections, confining our attention to a collisionless nonrelativistic plasma, we shall reduce the system (2.3.1) - (2.3.10) to suitable Poisson-type equations for the diverse physical assumptions we shall adopt. To this end, we assume that density and fluid velocity of the driver are, respectively, of the form:

$$n_b(\mathbf{r}, t) = n_b(\mathbf{r}_\perp, \xi)\,, \tag{2.3.11}$$

$$\mathbf{V}_b(\mathbf{r}, t) = \hat{z}\beta c + \mathbf{v}_b(\mathbf{r}_\perp, \xi)\,, \tag{2.3.12}$$

where $\xi = z - \beta ct$ and $\mathbf{v}_b$ is a fluid component such that: $|\mathbf{v}_b| \ll c$, with $\beta \sim 1$. Equation (2.3.12) states that the driver's velocity is basically relativistic along with a 3D nonrelativistic instantaneous displacement, $\mathbf{v}_b$, with instantaneous orientation, that accounts for both the longitudinal and transverse beam dynamics.

2.4 Poisson-type equation in overdense regime: collisionless nonrelativistic plasma

We assume that the driver has the maximum density, say n_{bmax}, much smaller than the unperturbed plasma density, i.e.,

$$n_{bmax} \ll n_0\,. \tag{2.4.1}$$

This condition defines the so-called *overdense regime*. It implies that the driver introduces a small perturbation in terms of charge density and current density into the plasma. Let us assume that initially the plasma is in the following equilibrium state: $n_e = n_0$, $\mathbf{V}_e = 0$,

$\mathbf{E} = 0$, $\mathbf{B} = \mathbf{B}_0 = B_0\hat{z}$ = constant, and $\hat{\Pi}_e = \hat{\Pi}_0$ = constant. Here $\mathbf{B}_0$ is a uniform and constant magnetic field which is oriented along the longitudinal direction. It is evident that it represents an external magnetic field. Once the driver is supposed to travel through the plasma, the resulting excited PWF is a quantity of the order of n_b/n_0. According to the assumption of overdense regime, this ratio is much smaller than 1. Therefore, it is clear that the driver density n_b is a first-order quantity and produces first-order displacement in all physical quantities. So that, it is possible to linearize the system of Eqs. (2.3.1) - (2.3.10) with the additional assumptions (2.3.11) and (2.3.12) and assume that the plasma motion is nonrelativistic, i.e., $\mathbf{P}_e(\mathbf{r}, t) \approx m_{e0}\mathbf{V}_e(\mathbf{r}, t)$.

In order to find the appropriate Poisson-type equation for the system under consideration, we do the following steps.

(i) We express both electric and magnetic fields, $\mathbf{E}$ and $\mathbf{B}$, in terms of the four-potential $(\mathbf{A}, \phi)$, according to Eqs. (2.1.3) and (2.1.4) and adopt the Lorentz gauge, i.e.,

$$\nabla \cdot \mathbf{A} + \frac{1}{c}\frac{\partial \phi}{\partial t} = 0\,. \tag{2.4.2}$$

(ii) We linearize the system of Eqs. (2.3.1) - (2.3.12). To this end, we introduce first-order perturbations of all the physical quantities (denoted by the subscript 1) around the above mentioned equilibrium states, i.e., $n_e = n_0 + n_1$, $\mathbf{V}_e = \mathbf{V}_1$, $\mathbf{E} = \mathbf{E}_1$, $\mathbf{B} = \mathbf{B}_0 + \mathbf{B}_1$, $\mathbf{A} = \mathbf{A}_0 + \mathbf{A}_1$, $\phi = \phi_1$, and $\hat{\Pi} = \hat{\Pi}_0 + \hat{\Pi}_1$. Consequently, the Lorentz-Maxwell system of equations becomes,

$$\frac{\partial n_1}{\partial t} + n_0 \nabla \cdot \mathbf{V}_1 = 0, \tag{2.4.3}$$

$$\frac{\partial \mathbf{V}_1}{\partial t} = \frac{e}{m_{e0}}\left[\nabla\phi_1 + \frac{1}{c}\frac{\partial \mathbf{A}_1}{\partial t}\right] - \frac{eB_0}{m_{e0}\,c}\mathbf{V}_1 \times \hat{\mathbf{z}} - \frac{\nabla \cdot \hat{\Pi}_1}{m_{e0}\,n_0}, \tag{2.4.4}$$

$$\frac{1}{c^2}\frac{\partial^2 \phi_1}{\partial t^2} - \nabla^2\phi_1 = 4\pi\left[qn_b - en_1\right], \tag{2.4.5}$$

$$\frac{1}{c^2}\frac{\partial^2 \mathbf{A}_1}{\partial t^2} - \nabla^2\mathbf{A}_1 = \frac{4\pi}{c}\left(qn_b\beta c\hat{z} - en_0\mathbf{V}_1\right), \tag{2.4.6}$$

where Eqs. (2.1.3) and (2.1.4) become,

$$\mathbf{E}_1 = -\nabla\phi_1 - \frac{1}{c}\frac{\partial \mathbf{A}_1}{\partial t}\,, \tag{2.4.7}$$

$$\mathbf{B}_0 + \mathbf{B}_1 = \nabla \times \mathbf{A}_0 + \nabla \times \mathbf{A}_1\,. \tag{2.4.8}$$

Here, $\mathbf{A}_0$ denotes the zero-order vector potential, i.e., $\mathbf{B}_0 = \nabla \times \mathbf{A}_0(\mathbf{r})$. Note that $\mathbf{A}_0(\mathbf{r}) = (\mathbf{B}_0 \times \mathbf{r})/2$. Correspondingly, the Lorentz gauge can be split into the following conditions:

$$\nabla \cdot \mathbf{A}_0 = 0, \tag{2.4.9}$$

$$\nabla \cdot \mathbf{A}_1 + \frac{1}{c}\frac{\partial \phi_1}{\partial t} = 0. \tag{2.4.10}$$

(iii) We split the vector quantities and the gradient operator (∇) into perpendicular (denoted by the subscript $\perp$) and longitudinal components (denoted by the subscript z), i.e., Eqs. (2.4.3) - (2.4.6) give:

$$\frac{\partial n_1}{\partial t} + n_0\frac{\partial V_{1z}}{\partial z} + n_0\nabla_\perp \cdot \mathbf{V}_{1\perp} = 0, \tag{2.4.11}$$

$$\frac{\partial V_{1z}}{\partial t} = \frac{e}{m_{e0}}\left(\frac{\partial \phi_1}{\partial z} + \frac{1}{c}\frac{\partial A_{1z}}{\partial t}\right) - \frac{\Gamma_z k_B T_{0z}}{m_{e0} n_0}\frac{\partial n_1}{\partial z}, \tag{2.4.12}$$

$$\frac{\partial \mathbf{V}_{1\perp}}{\partial t} = \frac{e}{m_{e0}}\left(\nabla_\perp\phi_1 + \frac{1}{c}\frac{\partial \mathbf{A}_{1\perp}}{\partial t}\right) + \omega_c(\mathbf{V}_{1\perp} \times \hat{\mathbf{z}}) - \frac{\Gamma_\perp k_B T_{0\perp}}{m_{e0} n_0}\nabla_\perp n_1, \tag{2.4.13}$$

$$\frac{1}{c^2}\frac{\partial^2 \phi_1}{\partial t^2} - \frac{\partial^2 \phi}{\partial z^2} - \nabla_\perp^2 \phi_1 = 4\pi\left[q n_b - e n_1\right], \tag{2.4.14}$$

$$\frac{1}{c^2}\frac{\partial^2 A_{1z}}{\partial t^2} - \frac{\partial^2 A_{1z}}{\partial z^2} - \nabla_\perp^2 A_{1z} = \frac{4\pi}{c}\left(q n_b \beta c - e n_0 V_{1z}\right), \tag{2.4.15}$$

$$\frac{1}{c^2}\frac{\partial^2 \mathbf{A}_{1\perp}}{\partial t^2} - \frac{\partial^2 \mathbf{A}_{1\perp}}{\partial z^2} - \nabla_\perp^2 \mathbf{A}_{1\perp} = -\frac{4\pi e n_0}{c}\mathbf{V}_{1\perp}, \tag{2.4.16}$$

where $\omega_c = -eB_0/m_{e0}c$ is the electron cyclotron frequency.

(iv) We perform the coordinate transformation:

$$\xi = z - \beta c t\,, \quad \mathbf{r}'_\perp = \mathbf{r}_\perp\,, \quad \tau = t\,. \tag{2.4.17}$$

Consequently,

$$\partial/\partial z = \partial/\partial\xi\,, \quad \nabla_\perp = \nabla'_\perp\,, \quad \partial/\partial t = -\beta c\partial/\partial\xi \; + \; \partial/\partial\tau\,, \tag{2.4.18}$$

where $\nabla'_\perp$ denotes the transverse gradient with respect to the new transverse co-ordinates.

(v) In addition, we assume the *quasi-static approximation* (see the previous chapter) by imposing that all the quantities are independent of τ, i.e.,

$$\partial/\partial\tau = 0\,. \tag{2.4.19}$$

As we have seen already in section 2.2, this corresponds to a sort of electrostatic approximation on fast time scale.

(vi) Under transformations (2.4.17) - (2.4.19), system of Eqs. (2.4.11)-(2.4.16), after a relatively long but straightforward procedure, can be reduced to the following Poisson-type equation (for simplicity, we have replaced $\nabla'_\perp$ by $\nabla_\perp$):

$$\left\{\left(\frac{\partial^2}{\partial\xi^2}+\frac{k_{uh}^2}{\beta^2}-\alpha_z\frac{\partial^2}{\partial\xi^2}-\alpha_\perp\nabla_\perp^2-\alpha_z\frac{k_c^2}{\beta^2}\right)\left[\frac{1}{\gamma_0^2}\frac{\partial^2}{\partial\xi^2}+\nabla_\perp^2-k_p^2\right]+(1-\beta^2\alpha_z)\frac{k_p^2k_c^2}{\beta^4}\right\}\Omega$$
$$=\frac{k_p^2}{\beta^2}\frac{qm_{e0}c^2}{e^2}\left[\frac{1}{\gamma_0^2}\left(\beta^2\frac{\partial^2}{\partial\xi^2}+k_c^2-\beta^2\alpha_z\frac{\partial^2}{\partial\xi^2}-\beta^2\alpha_\perp\nabla_\perp^2-\alpha_zk_c^2\right)-(1-\alpha_z)\beta^2k_p^2\right]\frac{n_b}{n_0}\,, \tag{2.4.20}$$

where we have observed that $\gamma_0 = 1/\sqrt{1-\beta^2}$ is the unperturbed relativistic energy factor, $\alpha_z = \Gamma_z v_{Tz}/\beta^2c^2$, $\alpha_\perp = \Gamma_\perp v_{T_\perp}/\beta^2c^2$ (v_{Tz} and $v_{T_\perp}$ being longitudinal and transverse thermal velocities, respectively), $k_p = \left(4\pi e^2n_0/m_{e0}c^2\right)^{1/2} \equiv \omega_p/c$ is the electron plasma wavenumber ($\omega_p = \sqrt{4\pi e^2n_0/m_{e0}}$, being the electron plasma frequency), $k_{uh} = \left(k_p^2+k_c^2\right)^{1/2}$ ($k_c \equiv \omega_c/c$ being the electron cyclotron wavenumber). Equation (2.4.20) is of the type (2.2.4) which relates the beam density $n_b(\mathbf{r}_\perp,\xi)$ to the plasma wake potential $\Omega(\mathbf{r}_\perp,\xi)$ for a collisionless, non-relativistic, magnetized, warm plasma with non isotropic temperature. In addition, we have derived this equation by assuming arbitrary conditions of both sharpness and relativistic motion of the driver along the longitudinal direction. It represents a very significant generalization of the Poisson-type equation derived in the original treatment of the PWF excitation [4]. By imposing appropriate boundary and initial conditions, the formal solution of Eq. (2.4.20) gives Ω as the functional of n_b. Then, the explicit form of the latter will give the related solution of the wake potential. Furthermore, given the linearity of the system of Eqs. (2.4.11) - (2.4.16), once Eq. (2.4.20) is solved for Ω, in principle the other physical first-order quantities involved in this system can be easily found in terms of n_b, as well, provided

that appropriate boundary and initial conditions are imposed. Note that, although here $\beta \sim 1$, in order to distinguish between the simple relativistic case with respect to more extreme conditions, such as the ultra-relativistic one, in Eq. (2.4.20) this constant has not yet replaced by 1. At this regard, we may suitably distinguish among three different energy regimes: *non-relativistic regime*, i.e., $\gamma_0 \gtrsim 1$; *relativistic regime*, i.e., $\gamma_0 > 1$; *ultrarelativistic regime*, i.e., $\gamma_0 \gg 1$. Here, we focus only on relativistic and ultrarelativistic drivers. Then, provided that γ_0 can be $\gg 1$ or > 1 only, we can distinguish among different sharpness of the longitudinal driver density profile as well as different sharpness of the transverse driver density profile. By denoting σ_z as the longitudinal effective size of the driver (i.e., rms of the longitudinal density profile), we may distinguish among three diverse longitudinal sharpnesses (note that $|\partial/\partial\xi| \sim 1/\sigma_z$): *ultrashort bunch*, i.e., $k_p\sigma_z \ll 1$; *moderately short bunch*, i.e., $k_p\sigma_z \sim 1$; *long beam*, i.e., $k_p\sigma_z \gg 1$.

Let us specialize Eq. (2.4.20), in some of the above limiting cases prescribed by the combination of energy and longitudinal sharpness regimes. To this end, we note that such a combination should be done with care because of the competition that the physical conditions, fixed by a given energy regime, has with the ones that are fixed by a given sharpness regime. For instance, in the ultrarelativistic case, the product $\gamma_0 k_p\sigma_z$ may give a quantity ~ 1 (which means that $1/\gamma_0|\partial/\partial\xi| \sim k_p$); whilst, in the simple relativistic case, the same product may give a quantity $\ll 1$ or < 1 (which means $(1/\gamma_0)|\partial/\partial\xi| \ll k_p$ or $(1/\gamma_0)|\partial/\partial\xi| < k_p$, respectively). One can repeat analogous arguments for other combinations.

Let us now denote by $\sigma_\perp$ the transverse effective size of the driver (i.e., rms of the transverse density profile). Regarding the transverse sharpness, we may distinguish among three regimes of transverse sharpness (note that $|\nabla_\perp| \sim 1/\sigma_\perp$): *strongly focussed beam*, i.e., $k_p\sigma_\perp \ll 1$; *moderately focussed beam*, i.e., $k_p\sigma_\perp \sim 1$; *wide beam*, i.e., $k_p\sigma_\perp \gg 1$.

2.5 Ultrarelativistic driver in a cold plasma: longitudinal sharpness regimes

We assume that the driver is ultra-relativistic. This means that the condition $\gamma_0 \gg 1$, implies that in Eq. (2.4.20) we can surely replace β with 1. Furthermore, the cold plasma assumption implies that $\alpha_z = \alpha_\perp = 0$. In this framework we consider two cases: strongly magnetized and unmagnetized cases.

2.5.1 Magnetized plasma

The strongly magnetized plasma assumption stands for the condition $k_c \gtrsim k_p$. The latter means that the effect of the external magnetic field, i.e., B_0, in terms of gyromotion has to be at least comparable to the collective plasma motion. Given the present technology to produce magnetic field amplitudes up to tens of tesla, in laboratory we may have at most $k_c \lesssim k_p$. However, in the astrophysical environments, B_0 can assume values such that also the condition $k_c \gg k_p$ can be easily fulfilled.

Ultrashort bunch

According to the arguments presented in the previous sections, the assumptions taken here allow us to reduce Eq. (2.4.20) to the following:

$$\left[\left(\frac{\partial^2}{\partial\xi^2}+k_{uh}^2\right)\left(\frac{1}{\gamma_0^2}\frac{\partial^2}{\partial\xi^2}+\nabla_\perp^2-k_p^2\right)+k_p^2k_c^2\right]\Omega = k_p^2\frac{qm_{e0}c^2}{e^2}\left[\frac{1}{\gamma_0^2}\left(\frac{\partial^2}{\partial\xi^2}+k_c^2\right)-k_p^2\right]\frac{n_b}{n_0}\,, \quad (2.5.1)$$

which is based on the very delicate interplay between the longitudinal strong sharpness and the extreme relativistic energy conditions. They compensate each other, in such a way to ensure that the term $(1/\gamma_0)\,|\partial/\partial\xi|$ is non negligible.

Moderately short bunch

Excluding the extreme astrophysical magnetized plasma conditions, if the driver is simply a moderately short bunch, Eq. (2.4.20) reduces to:

$$\left[\left(\frac{\partial^2}{\partial\xi^2}+k_{uh}^2\right)\left(\nabla_\perp^2-k_p^2\right)+k_p^2k_c^2\right]\Omega = -k_p^4\frac{qm_{e0}c^2}{e^2}\frac{n_b}{n_0}\,, \quad (2.5.2)$$

where the sharpness no longer compensates the effect of the extreme energy conditions. Equation (2.5.2) has been derived for the first time in Ref. [56].

Long beam

When the beam length is long enough to fulfill the condition $k_p\sigma_z \gg 1$, then the second-order derivative with respect to ξ in Eq. (2.5.2) can be neglected and, it simplifies as:

$$\left[\left(\nabla_\perp^2 - k_p^2\right) + \frac{k_p^2 k_c^2}{k_{uh}^2}\right]\Omega = -\frac{k_p^4}{k_{uh}^2}\frac{qm_{e0}c^2}{e^2}\frac{n_b}{n_0}\,, \tag{2.5.3}$$

which has been used in [56] to investigate the PWF excitation in quantum regime. Note that now the longitudinal coordinate ξ appears only as parameter in Eq. (2.5.3). As we will see better later, it can be used as one of the governing equation of the purely transverse dynamics of a paraxial nonlaminar beam, provided that ξ plays the role of a timelike variable.

2.5.2 Unmagnetized plasma

If the ambient magnetic field is absent or its effects can be considered negligible, in Eq. (2.4.20) we can impose the condition $B_0 = 0$ which corresponds to put $k_c = 0$. Then, the various cases of longitudinal sharpness are straightforwardly obtaine as follows.

Ultrashort bunch

According to the arguments presented in the previous sections, the assumptions taken here allow us to reduce Eq. (2.5.1) to the following:

$$\left(\frac{\partial^2}{\partial\xi^2} + k_p^2\right)\left(\frac{1}{\gamma_0^2}\frac{\partial^2}{\partial\xi^2} + \nabla_\perp^2 - k_p^2\right)\Omega = k_p^2\frac{qm_{e0}c^2}{e^2}\left[\frac{1}{\gamma_0^2}\frac{\partial^2}{\partial\xi^2} - k_p^2\right]\frac{n_b}{n_0}\,. \tag{2.5.4}$$

Also Eq. (2.5.4) is based on the very delicate interplay between the longitudinal strong sharpness and the extreme relativistic energy conditions, in such a way they compensate each other to ensure that the term $(1/\gamma_0)\,|\partial/\partial\xi|$ is non negligible. Note that Eq. (2.5.4) has been derived in a recent work where it was used to investigate the formation and stability of a hollow electron beam in the presence of a PWF excitation driven by an ultra-short electron bunch in a unmagnetized cold plasma [57].

Moderately short bunch

Once the condition, $k_c = 0$, is imposed, Eq. (2.5.2) reduces to:

$$\left(\frac{\partial^2}{\partial\xi^2} + k_p^2\right)\left(\nabla_\perp^2 - k_p^2\right)\Omega = -k_p^4 \frac{q m_{e0} c^2}{e^2}\frac{n_b}{n_0}\,, \tag{2.5.5}$$

which is equivalent, in case of electrons/positron beams, to the set of equations that has been derived for the first time in Ref. [4].

Long beam

By substituting $k_c = 0$ in Eq. (2.5.2), we obtain:

$$\left(\nabla_\perp^2 - k_p^2\right)\Omega = -k_p^2 \frac{q m_{e0} c^2}{e^2}\frac{n_b}{n_0}\,, \tag{2.5.6}$$

which has been recently used to investigate the self-modulated transverse dynamics in both classical [58–60] and quantum-like [61, 62] domains. Note that, as in the magnetized case, also here the longitudinal coordinate ξ appears only as parameter.

2.6 Ultrarelativistic driver in a cold plasma: transverse sharpness regimes

Similarly to the previous section, we specialize Eq. (2.4.20) for the diverse cases of transverse sharpness that can be obtained in combination with the ultrarelativistic regime of a driver travelling in a cold plasma ($\alpha_z = \alpha_\perp = 0$). Also here we consider the two cases of a strongly magnetized and unmagnetized plasma, respectively.

2.6.1 Magnetized plasma

Strongly focussed beam

According to the classification presented in the previous section, the strongly focussed beam assumption corresponds to the condition $k_p\sigma_\perp \ll 1$. Therefore, by imposing it in Eq. (2.4.20)

we easily obtain:

$$\left[\left(\frac{\partial^2}{\partial\xi^2}+k_{uh}^2\right)\left(\frac{1}{\gamma_0^2}\frac{\partial^2}{\partial\xi^2}+\nabla_\perp^2\right)+k_p^2\,k_c^2\right]\Omega=k_p^2\frac{qm_{e0}c^2}{e^2}\left[\frac{1}{\gamma_0^2}\left(\frac{\partial^2}{\partial\xi^2}+k_c^2\right)-k_p^2\right]\frac{n_b}{n_0}\,. \tag{2.6.1}$$

Here, the derivatives with respect to ξ are not affected by any approximation, because the longitudinal sharpness is considered to be arbitrary (therefore to be specified for each specific case).

Moderately focussed beam

In this case, since $k_p\sigma_\perp \sim 1$, it is obvious that in Eq. (2.4.20) we have just to put: $\alpha_z = \alpha_\perp = 0$, and no comparison between transverse and longitudinal sharpness is assumed in special cases. Then, the corresponding expression coincides with Eq. (2.5.1).

Wide beam

When the beam is wide enough to fulfill the condition $k_p\sigma_\perp \gg 1$, then Eq. (2.4.20) can be reduced as the following:

$$\left[\left(\frac{\partial^2}{\partial\xi^2}+k_{uh}^2\right)\left(\frac{1}{\gamma_0^2}\frac{\partial^2}{\partial\xi^2}-k_p^2\right)+k_p^2k_c^2\right]\Omega=k_p^2\frac{qm_{e0}c^2}{e^2}\left[\frac{1}{\gamma_0^2}\left(\frac{\partial^2}{\partial\xi^2}+k_c^2\right)-k_p^2\right]\frac{n_b}{n_0}\,. \tag{2.6.2}$$

2.6.2 Unmagnetized plasma

If the ambient magnetic field is absent or its effects can be considered negligible, in Eq. (2.4.20) we put $k_c = 0$. Then, the various cases of longitudinal sharpness are straightforwardly obtained as follows.

Strongly focussed beam

When the condition $k_c = 0$ is replaced in Eq. (2.6.1), we easily obtain the following Poisson-type equation:

$$\left(\frac{\partial^2}{\partial\xi^2}+k_p^2\right)\left(\frac{1}{\gamma_0^2}\frac{\partial^2}{\partial\xi^2}+\nabla_\perp^2\right)\Omega=k_p^2\frac{qm_{e0}c^2}{e^2}\left(\frac{1}{\gamma_0^2}\frac{\partial^2}{\partial\xi^2}-k_p^2\right)\frac{n_b}{n_0}\,. \tag{2.6.3}$$

Moderately focussed beam

Once the condition $k_c = 0$ is imposed, Eq. (2.5.1) reduces to:

$$\left(\frac{\partial^2}{\partial\xi^2} + k_p^2\right)\left(\frac{1}{\gamma_0^2}\frac{\partial^2}{\partial\xi^2} + \nabla_\perp^2 - k_p^2\right)\Omega = k_p^2\frac{qm_{e0}c^2}{e^2}\left(\frac{1}{\gamma_0^2}\frac{\partial^2}{\partial\xi^2} - k_p^2\right)\frac{n_b}{n_0}\,, \tag{2.6.4}$$

which is equivalent, in case of electrons/positron beams, to the set of equations that has been derived for the first time in Ref. [4].

Wide beam

By substituting $\nabla_\perp = 0$ in Eq. (2.5.4), we obtain:

$$\left(\frac{\partial^2}{\partial\xi^2} + k_p^2\right)\left(\frac{1}{\gamma_0^2}\frac{\partial^2}{\partial\xi^2} - k_p^2\right)\Omega = k_p^2\frac{qm_{e0}c^2}{e^2}\left(\frac{1}{\gamma_0^2}\frac{\partial^2}{\partial\xi^2} - k_p^2\right)\frac{n_b}{n_0}\,. \tag{2.6.5}$$

2.7 Poisson-type equation for purely longitudinal case

We can also confine our attention on 1D case of purely longitudinal beam profile. In this case, in Eq. (2.4.20), all the transverse derivative should be suppressed while retaining the longitudinal ones.

2.7.1 Magnetized plasma

Warm plasma

By putting $\alpha_\perp = 0$ and $\nabla_\perp = 0$, we easily get:

$$\begin{aligned}&\left[\left(\frac{\partial^2}{\partial\xi^2} + k_{uh}^2 - \alpha_z\frac{\partial^2}{\partial\xi^2} - \alpha_z k_c^2\right)\left(\frac{1}{\gamma_0^2}\frac{\partial^2}{\partial\xi^2} - k_p^2\right) + (1-\alpha_z)k_p^2k_c^2\right]\Omega\\ &= k_p^2\frac{qm_{e0}c^2}{e^2}\left[\frac{1}{\gamma_0^2}\left(\frac{\partial^2}{\partial\xi^2} + k_c^2 - \alpha_z\frac{\partial^2}{\partial\xi^2} - \alpha_z k_c^2\right) - (1-\alpha_z)k_p^2\right]\frac{n_b}{n_0}\,.\end{aligned} \tag{2.7.1}$$

Cold plasma

If in addition we put $\alpha_z = 0$, we have the Poisson-type equation for the case of cold plasma,

$$\left[\left(\frac{\partial^2}{\partial\xi^2} + k_{uh}^2\right)\left(\frac{1}{\gamma_0^2}\frac{\partial^2}{\partial\xi^2} - k_p^2\right) + k_p^2k_c^2\right]\Omega = k_p^2\frac{qm_{e0}c^2}{e^2}\left[\frac{1}{\gamma_0^2}\left(\frac{\partial^2}{\partial\xi^2} + k_c^2\right) - k_p^2\right]\frac{n_b}{n_0}\,. \tag{2.7.2}$$

2.7.2 Unmagnetized plasma

Warm plasma

By putting $\alpha_\perp = \nabla_\perp = k_c = 0$, we easily get:

$$\left(\frac{\partial^2}{\partial\xi^2} + k_p^2 - \alpha_z\frac{\partial^2}{\partial\xi^2}\right)\left(\frac{1}{\gamma_0^2}\frac{\partial^2}{\partial\xi^2} - k_p^2\right)\Omega = \frac{k_p^2\, qm_{e0}c^2}{e^2}\left[\frac{1}{\gamma_0^2}\left(\frac{\partial^2}{\partial\xi^2} - \alpha_z\frac{\partial^2}{\partial\xi^2}\right) - (1-\alpha_z)k_p^2\right]\frac{n_b}{n_0}\,. \tag{2.7.3}$$

Cold plasma

If in addition we put $\alpha_z = 0$, we have the Poisson-type equation for the case of cold plasma,

$$\left(\frac{\partial^2}{\partial\xi^2} + k_p^2\right)\left(\frac{1}{\gamma_0^2}\frac{\partial^2}{\partial\xi^2} - k_p^2\right)\Omega = k_p^2\frac{qm_{e0}c^2}{e^2}\left[\frac{1}{\gamma_0^2}\frac{\partial^2}{\partial\xi^2} - k_p^2\right]\frac{n_b}{n_0}\,. \tag{2.7.4}$$

If $1/\gamma_0\partial/\partial\xi \ll k_p$, then above equation becomes

$$\left(\frac{\partial^2}{\partial\xi^2} + k_p^2\right)\Omega = k_p^2\frac{qm_{e0}c^2}{e^2}\frac{n_b}{n_0}\,. \tag{2.7.5}$$

2.8 Poisson-type equation for purely transverse case

Now we confine our attention on 2D case of purely transverse beam profile. In Eq. (2.4.20) all the longitudinal derivative should be suppressed while retaining the transverse ones.

2.8.1 Magnetized plasma

Warm plasma

By putting $\alpha_z = 0 = \partial/\partial\xi = 0$, we easily get:

$$\left[\left(k_{uh}^2 - \alpha_\perp\nabla_\perp^2\right)\left(\nabla_\perp^2 - k_p^2\right) + k_p^2k_c^2\right]\Omega = k_p^2\frac{qm_{e0}c^2}{e^2}\left[\frac{1}{\gamma_0^2}\left(k_c^2 - \alpha_\perp\nabla_\perp^2\right) - k_p^2\right]\frac{n_b}{n_0}\,. \tag{2.8.1}$$

Cold plasma

If in addition we put $\alpha_\perp = 0$, we have the Poisson-type equation for the case of cold plasma,

$$\left[\left(\nabla_\perp^2 - k_p^2\right) + \frac{k_p^2k_c^2}{k_{uh}^2}\right]\Omega = \frac{k_p^2}{k_{uh}^2}\frac{qm_{e0}c^2}{e^2}\left(\frac{k_c^2}{\gamma_0^2} - k_p^2\right)\frac{n_b}{n_0}\,. \tag{2.8.2}$$

2.8.2 Unmagnetized plasma

Warm plasma

By putting $\alpha_z = \partial/\partial\xi = k_c = 0$, we easily find:

$$\left(k_p^2 - \alpha_\perp \nabla_\perp^2\right)\left(\nabla_\perp^2 - k_p^2\right)\Omega = -k_p^2 \frac{q m_{e0} c^2}{e^2}\left(\frac{1}{\gamma_0^2}\alpha_\perp \nabla_\perp^2 + k_p^2\right)\frac{n_b}{n_0}\,. \tag{2.8.3}$$

Cold plasma

If in addition we put $\alpha_\perp = 0$, we have the Poisson-type equation for the case of cold plasma,

$$\left(\nabla_\perp^2 - k_p^2\right)\Omega = -k_p^2 \frac{q m_{e0} c^2}{e^2}\frac{n_b}{n_0}\,. \tag{2.8.4}$$

2.9 Conclusions

We have presented the general theory of plasma wake field excitation in a magnetoactive, nonrelativistic, warm, overdense, and collisionless plasma. This has been accomplished by using the set of 3D fluid equations, comprising continuity and the motion equations, that are coupled with the Maxwell equations (i.e., Lorentz-Maxwell system) in the adiabatic approximation (see Chapter 1), in the presence of an ultra-relativistic driving beam. We have first put forward the simple concept of plasma wake field and plasma wake potential by starting from the expression of the Lorentz force experienced by a test particle, in its co-moving frame, in the presence of the self-consistent EM field provided by the 'beam-plasma' system. In the quasi-static approximation, we have reduced the above Lorentz-Maxwell system to a novel 3D partial differential equation, called here the *generalized Poisson-type equation*. It relates the beam density to the wake potential and extends the PWF theory to the case of warm plasmas. Additionally, it accounts for the presence of an ambient magnetic field, the longitudinal and transverse plasma pressure terms, and the generalized conditions of beam energy and sharpness of the beam profile. We have finally specialized this novel equation to several limiting cases in order to recover the particular equations that have been used in the literature.

Chapter 3

Models for charged particle beams and its self-consistent interaction with the surrounding medium

We formulate the kinetic description of an relativistic driving beam while self-consistently interacting with the plasma wake field excited in a warm, magnetized, collisionless plasma in overdense regime. The driver is supposed to be in the arbitrary conditions of sharpness of its density profile. Such a general formulation is provided by starting from the relativistic single-particle 3D Hamiltonian in the presence of an ambient magnetic field. In the reference frame of the unperturbed particle, we express the Hamiltonian of the perturbed particle in terms of a slight variation from the one of the unperturbed particle that is associated with the relativistic unperturbed beam state. After expanding the four potential to the first-order and performing the non-relativistic expansion with respect to the unperturbed state, we get the effective single-particle Hamiltonian. The latter is used to construct the 3D Vlasov equation for the beam motion in the reference frame of the unperturbed particle. This way, by coupling the Vlasov equation with the generalized Poisson-type equation obtained in Chapter 2, we provide the self-consistent 3D kinetic description to be used in the next chapters to study the self-modulated dynamics of the driver while interacting with the surrounding plasma.

3.1 Preliminary considerations

In this chapter, according to the *Introduction*, we refer to the concept of beam as a paraxial and nonlaminar system of many charged particles, whose dynamics is affected by the interaction with the surrounding plasma. Such an interaction typically involves the *self-consistent fields* as well as any eventual *external field* that has been generated by sources that are *external* to the beam-plasma system. The self-consistent fields are involved in the PWF excitation, as described in Chapter 2. They are generated by all the sources that are *internal* to the beam-plasma system, such as the beam charge and current distributions and the plasma charge and current distributions, respectively. In general, the internal sources are dynamically involved in the Lorentz-Maxwell system of equations, as extensively described in Chapter 2. The approach used has, in particular, shown how to reduce such a system of equation to the appropriate Poisson-type equation. This has been accomplished for a number of physical examples. However, only the Poisson-type equation fixes a functional relation between the beam number density and plasma wake potential Ω. In other words, by referring to Chapter 2, for any beam number density n_b, we can solve the Poisson-type equation for Ω. Therefore, the knowledge of Ω allows us to determine the wake fields. The latter, in turn, affect the behaviour of the beam and, consequently, its particle distribution (i.e., n_b). We conclude that, according to the self-consistency of the beam-plasma interaction, an equation that governs the reaction of the wake fields on the beam itself, to be coupled with the Poisson-type equation, is necessary. Such an equation, which hereafter we call the *beam motion equation*, would account for the instantaneous forces exserted by the plasma wake fields (PWFs) on the beam particles.

In the next sections, we will find the appropriate motion equations of the problem we want to discuss. To this end, we will proceed according to the following scheme.

- We start from the Hamiltonian for a relativistic single-particle that is moving under the action of the EM fields (self-consistent plus external fields) and define the unperturbed state as the one in the absence of the self-consistent fields.

- We split the vector quantities in longitudinal (parallel to the beam propagation direction) and radial (perpendicular to the beam propagation direction) components.
- We perturb the physical quantities around the unperturbed state.
- We finally find the effective Hamiltonian associated with the single-particle motion in the beam co-moving frame.

3.2 Relativistic Hamiltonian for a single-particle motion in the presence of EM fields

Let us consider a relativistic charged particle of charge q and rest mass m_{b0}, moving with an arbitrary velocity $\mathbf{v}$ in the presence of an EM field, i.e., $\mathbf{E} = \mathbf{E}(\mathbf{r}, t)$, $\mathbf{B} = \mathbf{B}(\mathbf{r}, t)$. It is well known that the Hamiltonian for such a motion is given by [63]:

$$H(\mathbf{r}, \mathbf{P}, t) = c\left[\left(\mathbf{P} - \frac{q}{c}\mathbf{A}\right)^2 + m_{b0}^2 c^2\right]^{1/2} + q\phi\,, \tag{3.2.1}$$

where $\mathbf{A} = \mathbf{A}(\mathbf{r}, t)$ and $\phi = \phi(\mathbf{r}, t)$ are vector and scalar potential, respectively, that are associated with the fields $\mathbf{E}(\mathbf{r}, t)$ and $\mathbf{B}(\mathbf{r}, t)$ by means of the relations (2.1.3) and (2.1.4), respectively. In Eq. (3.2.1), $\mathbf{P}$ is the canonical momentum which is related to the particle kinetic linear momentum, $\mathbf{p} = m_{b0}\gamma\mathbf{v}$, by:

$$\mathbf{P} = m_{b0}\gamma\mathbf{v} + \frac{q}{c}\mathbf{A}\,, \tag{3.2.2}$$

where $\gamma = \left(1 - v^2/c^2\right)^{-1/2}$ is the relativistic gamma factor.

In the absence of the fields, i.e., $\mathbf{E} = \mathbf{B} = 0$, we can define the unperturbed state of the particle, i.e., $\mathbf{v} = \mathbf{v}_0 \equiv \beta c\hat{z}$ ($\beta \sim 1$) and $\gamma = \gamma_0 \equiv (1 - \beta^2)^{-1/2}$, in which the particle trajectory is a straight line that we have assumed to be the $z-$ axis.

Note that the state of the particle remains unperturbed also if we consider the presence of an uniform and constant magnetic field $\mathbf{B}_0 = B_0\hat{z}$, oriented along the $z-$ axis. In fact, since the particle velocity in this state, i.e., $\mathbf{v} = \mathbf{v}_0$, is constant of motion and has the longitudinal component only, the particle does not interact with $\mathbf{B}_0$ and therefore, does not assume a

transverse component during the time. Therefore, it is easy to see that the Hamiltonian associated with such an unperturbed state is:

$$H_0 = m_{b0}\gamma_0 c^2 \,. \tag{3.2.3}$$

3.2.1 Slightly perturbed motion

If we now consider a paraxial relativistic charged-particle travelling along the $z-$ axis in the presence of the same uniform and constant magnetic field $\mathbf{B}_0$, we can state that each beam particle has an instantaneous velocity that can be cast in the following form:

$$\mathbf{v} = \beta c\hat{z} + \mathbf{u} \,, \tag{3.2.4}$$

where $\mathbf{u}$ represents slight displacement of $\mathbf{v}$ from the unperturbed state $\mathbf{v}_0 = \beta c\hat{z}$, i.e.,

$$u \ll c \,, \tag{3.2.5}$$

with an arbitrary instantaneous orientation. Therefore, taking into account all the possible slight displacements that are possible in a paraxial beam, the unperturbed state particle plays the role of an ideal condition of the beam particle. Note that the perturbed state requires the presence of an EM field, whose strengths have to be compatible with Eq. (3.2.4) and condition (3.2.5). Note also that the quantity $\mathbf{u}$ has in general longitudinal and transverse components, i.e.,

$$\mathbf{u} = u_z\hat{z} + \mathbf{u}_\perp \,. \tag{3.2.6}$$

3.2.2 Perturbed effective single particle Hamiltonian

We perturb all the physical quantities of our interest around the state of the unperturbed particle, i.e.,

$$\gamma = \gamma_0 + \gamma_1 \,, \tag{3.2.7}$$

$$\mathbf{P} = \mathbf{P}_0 + \mathscr{P} = m_{b0}\gamma_0\beta c\,\hat{z} + \mathscr{P}_z\hat{z} + \mathscr{P}_\perp \,, \tag{3.2.8}$$

$$\mathbf{A} = A_{1_z}\hat{z} + \mathbf{A}_{0\perp} + \mathbf{A}_{1_\perp} \,, \tag{3.2.9}$$

$$\phi = \phi_1 \,, \tag{3.2.10}$$

where we have also split the vector quantities into longitudinal and transverse components. Note that the term $\mathbf{A}_{0\perp}$ accounts for the presence of the magnetic field $\mathbf{B}_0$ [63], i.e.,

$$\mathbf{A}_{0\perp} = -\frac{1}{2}\mathbf{r}_\perp \times \mathbf{B}_0 \,, \tag{3.2.11}$$

where $\mathbf{r}_\perp$ is the transverse component of the position vector $\mathbf{r}$, i.e.,

$$\mathbf{r} = z\hat{z} + \mathbf{r}_\perp \,. \tag{3.2.12}$$

We replace Eq. (3.2.2) in Eq. (3.2.1), obtaining:

$$H = m_{b0}c^2\left[1 + \gamma^2\frac{v^2}{c^2}\right] + q\phi \,. \tag{3.2.13}$$

Then, we perturb Eq. (3.2.2) according to Eqs. (3.2.4) - (3.2.6) and (3.2.7) - (3.2.10) and separate the orders and longitudinal from transverse components. In addition, we perturb also Eq. (3.2.13) according to Eqs. (3.2.4) - (3.2.6) and (3.2.7) - (3.2.10); then, we perform the non-relativistic expansion. By combining the results of the two expansions, we easily get the following effective Hamiltonian:

$$\begin{aligned}\mathcal{H}\left(\mathbf{r}_\perp, z, \mathcal{P}_\perp, \mathcal{P}_z, s\right) = \frac{1}{2}{\mathcal{P}_z}^2 + \beta\mathcal{P}_z + \frac{1}{2}{\mathcal{P}_\perp}^2 + \frac{1}{2}k_c\,\hat{z}\cdot\left(\mathbf{r}_\perp\times\mathcal{P}_\perp\right) \\ + \frac{1}{2}Kr_\perp^2 - \frac{q}{m_{b0}\gamma_0 c^2}\left[\beta A_{1z}\left(\mathbf{r}_\perp, z, s\right) - \phi_1\left(\mathbf{r}_\perp, z, s\right)\right] \,,\end{aligned} \tag{3.2.14}$$

where we have introduced the time-like variable $s = ct$, $\mathcal{H} = (H - H_0)/H_0$, $\mathcal{P}_z = \mathscr{P}_z/m_{b0}\gamma_0 c$, $\mathcal{P}_\perp = \mathscr{P}_\perp/m_{b0}\gamma_0 c$, $k_c = -qB_0/m_{b0}\gamma_0 c^2$, and $K = \left(qB_0/2m_{b0}\gamma_0 c^2\right)^2 = (k_c/2)^2$. This is the Hamiltonian of a generic single-particle of the beam whose motion slightly deviates from the one of the unperturbed particle. The last term, i.e., $-\left(q/m_{b0}\gamma_0 c^2\right)(\beta A_{1z} - \phi_1)$, corresponds to an effective self-consistent potential term, whose gradient gives the self-consistent EM fields that the beam itself has created via the interaction with the plasma. Furthermore, the term $(1/2)\,k_c\,\hat{z}\cdot(\mathbf{r}_\perp\times\mathcal{P}_\perp)$ accounts for the longitudinal component of the single-particle angular momentum related to the beam particle gyro-motion around the ambient magnetic field $\mathbf{B}_0$, whereas the term $(1/2)\,Kr_\perp^2$ comes from $A_{0\perp}^2$ and, since $K > 0$, represents the potential well, whose gradient gives the focusing transverse force that is experienced by the perturbed

single-particle in the presence of $\mathbf{B}_0$.

Let us now consider the coordinate transformation; $\xi = z - \beta' s$, $\mathcal{R}_\perp = \mathbf{r}_\perp$, $\tau = s$, $\mathcal{P}_z' = \mathcal{P}_z + \alpha$, and $\mathcal{P}_\perp' = \mathcal{P}_\perp$, where α is an arbitrary real constant. Its inverse is; $z = \xi + \beta'\tau$, $\mathbf{r}_\perp = \mathcal{R}_\perp$, $s = \tau$, $\mathcal{P}_z = \mathcal{P}_z' - \alpha$, and $\mathcal{P}_\perp = \mathcal{P}_\perp'$. In addition, we write the Hamilton equations associated with Hamiltonian 3.2.14, i.e.,

$$\frac{dz}{ds} = \frac{\partial \mathcal{H}}{\partial \mathcal{P}_z} = \mathcal{P}_z + \beta, , \tag{3.2.15}$$

$$\frac{d\mathcal{P}_z}{ds} = -\frac{\partial \mathcal{H}}{\partial z} = \frac{\partial}{\partial z}\left\{\frac{q}{m_{b0}\gamma_0 c^2}\left[\beta A_{1z}(\mathbf{r}_\perp, z, s) + \phi_1(\mathbf{r}_\perp, z, s)\right]\right\} . \tag{3.2.16}$$

Then, by using above mentioned transformations, Eqs. (3.2.15) and (3.2.16) can be easily reduced to

$$\frac{d\xi}{d\tau} = \mathcal{P}_z' + \left(\beta - \beta'\right) - \alpha \equiv \frac{\partial \mathscr{H}}{\partial \mathcal{P}_z'} , \tag{3.2.17}$$

$$\frac{d\mathcal{P}_z'}{d\tau} = \frac{\partial}{\partial \xi}\left[\frac{q}{m_{b0}\gamma_0 c^2}\left(\beta A_{1z}' - \phi_1'\right)\right] \equiv -\frac{\partial \mathscr{H}}{\partial \xi} , \tag{3.2.18}$$

where $A_{1z}' = A_{1z}'(\mathcal{R}_\perp, \xi, \tau)$, $\phi_1' = \phi_1'(\mathcal{R}_\perp, \xi, \tau)$ and $\mathscr{H} = \mathscr{H}\left(\mathcal{R}_\perp, \xi, \mathcal{P}_\perp', \mathcal{P}_z', \tau\right)$ stand for the image of $A_{1z}(\mathbf{r}_\perp, z, s)$, $\phi_1(\mathbf{r}_\perp, z, s)$ and $\mathcal{H}$, respectively, under the transformations.

If we now require that the above transformation leads to $d\xi/d\tau = \mathcal{P}_z'$, we get that $\alpha = \beta - \beta'$. Consequently, Eq. (3.2.17) becomes:

$$\frac{d\xi}{d\tau} = \mathcal{P}_z' \equiv \frac{\partial \mathscr{H}}{\partial \mathcal{P}_z'} . \tag{3.2.19}$$

If, in addition, we impose the rigidity condition, i.e., $\beta' = \beta$, which means that our reference frame corresponds to the one where the unperturbed particle is at rest, the fourth of transformations becomes simply

$$\mathcal{P}_z' = \mathcal{P}_z , \tag{3.2.20}$$

and the effective potential $\Omega(\mathcal{R}_\perp, \xi, \tau) = \left[\beta A_{1z}'(\mathcal{R}_\perp, \xi, \tau) - \phi_1'(\mathcal{R}_\perp, \xi, \tau)\right]$ becomes the plasma wake potential that has been introduced in Chapter 2. Furthermore, Eqs. (3.2.20), (3.2.19) and (3.2.18) allow us finally to get easily the transformed Hamiltonian, viz.,

$$\mathscr{H}(\mathcal{R}_\perp, \xi, \mathcal{P}_\perp, \mathcal{P}_z, \tau) = \frac{1}{2}{\mathcal{P}_z}^2 + \frac{1}{2}{\mathcal{P}_\perp}^2 + \frac{1}{2}k_c\,\hat{z}\cdot(\mathcal{R}_\perp \times \mathcal{P}_\perp) + \frac{1}{2}K\mathcal{R}_\perp^2 + U_w(\mathcal{R}_\perp, \xi, \tau) , \tag{3.2.21}$$

where we have introduced the dimensionless plasma wake potential energy:

$$U_w(\mathcal{R}_\perp, \xi, \tau) = -\frac{q\,\Omega(\mathcal{R}_\perp, \xi, \tau)}{m_{b0}\gamma_0 c^2}\,. \tag{3.2.22}$$

3.3 The Vlasov equation for a relativistic charged-particle beam

In this section, we find the kinetic equation that describes the phase space evolution of the perturbed charged particles, whose Hamiltonian is given by Eq. (3.2.21), that belong to a relativistic paraxial beam. To this end, we first of all introduce the six-dimensional μ-space, i.e., $(\mathcal{R}_\perp, \xi, \mathcal{P}_\perp, \mathcal{P}_z)$. Then, we denote by $f = f(\mathcal{R}_\perp, \xi, \mathcal{P}_\perp, \mathcal{P}_z, \tau)$ the single-particle distribution function in such a phase space. According to Chapter 1, the kinetic equation is given by the total derivative of f, viz.,

$$\frac{\partial f}{\partial \tau} + \frac{d\xi}{d\tau}\frac{\partial f}{\partial \xi} + \frac{d\mathcal{R}_\perp}{d\tau}\cdot\frac{\partial f}{\partial \mathcal{R}_\perp} + \frac{d\mathcal{P}_z}{d\tau}\frac{\partial f}{\partial \mathcal{P}_z} + \frac{\partial \mathcal{P}_\perp}{\partial \tau}\cdot\frac{\partial f}{\partial \mathcal{P}_\perp} = 0\,. \tag{3.3.1}$$

By substituting Eq. (3.2.21) in Eq. (3.3.1), we easily get the following Vlasov equation:

$$\frac{\partial f}{\partial \tau} + \mathcal{P}_z\frac{\partial f}{\partial \xi} + \left[\mathcal{P}_\perp + \frac{1}{2}k_c\,(\hat{z}\times\mathcal{R}_\perp)\right]\cdot\frac{\partial f}{\partial \mathcal{R}_\perp} - \frac{\partial U_w}{\partial \xi}\frac{\partial f}{\partial \mathcal{P}_z} - \left[K\mathcal{R}_\perp - \frac{1}{2}k_c\,(\hat{z}\times\mathcal{P}_\perp) + \frac{\partial U_w}{\partial \mathcal{R}_\perp}\right]\cdot\frac{\partial f}{\partial \mathcal{P}_\perp} = 0\,, \tag{3.3.2}$$

which describes the collective behavior of the charged-particle beam while interacting with the plasma via the plasma wake potential and in the presence of an ambient magnetic field. It is worthy noting that, if N is the total number of particles in the beam, $-m_{b0}\gamma_0 c^2\,\hat{z}\partial U_w(\mathcal{R}_\perp, \xi, \tau)/\partial\xi$ and $-m_{b0}\gamma_0 c^2\,\partial U_w(\mathcal{R}_\perp, \xi, \tau)/\partial\mathcal{R}_\perp$ are the effective longitudinal and transverse components, respectively, of the force on the single particle at the Eulerian position $(\mathcal{R}_\perp, \xi, \tau)$ that have been generated by the other $N-1$ particles of the beam (mean field approximation).

3.4 The Vlasov-Poisson-type system of equations

From the previous section, it is clear that the gradient of U_w accounts for the self-consistent collective interaction, via the plasma, among the beam particles (beam self-interaction), in

the mean field approximation. However, to describe in a self-consistent way the beam-plasma evolution we need to couple the Vlasov Eq. (3.3.1) for f with the Poisson-type Eq. (2.4.20) for Ω (or U_w). To this end, we first simplify the notations in Eq. (3.3.1), just by performing the following substitutions:

$$\mathcal{R}_\perp \to \mathbf{r}_\perp\,,\ \mathcal{P}_\perp \to \mathbf{p}_\perp\,,\ \mathcal{P}_z \to p_z\,,\ \ \mathscr{H}\,(\mathcal{R}_\perp,\xi,\mathcal{P}_\perp,\mathcal{P}_z,\tau) \to H\,(\mathbf{r}_\perp,\xi,\mathbf{p}_\perp,p_z,\tau)\ . \tag{3.4.1}$$

Then, the self-consistent Vlasov-Poisson-type system of equations reads as follows:

$$\frac{\partial f}{\partial \tau} + p_z\,\frac{\partial f}{\partial \xi} + \left[\mathbf{p}_\perp + \frac{1}{2}k_c\,(\hat{z}\times\mathbf{r}_\perp)\right]\cdot\nabla_\perp f - \frac{\partial U_w}{\partial \xi}\,\frac{\partial f}{\partial p_z} - \left[Kr_\perp - \frac{1}{2}k_c\,(\hat{z}\times\mathbf{p}_\perp) + \nabla_\perp U_w\right]\cdot\nabla_{p_\perp} f = 0\,, \tag{3.4.2}$$

and

$$\left[\left(\frac{\partial^2}{\partial\xi^2} + \frac{k_{uh}^2}{\beta^2} - \alpha_z\frac{\partial^2}{\partial\xi^2} - \alpha_\perp\nabla_\perp^2 - \alpha_z\frac{k_c^2}{\beta^2}\right)\left(\frac{1}{\gamma_0^2}\frac{\partial^2}{\partial\xi^2} + \nabla_\perp^2 - k_p^2\right) + (1-\beta^2\alpha_z)\,\frac{k_p^2k_c^2}{\beta^4}\right]U_w =$$
$$-\left(\frac{q}{e}\right)^2\frac{m_{e0}}{m_{b0}}\frac{k_p^2}{\gamma_0\beta^2}\left[\frac{1}{\gamma_0^2}\left(\beta^2\frac{\partial^2}{\partial\xi^2} + k_c^2 - \beta^2\alpha_z\frac{\partial^2}{\partial\xi^2} - \beta^2\alpha_\perp\nabla_\perp^2 - \alpha_z k_c^2\right) - (1-\alpha_z)\beta^2k_p^2\right]\frac{n_b}{n_0}, \tag{3.4.3}$$

with the closure condition, i.e.,

$$n_b\,(\mathbf{r}_\perp,\xi,\tau) = \int f\,(\mathbf{r}_\perp,\xi,\mathbf{p}_\perp,p_z,\tau)\ d^2p_\perp\,dp_z\,. \tag{3.4.4}$$

Equation (3.4.4) defines the local beam number density as the projection (marginalization) of the beam distribution function to the configuration space, i.e., $(\mathbf{r}_\perp,\xi)$. Note that, in the above equations, $\nabla_\perp$ stands for the transverse component of the gradient in configuration space, i.e., $\nabla_\perp = \partial/\partial\mathbf{r}_\perp$, whereas $\nabla_{p_\perp}$ stands for the transverse component of the gradient in momentum space, i.e., $\nabla_{p_\perp} = \partial/\partial\mathbf{p}_\perp$.

In the next Chapters, we use the system (3.4.2) - (3.4.4) for several different cases concerning the self-modulated beam dynamics in a plasma.

3.5 Conclusions

The kinetic description of an ultra-relativistic driving beam travelling through a warm, magnetized, collisionless plasma in overdense regime has been presented. The driver has been

supposed to be in the arbitrary conditions of sharpness of its density profile while interacting with the surrounding plasma. We first started from the 3D Hamiltonian of a test particle that is experiencing the forces produced by the plasma wake fields. Then, we have expanded the Hamiltonian of the perturbed particle with respect to the one of the unperturbed particle that is associated with the unperturbed relativistic beam state. This has been accomplished by expanding the four potential to the first-order as well as by performing the non-relativistic expansion of the perturbed Hamiltonian with respect to the unperturbed state. We have, in this way, found the effective single-particle Hamiltonian that has been used to construct the Vlasov equation for the driver. The latter has been coupled with the generalized Poisson-type equation that we have found in Chapter 2. The pair of Vlasov-Poisson-type equations constitute the set of governing equation to provide the kinetic description of the self-consistent collective dynamics of the driving beam while interacting with the surrounding plasma. In the next chapters, it will be used to analyse the self-modulated dynamics of the driving beam.

Chapter 4

Transverse self-modulated beam dynamics of a nonlaminar, ultra-relativistic beam in a non relativistic cold plasma

An analysis of the self-modulated transverse dynamics of a cylindrically symmetric nonlaminar driving beam is carried out. To this end, we disregard the longitudinal dynamics. Therefore, the general 3D Vlasov-Poisson-type system of equation constructed in Chapter 3 is reduced to a 2D pair of equations governing the spatiotemporal evolution of the purely transverse dynamics of the driving beam, which is supposed to be very long compared to the plasma wavelength and travelling through a cold, magnetized and overdense plasma. Due to the conditions of very long beam, the self-consistent PWF mechanism is very efficient and it sensitively characterizes the self-modulated dynamics.

The analysis is carried out by using the pair of Vlasov-Poisson-type equations in cylindrical symmetry that are implemented by the virial equations to provide the analysis of the self-modulated dynamics of the driver envelope. We show the important role played by the constants of motions that are involved in such a description. We first carry out an analysis in two different limiting cases, i.e., the local case (the beam spot size is much greater than the plasma wavelength) and the strongly nonlocal case (the beam spot size is much smaller than the plasma wavelength) where several types of self-modulation, in terms of focusing, defocusing and betatron-like oscillations, are obtained and the criteria for instability, such as collapse and self-modulation instability, are formulated. To this ends, within the

context of the envelope description, we find suitable envelope equations, i.e., ordinary differential equations for the beam spot size, that are easily integrated analytically and that provide also suitable physical explanations in terms of the method of the pseudo potential or Sagdeev potential.
Then, the analysis is extended to the case where the beam spot size and the plasma wavelength are not necessarily constrained as in the local or strongly nonlocal cases. The analysis of the system can be still carried out with the virial equations and with the same methods used in the above limiting cases (envelope equations, Sagdeev potential) to provide a full semi-analytical and numerical investigation for the envelope self-modulation. To this end, criteria for predicting stability and self-modulation instability are suitably provided.

4.1 Introduction

In this chapter, we focus on the purely transverse dynamics of a nonlaminar driving beam, while experiencing the self-consistent PWF excitation, that has been extensively described in Chapters 2 and 3. To consider a specific case related to some typical experimental situation, we assume that our beam is constituted by ultra-relativistic electrons or positrons traveling along the constant and uniform magnetic field $\mathbf{B}_0 = \hat{z}B_0$, in overdense regime (i.e., $n_{bmax} \ll n_0$, n_{bmax} being the maximum value of the beam density). Furthermore, we assume that the plasma can be effectively thought as cold. This is physically justified by the very high energy that the ultra-relativistic driving beam transfers to the plasma by means of the PWF mechanism. According to Chapters 2 and 3, the typical wake field intensities are of the order of n_{bmax}/n_0 times E_{max}, i.e., the Dawson limit (see the Introduction of this thesis), which is given by $m_0\omega_p c/e$. For plasma densities ranging from 10^{17} to 10^{18}cm^{-3}, E_{max} ranges from ~ 0.1 to ~ 1 GV/cm. Correspondingly, for $n_{bmax}/n_0 \sim 10^{-2}$, the wake field intensities range from ~ 0.1 to ~ 1 GV/m. The corresponding electric pressure ranges from $\sim 10^5$ to $\sim 10^6$ erg/cm^3 (i.e., from $\sim 10^4$ to $\sim 10^5$ J/m^3). On the other hand, keeping the above values of plasma density and the temperature of a few 10^5K (i.e., $k_B T \sim 10$ eV), the kinetic plasma pressure ranges roughly from 1 to 10 erg/cm^3 (i.e., from 0.1 to 1 J/m^3). Therefore, it is clear

that the kinetic plasma pressure is several orders of magnitude less than the electric pressure to justify the assumption of cold plasma we have taken. Only relativistic temperatures ($k_B T \lesssim m_{e0}c^2 \approx 0.5$ MeV) can justify an assumption of warm plasma, but such a physical condition does not match with the typical features of a plasma for particle accelerator applications. It should be emphasized that, in the *underdense regime* (i.e., $n_{bmax} \gtrsim n_0$, the wake fields are much greater than in the overdense regime (those become of the order of Dawson limit). This way, the enormous quantity of energy transferred from the driving beam to the plasma makes the plasma electron motion relativistic. But, this does not imply that the thermal motion of the plasma electrons is relativistic to justify kinetic plasma pressures comparable to the electric pressures. In fact, for accelerator applications, the plasma is created with a non relativistic thermal motion. Once an ultra-relativistic driving beam is launched into the plasma, the part of the beam energy that is transferred to the plasma by means of the PWF mechanism contribute mainly to the *ordered* (i.e., fluid) plasma motion. A very small fraction of that energy contributes to the plasma heating.

In the next section, we start from the appropriate governing equations, i.e., the set of Vlasov-Poisson-type equations, that are written in the frame of the unperturbed particle, according to Chapter 3 (co-moving frame) and that are compatible with the above assumptions.

In this framework, we formulate the envelope description of the self-modulated beam dynamics. Such a description reveals to be very helpful to carry out a stability/instability analysis. Since the Vlasov-Poisson-type system of equations that we adopt is nonlinear and nonlocal, we specialize our analysis in three different regimes, where a specific nonlocal or local character of the nonlinearity plays a role.

It is worth pointing out that the reference of the problem under discussion in this chapter to the context of plasma-based acceleration is a little generic. Actually, the purely transverse case we have assumed implies absence of dynamics along the longitudinal direction, i.e., z-direction. On the other hand, the beam particles experience the action of the transverse PWF, while moving along z, with respect to the laboratory frame. However, in the unperturbed-particle frame, without longitudinal dynamics, all the particles are moving in

the transverse direction, only. Although the transverse action of the wake fields on the beam particles produces particle acceleration in a wider sense, this physical circumstance should be more conveniently referred to as a sort of *self-manipulation* of the beam. Note that this is actually a macroscopic feedback that the driving beam receives from the plasma after exciting the latter (i.e., the generation of the strong electric fields and electric pressures). It should be emphasized that such a feedback is more and more important as the *effective length* of the beam (i.e., σ_z), compared to the plasma wavelength, increases more and more. For this reason, we assume that the driving beam is relatively long to satisfy such a physical circumstance. Within the framework of the envelope description, given later in this chapter, the self-manipulation corresponds to a variety of electro-mechanical actions, such as *self-focusing* (leading eventually to the *beam collapse*), *self-defocusing* (leading eventually to the *envelope self-modulation instability*), or stable configurations (in particular, stable *envelope betatron-like oscillations*).

4.2 The governing equations of the transverse beam dynamics

To write the appropriate governing equation, we have to specialize the general set of Eqs. (3.4.2) - (3.4.4) to our assumptions. In particular, we have chosen to focus our analysis on a beam of electrons ($q = -e$, $m_{b0} = m_{e0}$) or positrons ($q = e$, $m_{b0} = m_{e0}$) as a driving beam. Therefore, the quantity $(q/e)^2$ (m_{e0}/m_{b0}) appearing at the right-hand side of Eq. (3.4.3) becomes 1. In addition, the assumptions of purely transverse beam dynamics can be imposed by formally putting $\partial/\partial\xi = \partial/\partial p_z = 0$ in Eqs. (3.4.2) - (3.4.4), whereas the cold plasma assumptions corresponds to put in this same equations $\alpha_z = \alpha_\perp = 0$. Finally, the assumptions of ultra-relativistic and long beam correspond to $\beta \approx 1$, $\gamma_0 \gg 1$, and $k_s\sigma_z \gg 1$, respectively. Then, similarly to what we have done in Chapter 2 to obtain the diverse Poisson-type equations, the above assumptions easily lead to the following pair of equations:

$$\frac{\partial f}{\partial \tau} + \left[\mathbf{p}_\perp + \frac{1}{2}k_c\,(\hat{z}\times\mathbf{r}_\perp)\right]\cdot\nabla_\perp f - \left[K\mathbf{r}_\perp - \frac{1}{2}k_c\,(\hat{z}\times\mathbf{p}_\perp) + \nabla_\perp U_w\right]\cdot\nabla_{p_\perp} f = 0\,, \qquad (4.2.1)$$

$$\left(\nabla_\perp^2 - k_s^2\right) U_w = k_s^2 \lambda_0 \int f \, d^2 p_\perp \,, \tag{4.2.2}$$

where $\lambda_0 = N/n_0 \gamma_0 \sigma_z$ (N being the total number of electrons or positrons of the driving beam) and $k_s = k_p^2/k_{uh}$. Note that here $f = f(\mathbf{r}_\perp, \mathbf{p}_\perp, \tau)$ stands for the single-particle distribution function in the 4D $(\mathbf{r}_\perp, \mathbf{p}_\perp)$-phase space; therefore, the local beam density, i.e., $n_b(\mathbf{r}_\perp, \tau)$, has been expressed in terms of this 4D distribution function, as follows:

$$n_b(\mathbf{r}_\perp, \tau) = \frac{N}{\sigma_z} \int f(\mathbf{r}_\perp, \mathbf{p}_\perp, \tau) \; d^2 p_\perp \,. \tag{4.2.3}$$

Note that definition (4.2.3) has been chosen in such a way that n_b is the number of particles per unity volume of the 3D configuration space $(\mathbf{r}_\perp, \xi)$. In fact, since in this chapter n_b is independent of ξ, the total number of beam particles is given by:

$$N = \sigma_z \int n_b(\mathbf{r}_\perp, \tau) d^2 \mathbf{r}_\perp \,, \tag{4.2.4}$$

where the integration in $d\xi$ is replaced by the simple multiplication by σ_z. Consequently, the integral of f in the 4D-phase space $(\mathbf{r}_\perp, \mathbf{p}_\perp)$ is fixed to unity, i.e.,

$$\int f(\mathbf{r}_\perp, \mathbf{p}_\perp, \tau) d^2 r_\perp, d^2 p_\perp = 1 \,. \tag{4.2.5}$$

It is worth noting that the nonlinearity of the above system of Eqs. (4.2.1) and (4.2.2) lies in the term $(\nabla_\perp U_w \cdot \nabla_{p_\perp} f)$ in Vlasov equation, whereas the local and nonlocal character of the system depend on the interplay between the terms $\nabla_\perp^2 U_w$ and $k_s^2 U_w$ in the Poisson-type equation.

In order to perform the analysis of our system in the diverse physical conditions, we distinguish among the following three different regimes of the beam dynamics, i.e.,

1. *Purely local regime*, where the beam spot size (i.e., $\sigma_\perp$) is much greater than the wavelength $\lambda_s \equiv 2\pi/k_s$, i.e., $k_s \sigma_\perp \gg 1$, which corresponds to impose formally $|\nabla_\perp| \ll k_s$.

2. *Moderately nonlocal regime*, where the beam spot size is of the order of λ_s, i.e., $k_s \sigma_\perp \sim 1$, which corresponds to impose formally $|\nabla_\perp| \sim k_s$.

3. *Strongly nonlocal regime*, where the beam spot size is much smaller than λ_s, i.e., $k_s\,\sigma_\perp \ll 1$, which corresponds to impose formally $|\nabla_\perp| \gg k_s$.

Note that, in absence of an external magnetic field, the above regimes are simply characterized by the following conditions:

1. *Purely local regime*, $k_p\sigma_\perp \gg 1$ (i.e., $|\nabla_\perp| \ll k_p$);

2. *Moderately nonlocal regime*, $k_p\sigma_\perp \sim 1$ (i.e., $|\nabla_\perp| \sim k_p$);

3. *Strongly nonlocal regime*, $k_p\sigma_\perp \ll 1$ (i.e., $|\nabla_\perp| \gg k_p$).

Note that, according to Chapter 2, the purely local, moderately nonlocal and strongly nonlocal regimes correspond also to the conditions for *wide*, *moderately focussed*, and *strongly focussed* beam, respectively, that we have introduced there as well.

4.3 Beam envelope description

In this section, we introduce the so-called *beam envelope description*, or *virial description*, that is obtained by taking the average of certain physical quantities by means of the distribution function $f = f(\mathbf{r}_\perp, \mathbf{p}_\perp, \tau)$. Such an approach is supported by a set of equations, usually referred to as the *virial equations*. The latter spring directly from the kinetic description, i.e., from the pair of Vlasov-Poisson-type equations. In order to obtain the virial equations, let us consider the Hamiltonian given in the unperturbed-particle frame, i.e., $H(\mathbf{r}_\perp, \mathbf{p}_\perp, \tau)$ [see, section (3.4)]. We can cast it as:

$$H(\mathbf{r}_\perp, \mathbf{p}_\perp, \tau) = T(\mathbf{p}_\perp) + U(\mathbf{r}_\perp, \mathbf{p}_\perp, \tau)\,, \tag{4.3.1}$$

where

$$T(p_\perp) = \frac{1}{2}p_\perp^2 \tag{4.3.2}$$

and

$$U(\mathbf{r}_\perp, \mathbf{p}_\perp, \tau) = \frac{1}{2}k_c\,\hat{z}\cdot(\mathbf{r}_\perp \times \mathbf{p}_\perp) + \frac{1}{2}Kr_\perp^2 + U_w(\mathbf{r}_\perp, \tau)\ . \tag{4.3.3}$$

Therefore, the spatiotemporal evolution of the beam is provided by the following Vlasov equation in phase space:

$$\frac{\partial f}{\partial \tau} + \frac{\partial H}{\partial \mathbf{p}_\perp} \cdot \frac{\partial f}{\partial \mathbf{r}_\perp} - \frac{\partial H}{\partial \mathbf{r}_\perp} \cdot \frac{\partial f}{\partial \mathbf{p}_\perp} = 0 \,. \tag{4.3.4}$$

If $F(\mathbf{r}_\perp, \mathbf{p}_\perp, \tau)$ is a generic physical quantity defined in the 4D-phase space, according to Eq. (4.2.5), the phase space average of F is defined as:

$$\langle F \rangle = \int F(\mathbf{r}_\perp, \mathbf{p}_\perp, \tau) f(\mathbf{r}_\perp, \mathbf{p}_\perp, \tau) d^2 r_\perp, d^2 p_\perp \,. \tag{4.3.5}$$

In particular, we introduce the following averaged quantities:

- the beam spot size (effective transverse beam size), i.e.,

$$\sigma_\perp(\tau) = \langle r_\perp^2 \rangle^{1/2} = \left[\int r_\perp^2 \, f \, d^2 r_\perp \, d^2 p_\perp \right]^{1/2} ; \tag{4.3.6}$$

- the momentum spread, i.e.,

$$\sigma_{p_\perp}(\tau) = \langle p_\perp^2 \rangle^{1/2} = \left[\int p_\perp^2 \, f \, d^2 r_\perp \, d^2 p_\perp \right]^{1/2} ; \tag{4.3.7}$$

-the average of the total energy, i.e.,

$$\mathcal{E}(\tau) = \langle H \rangle = \int H f \, d^2 r_\perp \, d^2 p_\perp = \langle T \rangle + \langle U \rangle \,, \tag{4.3.8}$$

where

$$\langle T \rangle = \int \frac{1}{2} p_\perp^2 f \left(\mathbf{r}_\perp, \mathbf{p}_\perp, \tau \right) \, d^2 r_\perp \, d^2 p_\perp = \frac{1}{2} \sigma_{p_\perp}^2(\tau) \tag{4.3.9}$$

and

$$\langle U \rangle = \int U \left(\mathbf{r}_\perp, \mathbf{p}_\perp, \tau \right) f \left(\mathbf{r}_\perp, \mathbf{p}_\perp, \tau \right) \, d^2 r_\perp d^2 r_\perp \,. \tag{4.3.10}$$

It should be emphasized that to define $\sigma_\perp$ and $\sigma_{p_\perp}$, we have assumed that $\langle \mathbf{r}_\perp \rangle = \langle \mathbf{p}_\perp \rangle = 0$, since in the unperturbed particle frame, the beam centroid is moving always along $\hat{z}$.

4.3.1 First virial equation

In order to find an evolution equation for $\sigma_\perp^2(\tau)$, we first differentiate the square of Eq. (4.3.6) with respect to τ, i.e.,

$$\frac{d\sigma_\perp^2}{d\tau} = \int r_\perp^2 \frac{\partial f}{\partial \tau}\, d^2 r_\perp\, d^2 p_\perp \,. \tag{4.3.11}$$

Then, we substitute $\partial f/\partial\tau$ by means of Eq. (4.3.4) obtaining

$$\frac{d\sigma_\perp^2}{d\tau} = -\int r_\perp^2 \left[\frac{\partial \mathcal{H}}{\partial \mathbf{p}_\perp}\cdot\frac{\partial f}{\partial \mathbf{r}_\perp} - \frac{\partial \mathcal{H}}{\partial \mathbf{r}_\perp}\cdot\frac{\partial f}{\partial \mathbf{p}_\perp}\right] d^2 r_\perp\, d^2 p_\perp \,. \tag{4.3.12}$$

After integrating by parts and imposing the boundary conditions at the infinity (compatible with the normalization of the distribution function) we get (for details see Appendix A):

$$\frac{d\sigma_\perp^2}{d\tau} = 2\left\langle \mathbf{r}_\perp \cdot \nabla_{p_\perp} H\right\rangle + \left\langle r_\perp^2 \left[\nabla_{r_\perp}\cdot(\nabla_{p_\perp} H) - \nabla_{p_\perp}\cdot(\nabla_{r_\perp} H)\right]\right\rangle \,. \tag{4.3.13}$$

By using the Hamilton's equations for the Hamiltonian (4.3.1), i.e.,

$$\frac{d\mathbf{r}_\perp}{d\tau} = \frac{\partial H}{\partial p_\perp} = \mathbf{p}_\perp + \frac{1}{2}k_c(\hat{z}\times\mathbf{r}_\perp)\,, \tag{4.3.14}$$

and

$$\frac{d\mathbf{p}_\perp}{d\tau} = -\frac{\partial H}{\partial \mathbf{r}_\perp} = -[K\mathbf{r}_\perp + \nabla_\perp U_w - \frac{1}{2}k_c(\hat{z}\times\mathbf{p}_\perp)]\,, \tag{4.3.15}$$

one can easily show that the second term at the right-hand side of Eq. (4.3.13) vanishes. Therefore Eq. (4.3.13) becomes:

$$\frac{d\sigma_\perp^2}{d\tau} = 2\langle \mathbf{r}_\perp\cdot\mathbf{p}_\perp\rangle = 2\int (\mathbf{r}_\perp\cdot\mathbf{p}_\perp) f\, d^2 r_\perp\, d^2 p_\perp \,, \tag{4.3.16}$$

which can be also cast as:

$$\sigma_\perp \frac{d\sigma_\perp}{d\tau} = \langle \mathbf{r}_\perp\cdot\mathbf{p}_\perp\rangle \,. \tag{4.3.17}$$

Note that Eq. (4.3.17) remains formally the same in the unmagnetized case ($B_0 = 0$). However, without external magnetic field, Hamilton's equation (4.3.14) gives (note that $\tau(= ct)$ can be thought as longitudinal length):

$$\frac{d\mathbf{r}_\perp}{d\tau} = \mathbf{p}_\perp \,. \tag{4.3.18}$$

Then, we observe that, within the context of the electron optics, $\mathbf{r}_\perp(\tau)$ and $\mathbf{p}_\perp(\tau)$ are the instantaneous position and slope in the instantaneous transverse plane with respect to the longitudinal direction of a generic electron ray (charged particle trajectory). In particular, the paraxial assumption imposes the condition: $|p_\perp| = |v/c| \ll 1$. In addition, Eq. (4.3.17) shows that the average of the product of position and slope of the electron rays is simply the product of $\sigma_\perp$ (i.e., rms of electron ray positions in the transverse plane) and its slope with respect to the longitudinal direction.

On the other hand, we observe that the product $\mathbf{r}_\perp \cdot \mathbf{p}_\perp = \mathbf{r}_\perp \cdot (d\mathbf{r}_\perp/d\tau) = 1/2\,(dr_\perp^2/d\tau)$ is, by definition, the *virial* of the generic single-particle.

Note that, by analogy with this definition, we may assume that $\sigma_\perp(\tau)$ and $\sigma'_\perp \equiv d\sigma_\perp/d\tau$ are the instantaneous position and velocity of a hypothetic particle. Then, the instantaneous virial is defined as,

$$\sigma_\perp \frac{d\sigma_\perp}{d\tau} = \frac{1}{2}\frac{d\sigma_\perp^2}{d\tau}.$$

We conclude that Eq. (4.3.17) defines statistically a sort of "effective" virial, i.e., $\sigma_\perp d\sigma_\perp/d\tau$, that corresponds to the average of the beam particle virial, i.e.,

$$\sigma_\perp \frac{d\sigma_\perp}{d\tau} = \left\langle \mathbf{r}_\perp \cdot \frac{d\mathbf{r}_\perp}{d\tau} \right\rangle . \tag{4.3.19}$$

If we now consider the magnetic field no longer negligible, according to Eq. (4.3.14), the meaning of $\mathbf{p}_\perp$ is no longer simply the slope of the electron ray. However, due to the orthogonality between $\mathbf{r}_\perp$ and $(\hat{z} \times \mathbf{r}_\perp)$, $\mathbf{r}_\perp \cdot \mathbf{p}_\perp = \mathbf{r}_\perp \cdot (d\mathbf{r}_\perp/d\tau)$. Consequently in the presence of $\mathbf{B}_0$, Eq. (4.3.19) still holds the same meaning of virial.

We now take the derivative of Eq. (4.3.16), obtaining:

$$\frac{d^2\sigma_\perp^2}{d\tau^2} = 2\int (\mathbf{r}_\perp \cdot \mathbf{p}_\perp)\frac{\partial f}{\partial \tau}\, d^2 r_\perp\, d^2 p_\perp\,. \tag{4.3.20}$$

We, once more, substitute $\partial f/\partial\tau$ by means of Eq. (4.3.4), i.e.,

$$\frac{d^2\sigma_\perp^2}{d\tau^2} = -2\int (\mathbf{r}_\perp \cdot \mathbf{p}_\perp)\left[\frac{\partial \mathcal{H}}{\partial \mathbf{p}_\perp}\cdot\frac{\partial f}{\partial \mathbf{r}_\perp} - \frac{\partial \mathcal{H}}{\partial \mathbf{r}_\perp}\cdot\frac{\partial f}{\partial \mathbf{p}_\perp}\right] d^2 r_\perp\, d^2 p_\perp\,. \tag{4.3.21}$$

Which can be integrated by parts, obtaining the following equation for the derivative of the averaged virial (see Appendix A):

$$\frac{d^2\sigma_\perp^2}{d\tau^2} = 2\left\langle \mathbf{p}_\perp \cdot \nabla_{p_\perp} H \right\rangle + 2\left\langle (\mathbf{r}_\perp \cdot \mathbf{p}_\perp)\nabla_{r_\perp} \cdot (\nabla_{p_\perp} H) \right\rangle - 2\left\langle \mathbf{r}_\perp \cdot (\nabla_{r_\perp} H) \right\rangle . \tag{4.3.22}$$

By using again the explicit form of the Hamiltonian (4.3.1) and the corresponding Hamiltonian equations, we finally obtain the following equation:

$$\frac{d^2\sigma_\perp^2}{d\tau^2} = 4\langle T \rangle - 2\langle \mathbf{r}_\perp \cdot \nabla_\perp V \rangle , \tag{4.3.23}$$

where,

$$V(\mathbf{r}_\perp, \tau) = \frac{1}{2} K r_\perp^2 + U_w(\mathbf{r}_\perp, \tau) . \tag{4.3.24}$$

We refer Eq. (4.3.23) to as the *first virial equation*.

It can be consequently cast in the following form, viz.,

$$\frac{d^2\sigma_\perp^2}{d\tau^2} = 2\sigma_{p_\perp}^2 - 2K\sigma_\perp^2 - 2\langle \mathbf{r}_\perp \cdot \nabla_\perp U_w \rangle , \tag{4.3.25}$$

or,

$$\frac{d^2\sigma_\perp^2}{d\tau^2} = 4(\mathcal{E} - \langle U \rangle) - 2\langle \mathbf{r}_\perp \cdot \nabla_{r_\perp} U \rangle + k_c \mathcal{L}_z , \tag{4.3.26}$$

where $\mathcal{L}_z = \langle L_z \rangle$, $L_z = \hat{z} \cdot (\mathbf{r}_\perp \times \mathbf{p}_\perp)$, and U is given in Eq. (4.3.3).

In case of unmagnetized plasma, the first virial equation becomes ($k_c = K = 0$):

$$\frac{d^2\sigma_\perp^2}{d\tau^2} = 4(\mathcal{E} - \langle U_w \rangle) - 2\langle \mathbf{r}_\perp \cdot \nabla_{r_\perp} U_w \rangle , \tag{4.3.27}$$

where

$$\mathcal{E} = \frac{1}{2}\langle p_\perp^2 \rangle + \langle U_w \rangle . \tag{4.3.28}$$

4.3.2 Second virial equation

In this section, we find an equation for the time evolution of the averaged total energy $\mathcal{E}(\tau) = \langle H \rangle$, according to its definition, i.e., Eq. (4.3.8). To this end, we differentiate Eq. (4.3.8) with respect to τ, obtaining:

$$\frac{d\mathcal{E}}{d\tau} = \int \frac{\partial H}{\partial \tau} f d^2 p_\perp d^2 r_\perp + \int H \frac{\partial f}{\partial \tau} d^2 p_\perp d^2 r_\perp , \tag{4.3.29}$$

which, by using Eq. (4.3.4), can be cast as:

$$\frac{d\mathcal{E}}{d\tau} = \left\langle \frac{\partial H}{\partial \tau} \right\rangle - \int H \left[\frac{\partial H}{\partial \mathbf{p}_\perp} \cdot \frac{\partial f}{\partial \mathbf{r}_\perp} - \frac{\partial H}{\partial \mathbf{r}_\perp} \cdot \frac{\partial f}{\partial \mathbf{p}_\perp} \right] d^2 p_\perp d^2 r_\perp \,. \tag{4.3.30}$$

Performing the integration by parts in the second term at the right-hand side, we easily find that this term vanishes, and therefore Eq. (4.3.30) becomes simply (for details see Appendix A):

$$\frac{d\mathcal{E}}{d\tau} = \left\langle \frac{\partial U_w}{\partial \tau} \right\rangle = \int \frac{\partial U_W}{\partial \tau} f d^2 r_\perp d^2 p_\perp \,, \tag{4.3.31}$$

where we have used the explicit form of H given by Eqs. (4.3.1) - (4.3.3) and observed that $U_w(\mathbf{r}_\perp, \tau)$ is the only term of the Hamiltonian that depends explicitly on τ.

We refer Eq. (4.3.31) to as the *second virial equation*, which describes the time evolution of the averaged energy $\mathcal{E}$.

4.3.3 Virial description and constants of motion

Equations (4.3.23) and (4.3.31) constitute a pair of coupled equations governing the time evolution of the beam envelope. However, this is not a complete set of equations, since it requires the knowledge of f and U_w. This implies that the envelope description is subordinated to the kinetic description. To satisfy the self-consistency, we have to couple the Vlasov-Poisson-type system of equations, i.e., Eqs. (4.2.1) and (4.2.2), with Eqs. (4.3.23) and (4.3.31). Provided that suitable initial and boundary conditions are imposed, in principle, we have first to solve Eqs. (4.2.1) and (4.2.2). Once $f(\mathbf{r}_\perp, \mathbf{p}_\perp, \tau)$ and $U_w(\mathbf{r}_\perp, \tau)$ are known, we can use the virial equations to describe the time evolution of the beam envelope. We refer this approach to as the *virial description*. Actually, often, the Vlasov-Poisson-type system is difficult to solve, then the virial description reveals to be very helpful. In fact, in the most fortunate cases, if for instance our beam-plasma system satisfies some suitable specific properties of symmetry, the virial description can be constructed without the explicit knowledge of the instantaneous distribution function, whereas the knowledge of the initial distribution would be necessary. This aspect is strictly connected to the existence of suitable constants of motion (due to, for instance, the properties of symmetry mentioned above), because the

constants of motions can allow us to fix conditions among the physical quantities given at arbitrary times. Therefore, one can fix these quantities, in particular, at the initial time or at any other time that could be convenient to the ends of our analysis. If Eqs. (4.3.23) and (4.3.31) can be combined into a single differential equation for the beam spot-size, called *beam envelope equation*, this approach allows to reduce the study of the time evolution of the beam envelope to the one of the beam spot size, i.e., $\sigma_\perp(\tau)$.

In the next sections, we describe specific problems of beam self-modulation within the context of the viral description, where the search of constants of motion associated with the spatiotemporal evolution of the system (4.2.1), (4.2.2), (4.3.23) and (4.3.31) is very helpful and plays a crucial role.

4.3.4 Constants of motion and envelope equations

We show here the existence of a constant of motion for the set of Eqs. (4.2.1), (4.2.2), (4.3.23) and (4.3.31). To this end, we observe that the integral in Eq. (4.3.31) can be cast as $\int d^2r_\perp \, (\partial U_w/\partial\tau) \int f \, d^2p_\perp$, since U_w is independent of $\mathbf{p}_\perp$. Then, by making use of Eq. (4.2.2), Eq. (4.3.31) becomes:

$$\frac{d\mathcal{E}}{d\tau} \;=\; \frac{1}{k_s^2\lambda_0}\left[\int \frac{\partial U_w}{\partial\tau}\nabla_\perp^2 U_w \, d^2r_\perp \;-\; k_s^2 \int U_w \, \frac{\partial U_w}{\partial\tau} \, d^2r_\perp \right], \tag{4.3.32}$$

which, after integrating by parts, can be cast as (for details, see Appendix B):

$$\frac{d\mathcal{E}}{d\tau} \;=\; -\frac{1}{2k_s^2\lambda_0}\,\frac{d}{d\tau}\int \left(|\nabla_\perp U_w|^2 + k_s^2 U_w^2\right) d^2r_\perp \,. \tag{4.3.33}$$

Consequently, from this equation we can define the following constant of motion:

$$C \;=\; \mathcal{E} \;+\; \frac{1}{2k_s^2\lambda_0}\int \left(|\nabla_\perp U_w|^2 + k_s^2 U_w^2\right) d^2r_\perp \,. \tag{4.3.34}$$

By expressing explicitly $\mathcal{E} = \langle H\rangle$ with Eqs. (4.3.1) - (4.3.3) in the above equation, we easily get:

$$C \;=\; \frac{1}{2}\sigma_{p\perp}^2 + \frac{1}{2}K\sigma_\perp^2 \;+\; \frac{1}{2k_s^2\lambda_0}\int \left(|\nabla_\perp U_w|^2 + k_s^2 U_w^2\right) d^2r_\perp + \langle U_w\rangle + \frac{1}{2}k_c\mathcal{L}_z \,. \tag{4.3.35}$$

Then, observing that

$$\langle U_w \rangle = -\frac{1}{k_s^2 \lambda_0} \int \left(|\nabla_\perp U_w|^2 + k_s^2 U_w^2 \right) d^2 r_\perp \,, \tag{4.3.36}$$

Eq. (4.3.35) becomes

$$C = \frac{1}{2}\sigma_{p\perp}^2 + \frac{1}{2} K \sigma_\perp^2 - \frac{1}{2k_s^2 \lambda_0} \int \left(|\nabla_\perp U_w|^2 + k_s^2 U_w^2 \right) d^2 r_\perp + \frac{1}{2} k_c \mathcal{L}_z \,. \tag{4.3.37}$$

By means of (4.3.37), we express $\mathcal{E}$ in terms of C and substitute it in the first virial equation. Then, using (4.3.37) and (4.3.3) into (4.3.26) we easily get:

$$\frac{d^2 \sigma_\perp^2}{d\tau^2} + 4\, K \sigma_\perp^2 = 4C - \frac{2}{k_s^2 \lambda_0} \int \left(|\nabla_\perp U_w|^2 + k_s^2 U_w^2 \right) d^2 r_\perp - 4\langle U_w \rangle - 2\langle \mathbf{r}_\perp \cdot \nabla_\perp U_w \rangle - 2 k_c \mathcal{L}_z \,. \tag{4.3.38}$$

After performing by parts the various integrations contained in the terms at the right-hand side of Eq. (4.3.38), we finally obtain the following envelope equation, i.e.,

$$\frac{d^2 \sigma_\perp^2}{d\tau^2} + 4\, K \sigma_\perp^2 = 4C + \frac{2}{k_s^2 \lambda_0} \int |\nabla_\perp U_w|^2 \, d^2 r_\perp - 2 k_c \mathcal{L}_z \,. \tag{4.3.39}$$

Note that, for the case of unmagnetized plasma ($B_0 = 0$), we easily get:

$$\frac{d^2 \sigma_\perp^2}{d\tau^2} = 4C' + \frac{2}{k_p^2 \lambda_0} \int |\nabla_\perp U_w|^2 \, d^2 r_\perp \,, \tag{4.3.40}$$

where $C' = 1/2\, \sigma_{p\perp}^2 - 1/(2k_s^2 \lambda_0) \int \left(|\nabla_\perp U_w|^2 + k_s^2 U_w^2 \right) d^2 r_\perp$.

4.3.5 Beam emittance

A useful quantity that is typically involved in the charged-particle beam transport is the so-called *thermal emittance* or simply *beam emittance*, that has been introduced by Lapostolle. It is defined in terms of all the second-order moments of the distribution function. The simplest definition of beam emittance is usually given in each 2D-subspace of the 6D-phase space. Let q_i and p_i be the i-component ($i = x, y, z$) of the single-particle position and conjugate momentum, respectively. By following the definition of average quantity given in

section 4.3, we introduce the second-order moments of the normalized distribution function $f(\mathbf{q}, \mathbf{p}, \tau)$ on the (q_i, p_i)-subspace, where $\mathbf{q} = (q_x, q_y, q_z)$, $\mathbf{p} = (p_x, p_y, p_z)$, i.e.,

$$\sigma_i(\tau) = \left\langle (q_i - \langle q_i \rangle)^2 \right\rangle^{1/2} = \left[\int (q_i - \langle q_i \rangle)^2 \, f d^3q \, d^3p \right]^{1/2} , \tag{4.3.41}$$

$$\sigma_{pi}(\tau) = \left\langle (p_i - \langle p_i \rangle)^2 \right\rangle^{1/2} = \left[\int (p_i - \langle p_i \rangle)^2 \, f d^3q \, d^3p \right]^{1/2} , \tag{4.3.42}$$

$$\sigma_{ip_i}(\tau) = \langle (q_i - \langle q_i \rangle)(p_i - \langle p_i \rangle) \rangle = \int (q_i - \langle q_i \rangle)(p_i - \langle p_i \rangle) \, f d^3q d^3p \, , \tag{4.3.43}$$

where

$$\langle q_i \rangle = \int q_i f(\mathbf{q}, \mathbf{p}, \tau) d^3q, d^3p \, , \tag{4.3.44}$$

$$\langle p_i \rangle = \int p_i f(\mathbf{q}, \mathbf{p}, \tau) d^3q, d^3p \, , \tag{4.3.45}$$

and $p_i = dq_i/d\tau$. In general, $\langle q_i \rangle$ and $\langle p_i \rangle$ are supposed not to be zero.

Note that $\sigma_i(\tau)$ is the instantaneous rms of the particle positions, $\sigma_{pi}(\tau)$ is the instantaneous rms of the particle momentum, i.e., momentum spread and $\sigma_{ip_i}(\tau)$ stands for the instantaneous position-momentum correlation term, along i-direction.

Note also that:

$$\sigma_i^2(\tau) = \left\langle q_i^2 \right\rangle - \langle q_i \rangle^2 \, , \tag{4.3.46}$$

$$\sigma_{pi}^2(\tau) = \left\langle p_i^2 \right\rangle - \langle p_i \rangle^2 \, , \tag{4.3.47}$$

$$\sigma_{ip_i}(\tau) = (\langle q_i p_i \rangle - \langle q_i \rangle \langle p_i \rangle) \, . \tag{4.3.48}$$

We can define the diffusion co-efficient, say ϵ_i, associated with the i-direction, in terms of the following combination of the above mentioned second order moments:

$$\epsilon_i(\tau) = 2 \left[\sigma_i^2(\tau) \sigma_{p_i}^2(\tau) - \sigma_{ip_i}^2(\tau) \right]^{1/2} , \tag{4.3.49}$$

or

$$\epsilon_i(\tau) = 2 \left[\left(\left\langle q_i^2 \right\rangle - \langle q_i \rangle^2 \right) \left(\left\langle p_i^2 \right\rangle - \langle p_i \rangle^2 \right) - (\langle q_i p_i \rangle - \langle q_i \rangle \langle p_i \rangle)^2 \right]^{1/2} , \tag{4.3.50}$$

which is the so-called *thermal emittance* (or simply *beam emittance*) associated with i-direction. If $\langle q_i \rangle = \langle p_i \rangle = 0$, then the emittance definition reduces simply to:

$$\epsilon_i(\tau) = 2\left[\left\langle q_i^2 \right\rangle \left\langle p_i^2 \right\rangle - \langle q_i p_i \rangle^2\right]^{1/2} . \tag{4.3.51}$$

It can be proven that, if $A_i(\tau)$ is the instantaneous area occupied by the beam in the 2D subspace (q_i, p_i), the following identification of $\epsilon_i(\tau)$ holds [64, 65]:

$$\epsilon_i(\tau) = \frac{A_i(\tau)}{\pi} \geq 0 . \tag{4.3.52}$$

This is also usually referred to as the *geometrical emittance*. Note that, in principle, $\epsilon_i(\tau)$ depends on time. Given the non-negativity of $\epsilon_i(\tau)$ from Eq. (4.3.52), Eq. (4.3.51) or (4.3.50) easily implies that:

$$\sigma_i(\tau)\sigma_{p_i}(\tau) \geq \frac{\epsilon_i(\tau)}{2} , \tag{4.3.53}$$

which represents a sort of uncertainty relation between the beam effective size and the corresponding momentum spread, along the i-direction. An interesting situation takes place when $\epsilon_i(\tau)$ is a conserved quantity. This is possible when the beam particles are drifting in absence of forces as well as they are moving in the presence of a linear force, such as $-k(\tau)q_i$ (harmonic oscillator force).

If we restrict the above definition to the transverse case only, $\epsilon_x(\tau)$ and $\epsilon_y(\tau)$ represent the emittances related to the phase space planes (x, p_x) and (y, p_y), respectively, while $\epsilon_z(\tau) = 0$. In addition, we can conveniently introduce the transverse emittance, i.e., $\epsilon_\perp$, generalizing Eq. (4.3.51) to the 2D case, i.e.,

$$\epsilon_\perp(\tau) = \left[\left\langle r_\perp^2 \right\rangle \left\langle p_\perp^2 \right\rangle - \langle \mathbf{r}_\perp \cdot \mathbf{p}_\perp \rangle^2\right]^{1/2} . \tag{4.3.54}$$

According to Eq. (4.3.17) and definitions (4.3.6) and (4.3.7), Eq. (4.3.54) can be re-cast as:

$$\epsilon_\perp(\tau) = \left[\sigma_\perp^2(\tau)\sigma_{p_\perp}^2(\tau) - \sigma_\perp^2(\tau)(\sigma'_\perp(\tau))^2\right]^{1/2} , \tag{4.3.55}$$

where $\sigma'_\perp(\tau) \equiv d\sigma_\perp(\tau)/d\tau$. Note that, if at a given time, $\tau = \tau_0$, $\sigma'_\perp(\tau_0) = 0$, then at this time the emittance reaches its minimum value, $\epsilon_0 = \sigma_\perp(\tau_0)\,\sigma_{p_\perp}(\tau_0)$.

4.3.6 Cylindrical Symmetry

In the cylindrical symmetry, $f = f(r_\perp, p_\perp, \tau)$, $n_b = n_b(r_\perp, \tau)$ and $U_w(r_\perp, \tau)$, where $r_\perp$ is the radial cylindrical position coordinate and $p_\perp$ is the corresponding radial conjugate momentum. Under this assumption, the time-derivative of the single-particle angular momentum, i.e., $\mathbf{L} = \mathbf{r}_\perp \times \mathbf{p}_\perp = r_\perp p_\perp \hat{z}$, after some transformations gives ($\nabla_\perp = \hat{e}_r \frac{\partial}{\partial r_\perp}$):

$$\frac{d\mathbf{L}}{d\tau} = (\hat{e}_r r_\perp) \times \left(\hat{e}_r \frac{\partial U_w}{\partial r_\perp} \right) = 0 , \tag{4.3.56}$$

which implies that $\mathbf{L}$ is a conserved quantity and, consequently, $\mathcal{L}_z$ is a conserved quantity, as well. This result allows us to re-write, finally, Eq. (4.3.39) as:

$$\frac{d^2\sigma_\perp^2}{d\tau^2} + 4K\sigma_\perp^2 = 4\mathcal{A} + \frac{2}{k_s^2\lambda_0} \int |\nabla_\perp U_w|^2 \, d^2 r_\perp , \tag{4.3.57}$$

where $\mathcal{A} = C - 1/2k_c\mathcal{L}_z$ is a new constant of motion, i.e.,

$$\mathcal{A} = \frac{1}{2}\sigma_{p\perp}^2 + \frac{1}{2}K\sigma_\perp^2 - \frac{1}{2k_s^2\lambda_0} \int \left(|\nabla_\perp U_w|^2 + k_s^2 U_w^2 \right) d^2 r_\perp = \frac{1}{2}\sigma_{p\perp}^2 + \frac{1}{2}K\sigma_\perp^2 + \frac{1}{2}\langle U_w \rangle . \tag{4.3.58}$$

In the unmagnetized case, Eq. (4.3.57) reduces to ($C = \mathcal{A}$):

$$\frac{d^2\sigma_\perp^2}{d\tau^2} = 4C + \frac{2}{k_p^2\lambda_0} \int |\nabla_\perp U_w|^2 \, d^2 r_\perp . \tag{4.3.59}$$

4.4 Self-modulated beam dynamics in purely local regime

In this section, we present a first application of the virial description to the self-modulated dynamics of a cylindrically symmetric beam in the purely local regime [58]. According to the classification introduced in section 4.2, in the purely local case, the beam spot size satisfies the condition $k_s\sigma_\perp \gg 1$, which implies that in the Poisson-type Eq. (4.2.2) the condition $|\nabla_\perp U_w| \ll k_s^2 |U_w|$ holds. Hereafter, for simplicity we make the following replacements: $r_\perp \to r$, $p_\perp \to p$. Then, $f = f(r, p, \tau)$, $n_b = n_b(r, \tau)$ and $U_w = U_w(r, \tau)$. Consequently, Eq. (4.2.2) becomes

$$U_w = -\lambda_0 \int f \, d^2 p . \tag{4.4.1}$$

Then, in the purely local regime, the evolution of the beam while travelling through the plasma is governed by the pair of Eqs. (4.2.1) and (4.4.1). It is worthy noting that the concept of strong magnetic field may differ in the laboratory and astrophysical plasma cases. In the laboratory case, the values of B_0 cannot exceed several tens of teslas. Therefore, for plasma density ranging from 10^{12} to 10^{19} (typical of the wide spectrum of possible plasma-based particle acceleration schemes), it results that $\omega_c \lesssim \omega_p$. This implies that the condition of purely local regime reduces to $k_p\sigma_\perp \gg 1$. On the other hand, we encounter a very different situation in the astrophysical environments, where the ambient magnetic fields can largely overcome $10\,T$ ($\omega_c \gg \omega_p$), and therefore the strictly purely local regime condition becomes $(k_p^2/k_c)\sigma_\perp \gg 1$, which represents a constraint for $\sigma_\perp$ that differs completely from the one for the laboratory case.

We observe that according to the assumption of purely local regime, the integrand at the right-hand side of Eq. (4.3.57) is proportional to $1/k_s\sigma_\perp \ll 1$. Therefore, it can be neglected, and Eq. (4.3.57) reduces to the following ordinary differential equation for $\sigma_\perp$ (i.e., envelope equation):

$$\frac{d^2\sigma_\perp^2}{d\tau^2} + 4K\sigma_\perp^2 = 4\mathcal{A}\,, \tag{4.4.2}$$

where

$$\mathcal{A} = \frac{1}{2}\sigma_p^2(\tau) + \frac{1}{2}K\sigma_\perp^2(\tau) - \frac{1}{2\lambda_0}\int U_w^2(r,\tau)\,d^2r = \text{constant}\,. \tag{4.4.3}$$

Here, we have observed that, since here $|\nabla_\perp U_w| \ll k_s|U_w|$, from Eq. (4.3.36)

$$\langle U_w\rangle = -\frac{1}{\lambda_0}\int U_w^2\,d^2r\,. \tag{4.4.4}$$

For the given initial conditions, viz.,

$$\sigma_0 = \sigma_\perp(\tau_0), \quad \sigma_0' = \left(\frac{d\sigma_\perp}{d\tau}\right)_{\tau_0} \equiv \sigma_\perp'(\tau_0), \tag{4.4.5}$$

the envelope equation (4.4.2) allows us to follow the evolution of the beam through the transformation of its rms envelope surface. As we have put forward in the previous section, the analysis of this time evolution can allow us also to predict the transverse stability of the beam motion without finding explicitly the solution of the Vlasov-Poisson system.

The suitable use of the constant of motion (i.e., $\mathcal{A}$) indicates that, besides the initial condition of $\sigma_\perp, \sigma'_\perp$, only the initial distribution function, i.e., $f(r, p, \tau_0)$, is needed (τ_0 being an arbitrary value of τ, here assumed to be the initial time). Then, according to Eq. (4.4.3), such initial conditions fix the constant $\mathcal{A}$, i.e.,

$$\mathcal{A} = \frac{1}{2}\sigma_{p_0}^2 + \frac{1}{2}K\sigma_0^2 - \frac{1}{2\lambda_0}\int U_w^2(r, \tau_0)\, d^2r, \tag{4.4.6}$$

where $\sigma_{p0} \equiv \sigma_p(\tau_0)$. To this end, we perform our analysis considering separately the cases of $B_0 = 0$ and $B_0 \neq 0$.

4.4.1 Unmagnetized plasma

In this regime we have, $K = 0$. Then

$$\mathcal{A} = \frac{1}{2}\sigma_{p0}^2 - \frac{1}{2\lambda_0}\int U_w^2(r, 0)\, d^2r \tag{4.4.7}$$

and Eq. (4.4.2) becomes

$$\frac{d^2\sigma_\perp^2}{d\tau^2} = 4\mathcal{A}\,, \tag{4.4.8}$$

which for $\sigma'_0 = 0$, readily gives:

$$\sigma_\perp^2(\tau) = \sigma_0^2 + 2\mathcal{A}(\tau - \tau_0)^2\,. \tag{4.4.9}$$

The sign of the constant $\mathcal{A}$ depends on the way in which the interplay is established between the kinetic energy, i.e., $\sigma_{p0}^2/2$ and the self energy (wake energy), i.e., $1/2\,\lambda_0 \int U_w^2(r, 0)\, d^2r = \langle U_w(r, 0)\rangle$ in Eq. (4.4.7). Since the beam has been assumed to be warm, in the Maxwellian conditions, we have $\sigma_{p0}^2 \sim k_B T/m_{b0}\gamma_0 c^2$. Therefore, if $\mathcal{A} > 0$, the thermal energy overcomes the self-energy; otherwise, $\mathcal{A}$ may be zero or negative. Consequently, Eq. (4.4.9) leads us to conclude that the beam self-defocusses when $\mathcal{A} > 0$, and that it is in equilibrium when $\mathcal{A} = 0$ (when the exact balance between the thermal energy and the self energy takes place) or it experiences the self-focusing when $\mathcal{A} < 0$, for which the self energy overcomes the thermal energy.

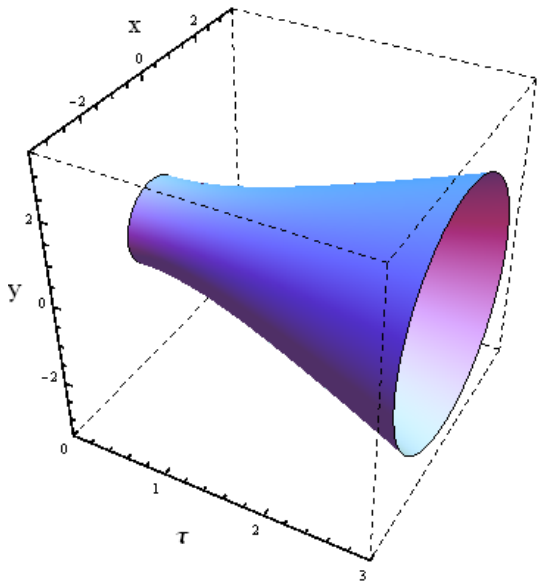

Figure 4.1: Beam envelope surface that, at each τ, is described by $x^2+y^2=\sigma_\perp^2(\tau)$, for $\mathcal{A}>0$ (self-defocusing of the beam for $B_0=0$). Here, $\sigma_0=1$, $\sigma_0'=0$, $\tau_0=0$ and $\mathcal{A}=0.4$.

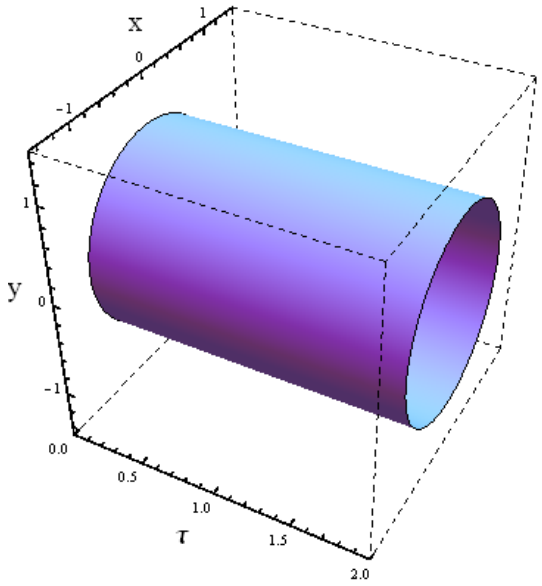

Figure 4.2: Beam envelope surface that, at each τ, is described by $x^2+y^2=\sigma_\perp^2(\tau)$, for $\mathcal{A}=0$ (self-equilibrium of the beam for $B_0=0$). Here, $\sigma_0=1$, $\sigma_0'=0$ and $\tau_0=0$.

Note that, in this case, $\sigma_\perp$ vanishes at a finite value of τ, say $\bar{\tau}$, such that $\bar{\tau}=\tau_0+\sigma_0/\sqrt{|\mathcal{A}|}$.

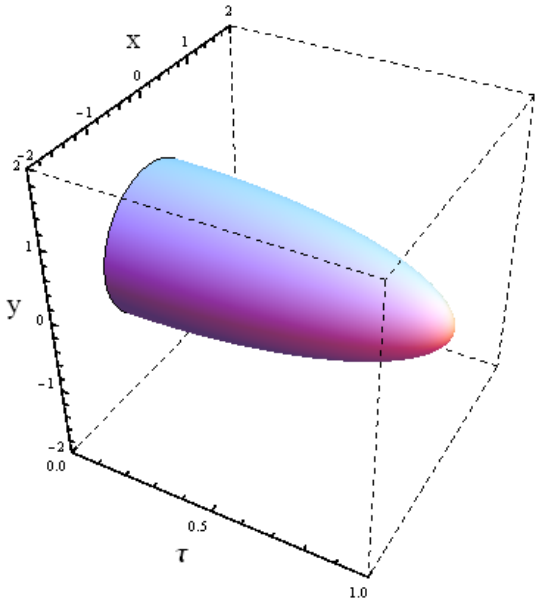

Figure 4.3: Beam envelope surface that, at each τ, is described by $x^2+y^2 = \sigma_\perp^2(\tau)$, for $\mathcal{A} < 0$ (self-focusing of the beam for $B_0 = 0$). Here, $\sigma_0 = 1$, $\sigma_0^{'} = 0$, $\tau_0 = 0$ and $\mathcal{A} = -0.5$.

It corresponds to the case of *beam collapse*. The above three physical circumstances are illustrated in Figures 4.1 - 4.3 through the behaviour of the envelope surface.

4.4.2 Magnetized plasma

Since in this regime we have $K \neq 0$, the full Eq. (4.4.2) needs to be considered. For the initial conditions (4.4.5), the solution of Eq. (4.4.2) is given by (note that, for simplicity, we have chosen $\tau_0 = 0$ and $\sigma_0' = 0$):

$$\sigma_\perp^2(\tau) = \sigma_0^2\left[2\left(\frac{\mathcal{A}}{K\sigma_0^2} - 1\right)\sin^2\left(\sqrt{K}\tau\right) + 1\right], \tag{4.4.10}$$

which clearly shows that:

1. For $\mathcal{A} < 0$ and $0 \leq \mathcal{A} \leq \frac{1}{2}K\sigma_0^2$, the beam is unstable, reaching the collapse condition, i.e., $\sigma_\perp = 0$ at the finite time value

$$\bar{\tau} = \frac{1}{\sqrt{K}}\arcsin\left\{\left[2\left(1 - \frac{\mathcal{A}}{K\sigma_0^2}\right)\right]^{-1/2}\right\}.$$

2. If $\mathcal{A} > 0$ and we choose $\sigma_0 = \sqrt{\mathcal{A}/K}$, then the beam is in the self-equilibrium condition, i.e., $\sigma_\perp = \sigma_0$.

3. Finally, for $\mathcal{A} > K\sigma_0^2/2$, the beam performs stable betatron-like oscillations describing the sausage-like rms beam envelope shape.

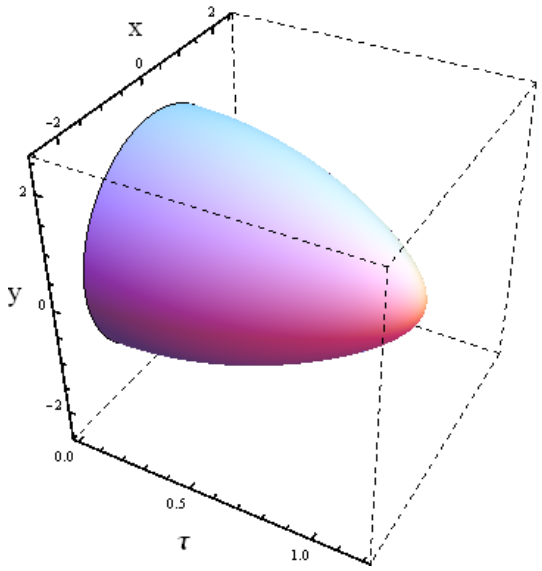

Figure 4.4: Beam envelope surface that, at each τ, is described by $x^2 + y^2 = \sigma_\perp^2(\tau)$, for $\mathcal{A} < 0$ and $0 \leq \mathcal{A} \leq \frac{1}{2}K\sigma_0^2$ (beam self-focusing leading to collapse for $B_0 \neq 0$). Here, $\sigma_0 = 2$, $\sigma_0^{'} = 0$, $K = 1$ and $\mathcal{A} = 1.5$.

Figures 4.4 - 4.6 illustrate the behaviour of the envelope surface corresponding to the instability/stability conditions discussed in this section.

4.4.3 Transverse beam emittance and equivalent Gaussian beam

It is easy to prove that the envelope Eq. (4.4.2) can be cast in the form of an Ermakov-Pinney equation, i.e.,

$$\frac{d^2\sigma_\perp}{d\tau^2} + K\sigma_\perp - \frac{A_0}{\sigma_\perp^3} = 0\,, \tag{4.4.11}$$

where A_0 is a constant of motion given by

$$A_0 = 2\sigma_\perp^2\left(\mathcal{A} - \frac{\sigma_\perp'^{\,2}}{2} - \frac{1}{2}K\sigma_\perp^2\right). \tag{4.4.12}$$

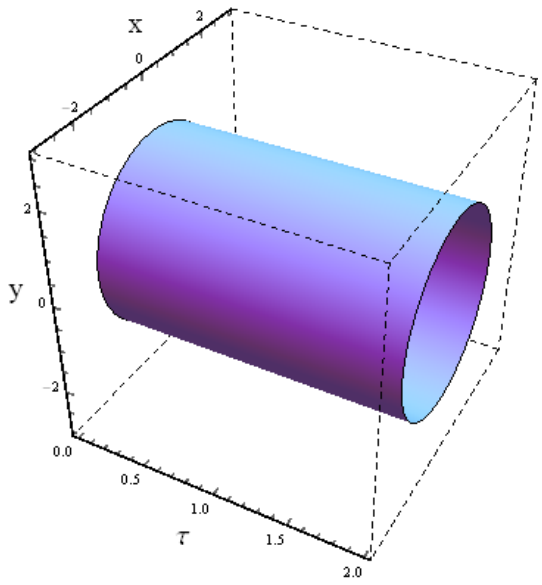

Figure 4.5: Beam envelope surface that, at each τ, is described by $x^2 + y^2 = \sigma_\perp^2(\tau)$, $\sigma_0 = \sqrt{\mathcal{A}/K}$ (beam self-equilibrium for $B_0 \neq 0$). Here, $\sigma_0 = 2$, $\sigma_0^{'} = 0$, $K = 1$ and $\mathcal{A} = 4$.

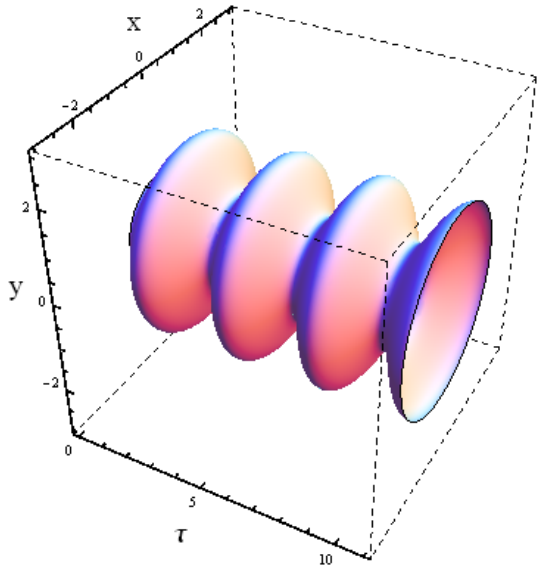

Figure 4.6: Beam envelope surface that, at each τ, is described by $x^2 + y^2 = \sigma_\perp^2(\tau)$, for $\mathcal{A} > K\sigma_0^2/2$ (beam self-modulation, i.e., betatron-like oscillation, for $B_0 \neq 0$). Here, $\sigma_0 = 1$, $\sigma_0^{'} = 0$, $K = 1$ and $\mathcal{A} = 2.5$.

This can be, in fact, accomplished by:

1. expanding the time derivative in Eq. (4.4.2) getting, i.e.,

$$2\left(\frac{d\sigma_\perp}{d\tau}\right)^2 + 2\sigma_\perp \frac{d^2\sigma_\perp}{d\tau^2} + 4K\sigma_\perp^2 = 4\mathcal{A}\,; \tag{4.4.13}$$

2. multiplying Eq. (4.4.2) by $d\sigma_\perp^2/d\tau$ and then integrating one time with respect to τ, i.e.,

$$2\left(\frac{d\sigma_\perp}{d\tau}\right)^2 + 2K\sigma_\perp^2 = 4\mathcal{A} + \frac{A_0}{\sigma_\perp^2}\,, \tag{4.4.14}$$

   where A_0 is an arbitrary integration constant;

3. combining, finally, Eqs. (4.4.13) and (4.4.14) to obtain Eq. (4.4.11).

Note that from Eq. (4.4.14) one can easily calculate the arbitrary constant A_0, once the initial conditions are imposed. After combining Eq. (4.4.3) with (4.4.12), we finally get:

$$A_0 = \sigma_p^2\sigma_\perp^2 - \sigma_\perp^2{\sigma'_\perp}^2 - \frac{\sigma_\perp^2}{\lambda_0}\int U_w^2(r,\tau)\,d^2r \tag{4.4.15}$$

$$\text{or,}\quad A_0 = \sigma_p^2\sigma_\perp^2 - \sigma_\perp^2{\sigma'_\perp}^2 + \langle U_w(r,\tau)\rangle\sigma_\perp^2\,, \tag{4.4.16}$$

where we have observed that, here $-(1/\lambda_0)\int U_w^2(r,\tau)\,d^2r = \langle U_w(r,\tau)\rangle$.

We now evaluate the constant of motion A_0, by assuming the following initial (normalized) transverse distribution function:

$$f_0(r,p) = f(r,p,0) = \frac{\exp\left[-\left(r^2/\sigma_0^2 + p^2/\sigma_{p0}^2\right)\right]}{\pi\sigma_0^2\sigma_{p0}^2}\,, \tag{4.4.17}$$

which is consistent with the initial conditions for the second-order moments, viz., $\sigma_0 = \sigma_\perp(0)$, $\sigma_{p0} = \sigma_p(0)$, and $\sigma_0' = \sigma'(0) = 0$. By using these initial conditions in Eqs. (4.4.15) and (4.4.16), we easily get

$$\langle U_w(r,0)\rangle = -\frac{1}{2}\frac{n_{b0}}{n_0\gamma_0} \tag{4.4.18}$$

and

$$A_0 = \sigma_0^2\left(\sigma_{p0}^2 - \frac{1}{2}\frac{n_{b0}}{n_0\gamma_0}\right), \tag{4.4.19}$$

where $n_{b0} = N/\sigma_z \pi \sigma_0^2$ estimates the unperturbed volumic number density of the beam. It is worthy noting that $\epsilon \equiv \sigma_0 \sigma_{p0}$ is the emittance and $\pi \sigma_0 \sigma_{p0} = \pi \epsilon$ is the conserved area of the rms ellipse associated with a Gaussian beam travelling in vacuo in the presence of the cylindrically symmetric quadrupole-like potential well $Kr^2/2$, whose initial condition is provided by Eq. (4.4.17). Consequently, Eq. (4.4.19) becomes

$$A_0 = \epsilon^2 + \langle U_w(r,0) \rangle \sigma_0^2 = \epsilon^2 - \frac{1}{2} \frac{n_b}{n_0 \gamma_0} \sigma_0^2 . \tag{4.4.20}$$

The latter shows clearly that, when the constant of motion A_0 is positive, $\sqrt{A_0}$ plays the role of the emittance of our beam travelling through the plasma, having in vacuo the same initial conditions assumed for the Gaussian beam. In these conditions, $\sqrt{A_0}$ represents the beam emittance that is *modified* by the presence of the collective effects provided by the PWF self-interaction. However, to the ends of the rms envelope evolution, the beam motion through the plasma can be associated with a Gaussian beam travelling in vacuo in the presence of the quadrupole-like potential well $Kr^2/2$, whose emittance is given by $\sqrt{A_0} = \sigma_0 \overline{\sigma}_{p0}$, i.e., whose initial conditions are $\sigma_0 = \sigma_\perp(0)$, $\overline{\sigma}_{p0} \equiv \sqrt{\sigma_{p0}^2 - n_b/2 n_0 \gamma_0}$ (the radicand is positive because $A_0 > 0$), and $\sigma_0' = \sigma'(0) = 0$. Therefore, the initial distribution function to be used for the *equivalent Gaussian beam* (EGB) is

$$\overline{f}_0(r,p) = \frac{\exp\left[-\left(r^2/\sigma_0^2 + p^2/\overline{\sigma}_{p0}^2\right)\right]}{\pi \sigma_0^2 \overline{\sigma}_{p0}^2} . \tag{4.4.21}$$

With these initial conditions, the EGB performs the betatron-like rms envelope oscillations described above for the beam travelling through the plasma.

If the initial conditions are such that A_0 is not positive, then it is easy to see that the EGB is no longer stable and, therefore, our beam travelling through the plasma is no longer stable either.

In general, on the basis of the above results, we can easily conclude that, for the given initial conditions:

- If $A_0 < 0$, i.e.,

$$\frac{\epsilon}{\sigma_0} < 0.7 \left(\frac{n_b}{n_0 \gamma_0}\right)^{1/2} , \tag{4.4.22}$$

then the beam will experience the collapse.

- If $A_0 = 0$, i.e.,

$$\frac{\epsilon}{\sigma_0} = 0.7\left(\frac{n_b}{n_0\gamma_0}\right)^{1/2}, \tag{4.4.23}$$

then the beam remains in the self-equilibrium ($\sigma(\tau) = \sigma_0$).

- Finally, if $A_0 > 0$, i.e.,

$$\frac{\epsilon}{\sigma_{0\perp}} > 0.7\left(\frac{n_b}{n_0\gamma_0}\right)^{1/2}, \tag{4.4.24}$$

then the beam will execute stable betatron oscillations.

4.5 Self modulation in strongly nonlocal regime

In this section we study the transverse dynamics of a cylindrically symmetric beam in the strongly nonlocal regime, i.e., when $k_s\sigma_\perp \ll 1$ or $|\nabla_\perp U_w|^2 \gg k_s^2|U_w|^2$. Once this condition is used, the Poisson-type equation (4.2.2) reduces to:

$$\nabla_\perp^2 U_w = k_s^2\lambda_0 \int f\, d^2p\,. \tag{4.5.1}$$

Furthermore, it is easy to see that in this limiting case, Eq. (4.3.57) is still valid and can be cast as:

$$\frac{d^2\sigma_\perp^2}{d\tau^2} + 4K\sigma_\perp^2 = 4\mathcal{A} - 2\langle U_w\rangle\,, \tag{4.5.2}$$

where the constant of motion $\mathcal{A}$ is given by:

$$\mathcal{A} = \frac{1}{2}\sigma_{p\perp}^2 + \frac{1}{2}K\sigma_\perp^2 + \frac{1}{2}\langle U_w\rangle = \text{constant}\,. \tag{4.5.3}$$

Note that the general expression for $\langle U_w\rangle$ given by Eq. (4.3.36) here reduces to

$$\langle U_w\rangle = -\frac{1}{k_s^2\lambda_0}\int\left(\frac{\partial U_w}{\partial r}\right)^2 d^2r\,. \tag{4.5.4}$$

Note also that Eq. (4.5.2) differs from the virial equation that holds for the local regime for the presence, at the right hand side, of the self-energy $\langle U_w\rangle$ (constant of motion in both cases

has formally the same expression). In other words, in the local case the beam envelope equation can be exactly cast as an harmonic oscillator equation, whilst in the strongly nonlocal case Eq. (4.5.2) cannot be reduced to such a form. This implies that the collective effects introduced by the self-energy characterizes a different behavior of the beam from the point of view of the stability/instability. In the next section, we deepen these aspects, by considering the beam self-modulation in cylindrical symmetry.

We here express our governing equations in cylindrical coordinate and assume that the distribution function is cylindrically symmetric, i.e., $f = f(r, p, \tau)$, where r is the cylindrical radial coordinate and p is the corresponding conjugate momentum. Therefore, the Vlasov equation is

$$\frac{\partial f}{\partial \tau} + p\frac{\partial f}{\partial r} - \frac{\partial V}{\partial r}\frac{\partial f}{\partial p} = 0\,, \tag{4.5.5}$$

where

$$V(r, \tau) = \frac{1}{2}Kr^2 + U_w(r, \tau)\,. \tag{4.5.6}$$

The Poisson-type equation (4.5.1) can be formally integrated as:

$$U_w(r, \tau) = 2\pi k_s^2 \lambda_0 \int_0^r \frac{1}{r'}\, dr' \int_0^{r'} r''\, dr'' \int_0^{\infty} f(r'', \tau, p)\, p\, dp\,.$$

4.5.1 Aberration-less approximation

Since in the strongly nonlocal regime the beam is mostly confined in a smaller region around the propagation axis, it is reasonable to assume that the total potential $V(r, \tau)$ has a minimum for $r = 0$. Furthermore, due to the beam confinement around the z-axis ($k_s \sigma_\perp \ll 1$), we can expand $V(r, \tau)$ in powers of r up to r^2 (aberration-less approximation), viz.,

$$V(r, \tau) \simeq V(0, \tau) + \left(\frac{\partial V}{\partial r}\right)_{r=0} r + \frac{1}{2}\left(\frac{\partial^2 V}{\partial r^2}\right)_{r=0} r^2. \tag{4.5.7}$$

By using above equation we easily find that:

$$V(0, \tau) = U_w(0, \tau) = 0,\ \left(\frac{\partial V}{\partial r}\right)_{r=0} = 0 \tag{4.5.8}$$

and

$$\left(\frac{\partial^2 V}{\partial r^2}\right)_{r=0} = K + \overline{K}(\tau) \equiv k(\tau)\,, \tag{4.5.9}$$

where

$$\overline{K}(\tau) = \pi k_s^2 \lambda_0 \int_0^\infty f(0,p,\tau)\, p\, dp\,. \tag{4.5.10}$$

Therefore:

$$V(r,\tau) \simeq \frac{1}{2}\, k(\tau)\, r^2\,. \tag{4.5.11}$$

Note that the request of a minimum in $r = 0$ implies that $k(\tau) > 0$. Therefore, from Eqs. (4.5.9) and (4.5.10), we get the condition

$$K > -k_s^2 \lambda_0 \int_0^\infty f(0,p,\tau)\, p\, dp\,, \tag{4.5.12}$$

which, according to the definitions of k_s and λ_0, is always satisfied. On the other hand, for an initially given Gaussian beam distribution, the solution of the Vlasov Eq. (4.5.5) with the potential (4.5.11) is given by

$$f(r,p,\tau) = A\, \exp\left\{-\frac{1}{\epsilon}\left[\gamma(\tau)\, r^2 + 2\,\alpha(\tau)\, rp + \beta(\tau)\, p^2\right]\right\}, \tag{4.5.13}$$

where A is a normalization constant, ϵ is the beam emittance and the functions $\alpha(\tau)$, $\beta(\tau)$ and $\gamma(\tau)$ (the analog of the Twiss parameters in electron/radiation beam optics) obey the following first-order ordinary differential equations, viz.,

$$\frac{d\gamma}{d\tau} = 2k\alpha,\ \ \frac{d\beta}{d\tau} = -2\alpha \text{ and } \ \frac{d\alpha}{d\tau} = -2\gamma + 2k\beta\,. \tag{4.5.14}$$

For given initial condition, i.e., $\alpha_0 = \alpha(\tau = 0)$, $\beta_0 = \beta(\tau = 0)$ and $\gamma_0 = \gamma(\tau = 0)$, the solutions $\alpha(\tau)$, $\beta(\tau)$ and $\gamma(\tau)$ provide the explicit solution of the Vlasov equation that includes the collective effects of the beam self-modulation in the strongly nonlocal regime (in the aberration-less approximation). By using Eq. (4.5.14), it is easy to prove that:

$$\gamma(\tau)\beta(\tau) - \alpha^2(\tau) = \gamma_0\beta_0 - \alpha_0^2 = \text{constant}. \tag{4.5.15}$$

It is useful to fix $\gamma_0\beta_0 - \alpha_0^2 = 1$. In this way initial conditions γ_0, β_0, and α_0 are no longer independent. Furthermore, we introduce the following second order moment (see section 4.3):

$$\sigma_{rp}(\tau) = \langle rp \rangle = \sigma \frac{d\sigma}{d\tau} \,. \tag{4.5.16}$$

It can be easily seen that, if we perform explicitly the averages $\sigma^2 = \langle r^2 \rangle$, $\sigma_{p\perp}^2 = \langle p^2 \rangle$ and $\sigma_{rp} = \langle rp \rangle$, by means of the distribution (4.5.13), we easily get

$$\sigma^2(\tau) = \epsilon\beta(\tau), \quad \sigma_p^2(\tau) = \epsilon\gamma(\tau), \quad \sigma_{rp}(\tau) = \epsilon\alpha(\tau) \,. \tag{4.5.17}$$

Consequently, Eq. (4.5.15) allows us to obtain

$$\sigma^2 \, \sigma_p^2 - \sigma_{rp}^2 = \epsilon^2(\gamma\beta - \alpha^2) = \epsilon^2 \,. \tag{4.5.18}$$

Furthermore, by combining Eq. (4.5.14) into a differential equation for β, we finally get the following Ermakov-Pinney equation

$$\frac{d^2\sigma}{d\tau^2} + k(\tau)\,\sigma - \frac{\epsilon^2}{\sigma^3} = 0 \,. \tag{4.5.19}$$

On the other hand, substituting Eq. (4.5.13) into (4.5.10) we obtain

$$\overline{K}(\tau) = \left(\frac{k_s^2 \lambda_0}{2\pi} \right) \frac{1}{\sigma^2} \,. \tag{4.5.20}$$

Then, substituting in turn the latter and Eq. (4.5.9) in Ermakov-Pinney equation we finally get the following envelope equation (Sacherer-type equation), viz.,

$$\frac{d^2\sigma}{d\tau^2} + K\,\sigma + \frac{\eta}{\sigma} - \frac{\epsilon^2}{\sigma^3} = 0 \,, \tag{4.5.21}$$

where $\eta = k_s^2\lambda_0/2\pi = k_s^2 N/2\pi\sigma_z n_0\gamma_0$, which accounts for the collective effects (through the presence of N and n_0) as well as the magnetic field through k_s. The above envelope equation resembles the Sacherer's equation governing the envelope description of a non-laminar beam in conventional particle accelerators in the presence of magnetic focusing and space charge effects.

4.5.2 Self-modulation analysis by means of the Sagdeev potential

In order to perform an analysis of the self-modulation due to the PWF interaction in the strongly nonlocal regime and aberration-less approximation, we use the method of Sagdeev potential (or pseudo-potential) that can be constructed from the envelope Eq. (4.5.21). To this end, we introduce the following dimensionless quantities:

$$\tilde{\tau} = k_s\tau\,,\quad \tilde{\sigma} = k_s\sigma\,,\quad \tilde{K} = K/k_s^2\,,\quad \tilde{\epsilon} = k_s\epsilon\,.$$

Then, Eq. (4.5.21) can be cast as the motion equation of a single particle of unitary mass

$$\frac{d^2\tilde{\sigma}}{d\tilde{\tau}^2} = -\frac{\partial V_s(\tilde{\sigma})}{\partial\tilde{\sigma}}\,, \tag{4.5.22}$$

where

$$V_s(\tilde{\sigma}) = \frac{1}{2}\tilde{K}\tilde{\sigma}^2 + \frac{1}{2}\eta\ln\tilde{\sigma}^2 + \frac{\tilde{\epsilon}^2}{2\tilde{\sigma}^2}\,. \tag{4.5.23}$$

Note that the initial conditions of Eq. (4.5.21) are:

$$\tilde{\sigma}_0 \equiv \tilde{\sigma}(\tilde{\tau}=0) \quad\text{and}\quad \tilde{\sigma}_0^{'} \equiv (d\tilde{\sigma}/d\tilde{\tau})_{\tilde{\tau}=0}\,.$$

Once these conditions are fixed, the mechanical energy (which is constant) of a representative point in the $\tilde{\sigma}$ - space is fixed, i.e.,

$$E = \frac{1}{2}\left(\frac{d\tilde{\sigma}}{d\tilde{\tau}}\right)^2 + \frac{1}{2}\tilde{K}\tilde{\sigma}^2 + \frac{1}{2}\eta\ln\tilde{\sigma}^2 + \frac{\tilde{\epsilon}^2}{2\tilde{\sigma}^2} = \frac{1}{2}\tilde{\sigma}_0'^2 + \frac{1}{2}\tilde{K}\tilde{\sigma}_0^2 + \frac{1}{2}\eta\ln\tilde{\sigma}_0^2 + \frac{\tilde{\epsilon}^2}{2\tilde{\sigma}_0^2}\,.$$

Then, we can analyse the features of the corresponding motion that characterizes the evolution of $\tilde{\sigma}(\tau)$. This evolution includes in particular the features related to the stability/instability.

Figures 4.7 and 4.8 display the Sagdeev potential $V_s(\tilde{\sigma})$, i.e., Eq. (4.5.23) and the corresponding numerical solution of the Eq. (4.5.22) [namely, solution of Eq. (4.5.21)] for given initial conditions ($\tilde{\sigma}_0 = 1.5$, $\tilde{\sigma}_0' = 0$) and different parameters $\tilde{K}$ and η. From all the displayed cases, it is clear that the self-modulation is stable. This is not only a result for the given initial conditions and the choices of the parameters. In fact, the analysis of Eq. (4.5.23) for arbitrary values of $\tilde{K}$ and η leads to conclude that the potential well is always trapping.

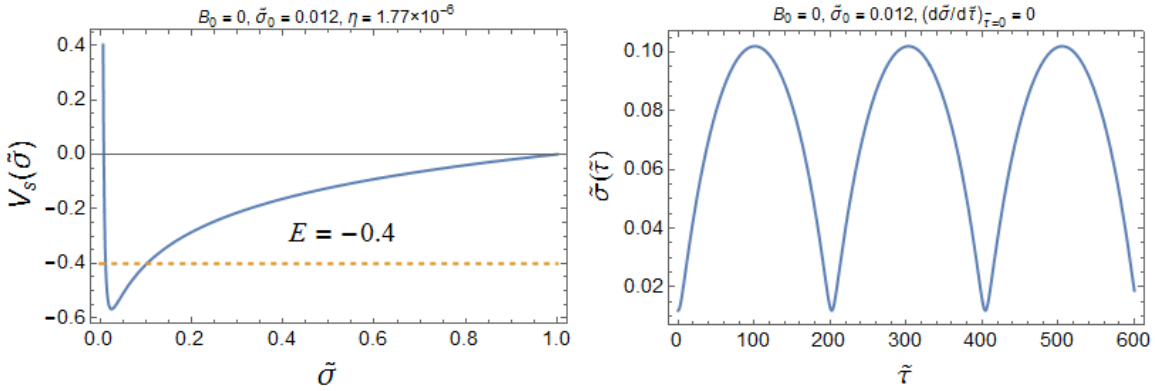

Figure 4.7: Sagdeev potential V_s (left) as defined by Eq. (4.5.23) and the corresponding numerical solution (right) of the Eq. (4.5.21) in absence of external magnetic field, where the plot of V_s is scaled by a factor 10^5.

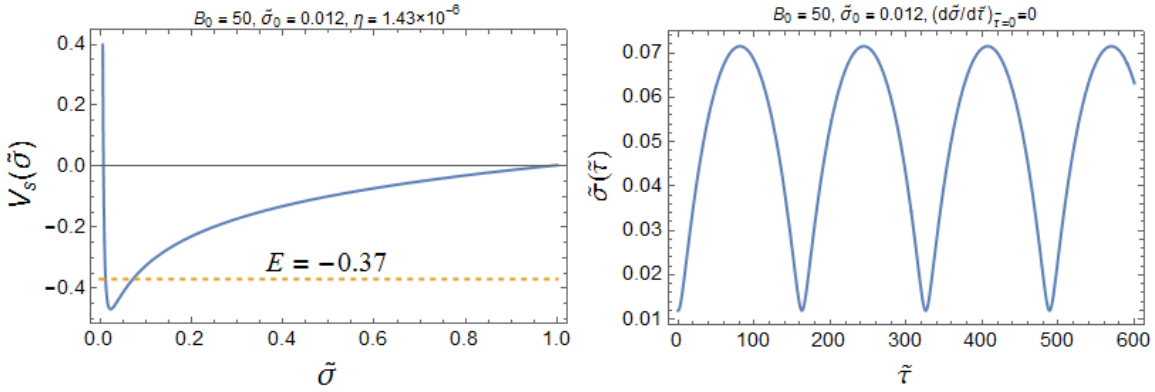

Figure 4.8: Sagdeev potential V_s (left) as defined by Eq. (4.5.23) and the corresponding numerical solution (right) of the Eq. (4.5.21) in the presence of a strong external magnetic field, where the plot of V_s is scaled by a factor 10^5.

If the energy E coincides with the minimum of the potential well ($\tilde{\sigma}_0 = \bar{\sigma}$), the beam is in a stationary state (self-equilibrium) and its spot size does not change, being fixed to the initial value $\tilde{\sigma}_0$ (note that $\tilde{\sigma'}_0 = 0$), according to Eq. (4.5.21), i.e.,

$$\tilde{K}\,\bar{\sigma} + \frac{\eta}{\bar{\sigma}} - \frac{\tilde{\epsilon}^2}{\bar{\sigma}^3} = 0\,, \tag{4.5.24}$$

where we have expressed Eq. (4.5.21) in terms of the dimensionless quantities and imposed the equilibrium condition $d^2\tilde{\sigma}/d\tilde{\tau}^2 = 0$. Note that in Figures 4.7 - 4.9, we have fixed the parameters in such a way that $\bar{\sigma} \sim 0.025$. This facilitates the analysis we are going to

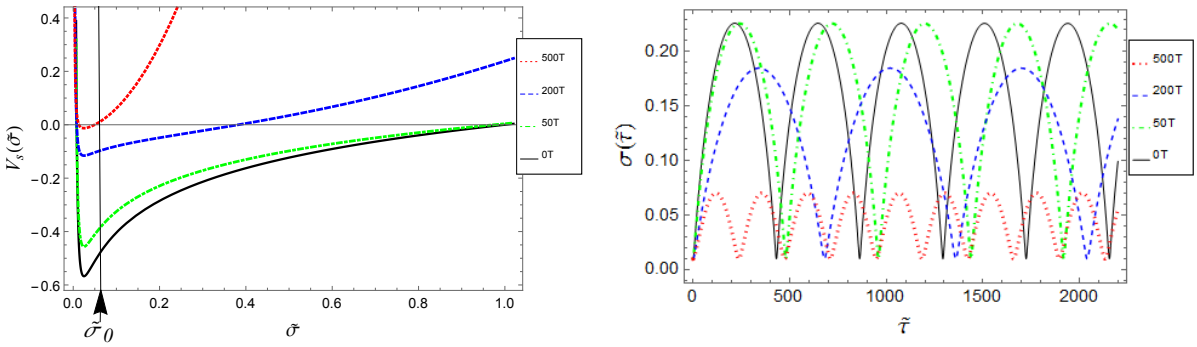

Figure 4.9: Sagdeev potential V_s as defined by Eq. (4.5.23) and corresponding oscillations of spot sizes for the different values of the external magnetic field amplitude B_0, ranging from laboratory to astrophysical environments. Initial conditions defined by $\tilde{\sigma}_0$ sufficiently small and $\tilde{\sigma}'_0 = 0$. Here, the plot of V_s is scaled by a factor 10^5

perform.

If the energy is fixed to a value above the minimum of the potential well with $\tilde{\sigma}_0 > \bar{\sigma}$ and, for simplicity, $\tilde{\sigma'}_0 = 0$, the motion of the representative point will be a nonlinear oscillation, provided that the condition $\tilde{\sigma} \ll 1$ is fulfilled. Therefore, the beam spot size will execute stable nonlinear transverse oscillations as a result of the stable beam self-modulation (see Figures 4.7 and 4.8). It would be emphasized that the features of the beam self-modulation strongly depend on the external magnetic field amplitude B_0. This is clear by observing that the nonlinear oscillations described by Eq. (4.5.21) depend on the magnetic focusing strength K which is proportional to B_0^2. Figures 4.7 and 4.8 show sensitive changes in both the structures of the Sagdeev potential and the period of the corresponding beam self-modulation as function of B_0, when all the beam and plasma parameters are fixed (note that in these conditions η depends on B_0 only). Figure 4.9 displays $V_s(\tilde{\sigma})$ for different values of B_0, ranging from 0 to 500T (i.e., from laboratory to astrophysical environments).

It is worthy noting that, although the condition $\tilde{\sigma} \ll 1$ is initially fulfilled, there are specific initial conditions that are leading to an unstable evolution of the beam modulation, i.e., the self-modulation instability (SMI). In fact, as illustrated in Figure 4.9, if we choose σ_0 sufficiently less than $\bar{\sigma}$, the corresponding energy E will be sufficiently high to allow $\tilde{\sigma}$ to grow until the kinetic energy of the representative point becomes zero, i.e., $\tilde{\sigma'}^2/2 = 0$. Then,

if the magnetic field is strong enough, its trapping effect limits the excursion of $\tilde{\sigma}$ oscillations to values that are still of the same order of magnitude of $\tilde{\sigma}_0$ (Figure 4.9). However, if B_0 is zero or assumes relatively small values, $\tilde{\sigma}$ can easily grow until one or two orders of magnitude greater than $\tilde{\sigma}_0$. This aspect is deepen in Section 4.6 from qualitative point of view, and in Section 4.7 from quantitative point of view.

4.6 Qualitative stability analysis

The analysis of the displayed plots leads to conclude that, during the beam evolution, provided that ideally the system is always in the strongly nonlocal regime, the self-modulation is stable and the potential well is always trapping. However, as we have already indicated above, this condition is fulfilled provided that $\left|\nabla_\perp^2 U_w\right| \gg k_s^2 |U_w|$ (i.e., $\tilde{\sigma} \ll 1$). Therefore, for a suitable choice of the initial conditions, such that σ satisfies this inequality, Figure 4.9 shows that the envelope self-modulation is stable and represents periodic solutions in σ. This corresponds to fix the total energy E to relatively small values, in Figure 4.9 for some of the profiles of the Sagdeev potential. If the energy E coincides with the minimum of the potential well (i.e., $\tilde{\sigma}_0 = \bar{\sigma}$), the beam is in a stationary state (self-equilibrium) and its spot size does not change, being fixed to the initial value $\tilde{\sigma}_0$ (note that $(d\tilde{\sigma}/d\tilde{\tau})_{\tilde{\tau}=0} = 0$), according to Eq. (4.5.22). If the energy is fixed to a value above the minimum of the potential well with $\tilde{\sigma}_0 > \bar{\sigma}$, the motion of the representative point will be a nonlinear oscillation, provided that the condition $\tilde{\sigma} \ll 1$ is still fulfilled. In particular, values of E that are very close to the minimum imply harmonic oscillations of σ. However, as B_0 increases, sensitive changes in both the structure of the Sagdeev potential and the period of the corresponding beam self-modulation are observed in such a way that the beam spot size will execute more and more stable nonlinear transverse oscillations. It is worthy noting that, although the condition $\tilde{\sigma} \ll 1$ is initially fulfilled, there are specific initial conditions that lead to an unstable evolution of the beam modulation, i.e., SMI. In fact, as illustrated in Figure 4.9, if we choose $\tilde{\sigma}_0$ sufficiently less than $\bar{\sigma}$, the corresponding energy E will be sufficiently high to allow $\tilde{\sigma}$ to

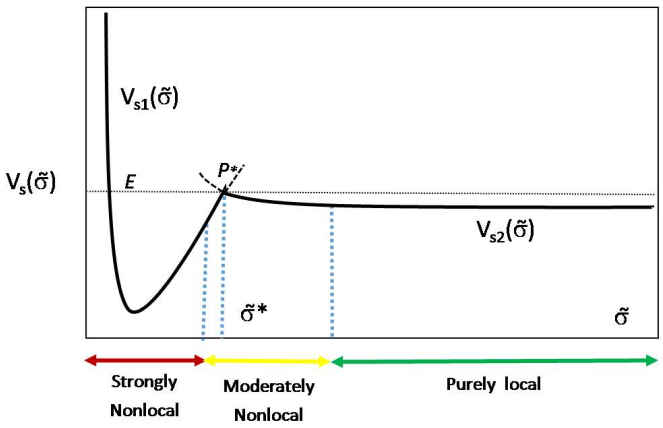

Figure 4.10: Qualitative plot of V_s over all the three different regimes.

grow until the kinetic energy of the representative point becomes zero, i.e., $1/2\,(d\tilde{\sigma}/d\tilde{\tau})^2 = 0$. Then, if the magnetic field is strong enough, its trapping effect limits the excursion of $\tilde{\sigma}$ oscillations to values that are still of the same order of magnitude of $\tilde{\sigma}_0$. However, if $B_0 = 0$

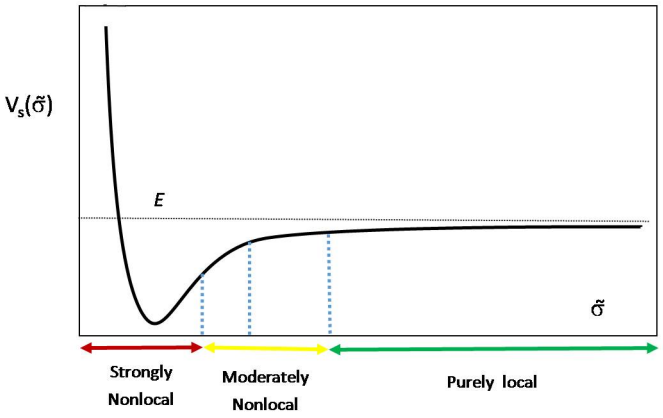

Figure 4.11: Qualitative plot of V_s over all the regimes with a qualitative smoothing of the moderately non-local regime.

or assumes relatively small values, $\tilde{\sigma}$ can easily grow and becomes much greater than $\tilde{\sigma}_0$. Otherwise, when this is just about to happen, the condition $\tilde{\sigma} << 1$ is no longer fulfilled and, therefore, the system enters progressively into the *moderately nonlocal regime* (i.e., $\tilde{\sigma} \sim 1$) and then into the *purely local regime* (i.e., $\tilde{\sigma} >> 1$) [58]. We conclude that, although

the system starts with an initial condition falling into the strongly nonlocal regime, it may rapidly violate the condition $\tilde{\sigma} << 1$ in such a way that its time evolution leads finally the beam to the region of local regime where the self modulation becomes unstable. To study this physical circumstance, we restrict our analysis to the case of $B_0 = 0$ ($k_s = k_p$). It is now useful to plot it as function of the dimensionless variable $\tilde{\sigma} \equiv k_p\sigma$. According to Figure 4.10, the plot can be qualitatively divided into the three regions of $\tilde{\sigma}$, ranging from $\tilde{\sigma} = 0$ to at least $\tilde{\sigma} \sim 10 - 10^2$, corresponding to strongly nonlocal (i.e., $\tilde{\sigma} \ll 1$), moderately non local (i.e., $\tilde{\sigma} \sim 1$) and purely local (i.e., $\tilde{\sigma} \gg 1$) regimes, respectively. Therefore, the Sagdeev potential should assume different shapes in the different regions. This implies that, out of the region $\tilde{\sigma} \ll 1$, the Sagdeev potential has to be determined starting with the appropriate Vlasov-Poisson-type system of equations. Since we are interested in providing a qualitative explanation of the unstable evolution of the self-modulation, we determine the analytical expression of the Sagdeev potential in the purely local region. Then, we try to approach qualitatively the moderately nonlocal region just by prolonging, one toward another, the plot of the strongly nonlocal region and the plot of the purely local region, respectively. The intersection of these two branches is illustrated in Figure 4.10, where the point of intersection is denoted by P^*. In the $\tilde{\sigma}$-space it corresponds to the value $\tilde{\sigma}^*$. On the scale of the potential adopted in Figure 4.10, the branch of the purely local region, compared to the nonlocal one, appears practically constant, because it varies much slowly in $\tilde{\sigma}$. According to the analytical treatment presented before, these two branches are respectively given by:

$$V_{s1}(\tilde{\sigma}) = \frac{1}{2}\eta \ln \tilde{\sigma}^2 + \frac{\tilde{\epsilon}^2}{2\tilde{\sigma}^2} \ , \ 0 < \tilde{\sigma} \leq \tilde{\sigma}^* \, , \tag{4.6.1}$$

$$V_{s2}(\tilde{\sigma}) = \frac{1}{2}\left(\frac{\tilde{\epsilon}^2}{\tilde{\sigma}_0^2} - \frac{1}{2}\frac{n_b}{n_0\gamma_0}\right)\frac{\tilde{\sigma}_0^2}{\tilde{\sigma}^2} + C_0 \ , \ \tilde{\sigma} \geq \tilde{\sigma}^* \, , \tag{4.6.2}$$

where $\tilde{\sigma}_0 = \tilde{\sigma}(0)$, and

$$C_0 = \frac{1}{2}\eta \ln \tilde{\sigma}^{*2} + \frac{1}{4}\frac{n_b}{n_0\gamma_0}\frac{\tilde{\sigma}_0^2}{\tilde{\sigma}^{*2}}$$

is the constant which allows the continuity between the two branches. Figure 4.11 displays qualitatively these two brunches once a qualitative smoothing of the moderately non-local

regime is done. This, of course, is only a qualitative way to connect the nonlocal region with the local one. From Figures 4.10 and 4.11 it is evident that, with initial conditions $\tilde{\sigma}_0$ falling in the strongly nonlocal region (i.e., $\tilde{\sigma}_0 \ll 1$) and such that the total energy of the representative point in the Sagdeev potential is $\leq E$, the variation in $\tilde{\sigma}$ are stable (periodic self-modulations). But if the initial conditions correspond to a total energy which is $> E$, then the representative point is no longer trapped in the potential. This corresponds to a progressive increasing of $\tilde{\sigma}$, i.e., to an unstable evolution of the beam envelope modulations.

It is worthy noting that the flatness of the asymptotic region of $\tilde{\sigma}$ (i.e., purely local regime) does not depend on the sign of the difference $\left(\frac{\tilde{\epsilon}^2}{\tilde{\sigma}_0^2} - \frac{1}{2}\frac{n_b}{n_0\gamma_0}\right)$. However, it is easy to see that the time evolution in the purely local region is given by

$$\tilde{\sigma}^2(\tilde{\tau}) = \left(\frac{\tilde{\epsilon}^2}{\tilde{\sigma}_0^2} - \frac{1}{2}\frac{n_b}{n_0\gamma_0}\right)(\tilde{\tau} - \tilde{\tau}^*)^2 + \tilde{\sigma}^{*2}\,, \tag{4.6.3}$$

where $\tilde{\tau} = k_p\tau$ and $\tilde{\tau}^*$ is the timelike value of $\tilde{\tau}$ such that $\tilde{\sigma}(\tilde{\tau}^*) = \tilde{\sigma}^*$. Therefore, the growth of $\tilde{\sigma}$ is compatible only with the positive value of the difference $\left(\frac{\tilde{\epsilon}^2}{\tilde{\sigma}_0^2} - \frac{1}{2}\frac{n_b}{n_0\gamma_0}\right)$.

4.7 Quantitative analysis of beam self-modulation in the arbitrary regime

4.7.1 General solution of U_w

In this section we provide a quantitative description of the self-modulated dynamics of a cylindrically symmetric beam beyond the diverse special regimes that have been considered in the previous section, such as the nonlocal (strong and moderate) and purely local cases. Here, we develop a more general approach finalised to carry out self-consistent envelope description associated with the Vlasov-Poisson-type system keeping both terms of the left-hand side of Eq. (4.2.2), i.e., $\nabla_\perp^2 U_w$ and $k_s^2 U_w$. To this end, we assume that the system is not far from the local thermal equilibrium. In this way, the solution of the Vlasov equation, i.e.,

$$\frac{\partial f}{\partial \tau} + p\frac{\partial f}{\partial r} - \frac{\partial V}{\partial r}\frac{\partial f}{\partial p} = 0\,, \tag{4.7.1}$$

where $f = f(r, p, \tau)$ is the cylindrically symmetric distribution function and

$$V = V(r, \tau) = \frac{1}{2} K r^2 + U_w(r, \tau)\,,$$

can be approximated by the following form:

$$f(r, p, \tau) = n_b(r, \sigma(\tau))\, \frac{e^{-p^2/\sigma_p^2}}{\pi \sigma_p^2}\,, \tag{4.7.2}$$

where $\sigma_p^2(\tau) = \langle p^2 \rangle$ and $\sigma^2(\tau) = \langle r^2 \rangle$. By introducing the dimensionless quantities: $\tilde{r} = k_s r$, $\tilde{\tau} = k_s \tau$, $\tilde{p} = k_s p$, $\tilde{\sigma} = k_s \sigma$, and $\tilde{\sigma}_p = k_s \sigma_p$, solution (4.7.2) can be cast as

$$f(\tilde{r}, \tilde{p}, \tilde{\tau}) = n_b(\tilde{r}, \tilde{\sigma}(\tilde{\tau}))\, \frac{e^{-\tilde{p}^2/\tilde{\sigma}_p^2}}{\pi \tilde{\sigma}_p^2}\,, \tag{4.7.3}$$

and the Poisson-type equation (4.2.2) in cylindrical co-ordinates, i.e.,

$$\frac{1}{r} \frac{\partial}{\partial r} \left(r \frac{\partial U_w}{\partial r} \right) - k_s^2 U_w = k_s^2 \lambda\, n_b\,, \tag{4.7.4}$$

can be cast as

$$\frac{\partial^2 U_w}{\partial \tilde{r}^2} + \frac{1}{\tilde{r}} \frac{\partial U_w}{\partial \tilde{r}} - U_w = \lambda\, n_b\,, \tag{4.7.5}$$

where, $U_w = U_w(\tilde{r}, \tilde{\sigma})$ and $\lambda = 1/n_0 \gamma_0$.

Note that we have explicitly indicated the dependence of f on $\tilde{\tau}$ also trhough the time dependence of $\tilde{\sigma}(\tilde{\tau})$ and $\tilde{\sigma}_p(\tilde{\tau})$, respectively. Once the time evolution of $\tilde{\sigma}$ is known, the time dependence of n_b is known, as well. Therefore, starting from an initial condition, i.e., $\tilde{\sigma}_0 = \tilde{\sigma}(\tilde{\tau} = 0)$ and $\tilde{\sigma}'_0 = \tilde{\sigma}'(\tilde{\tau} = 0)$, our analysis will allow us to study the envelope evolution of the beam not far from the local thermal equilibrium. However, such an evolution can be stable and unstable, being dependent on the initial conditions. Therefore, we are looking for suitable criteria that allows us to predict the stable or unstable evolution of the beam envelope, just on the basis of the given initial conditions. To this end, we need to find the envelope equation corresponding to our physical problem.

Equation (4.7.5) has the following solution

$$U_w(\tilde{r}, \tilde{\sigma}) = -\lambda \left[K_0(\tilde{r}) \int_0^{\tilde{r}} I_0(\tilde{r}_1) n_b(\tilde{r}_1, \tilde{\sigma}) \tilde{r}_1 d\tilde{r}_1 + I_0(\tilde{r}) \int_{\tilde{r}}^{\infty} K_0(\tilde{r}_2) n_b(\tilde{r}_2, \tilde{\sigma}) \tilde{r}_2 d\tilde{r}_2 \right] \tag{4.7.6}$$

(where $I_0(\tilde{r})$ and $K_0(\tilde{r})$ are the modified Bessel functions of the first and second kind, respectively) that satisfies the boundary conditions:

$$\lim_{\tilde{r}\to 0} U_w(\tilde{r},\tilde{\sigma}) < \infty\,, \quad \lim_{\tilde{r}\to\infty} U_w(\tilde{r},\tilde{\sigma}) = 0\,. \tag{4.7.7}$$

Figure 4.12 displays the initial beam density $n_b(\tilde{r},\tilde{\sigma}_0)$ for the following four different profiles:

- *Parabola-square*, i.e.,

$$n_{b1}(\tilde{r},\tilde{\sigma}) = \frac{3n_{b0}}{4\pi\tilde{\sigma}^2}\left(1-\frac{\tilde{r}^2}{4\tilde{\sigma}^2}\right)^2\Theta\left(1-\frac{\tilde{r}}{2\tilde{\sigma}}\right), \tag{4.7.8}$$

  where Θ is a Heaviside function.

- *Gaussian*, i.e.,

$$n_{b2}(\tilde{r},\tilde{\sigma}) = \frac{n_{b0}}{\pi\tilde{\sigma}^2}\,\exp\left(-\frac{\tilde{r}^2}{\tilde{\sigma}^2}\right). \tag{4.7.9}$$

- *Lorentzian square*, i.e.,

$$n_{b3}(\tilde{r},\tilde{\sigma}) = \frac{n_{b0}}{4\pi\tilde{\sigma}^2}\left(\frac{1}{1+\tilde{r}^2/(4\tilde{\sigma}^2)}\right)^2. \tag{4.7.10}$$

- *Cosine-square*, i.e.,

$$n_{b4}(\tilde{r},\tilde{\sigma}) = \frac{2\pi\, n_{b0}}{(2.07252\tilde{\sigma})^2(\pi^2-4)}\,\cos^2\left(\frac{\pi}{2}\frac{\tilde{r}}{(2.07252\tilde{\sigma})}\right)\Theta\left(1-\frac{\tilde{r}}{2.07252\tilde{\sigma}}\right). \tag{4.7.11}$$

For simplicity, in Figure 4.12, we have chosen $\tilde{\sigma}_0 = 1$. Figure 4.13 shows U_w as function of $\tilde{r}$ at $\tilde{\tau} = 0$, with $\tilde{\sigma}_0 = 1$, for all the above different profiles, whereas Figure 4.14 displays the $3D$ plot of U_w as function of $\tilde{x}$ and $\tilde{y}$ ($\tilde{r} = \sqrt{\tilde{x}^2+\tilde{y}^2}$) for the case of *parabola-square* density profile (see Eq. (4.7.8)). We note that in Figure 4.13 the shape of $U_w(\tilde{r},\tilde{\sigma}_0)$ is similar for all the profiles. Given this similarity, in the followings we will obtain the evolution of $\tilde{\sigma}$ for one of the above profiles, only. Most of both qualitative and quantitative considerations that we will develop for this case will be also applied to all the other cases. However, to the ends of determining the general expression of the envelope equation, for the time being we proceed by considering an arbitrary profile of n_b.

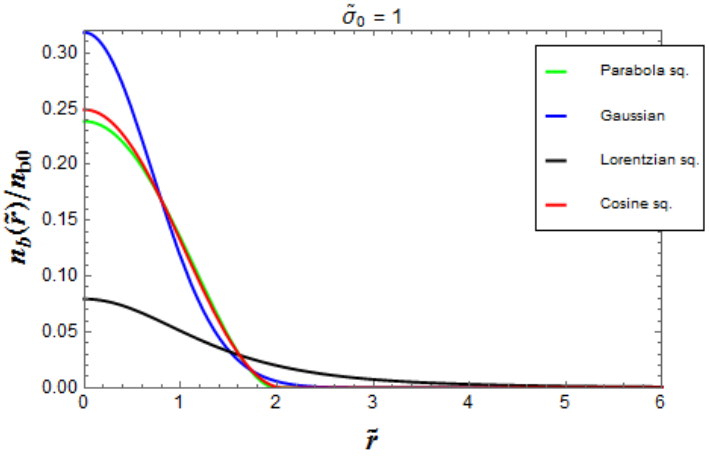

Figure 4.12: Plot of different initial profiles as function of $\tilde{r}$.

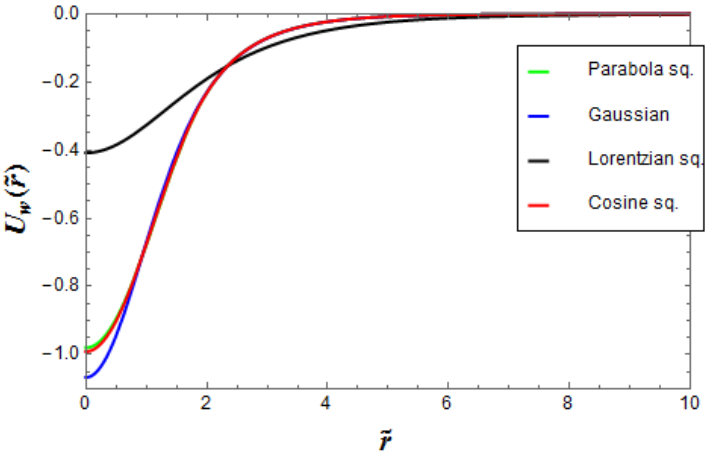

Figure 4.13: Plot of different Wake potential, U_w, for different density profiles. The plot is scaled here by a factor 10^6.

4.7.2 Envelope equation and Sagdeev potential in the general case

In this section, we derive the envelope equation starting from Eq. (4.3.57) that we rewrite in the dimensionless form, i.e.,

$$\frac{d^2\tilde{\sigma}^2}{d\tilde{\tau}^2} + 4\tilde{K}\tilde{\sigma}^2 = 4\mathcal{A} + \frac{4\pi}{k_s^2\lambda_0}\int_0^\infty \left|\frac{\partial U_w}{\partial \tilde{r}}\right|^2 \tilde{r}d\tilde{r}\,, \tag{4.7.12}$$

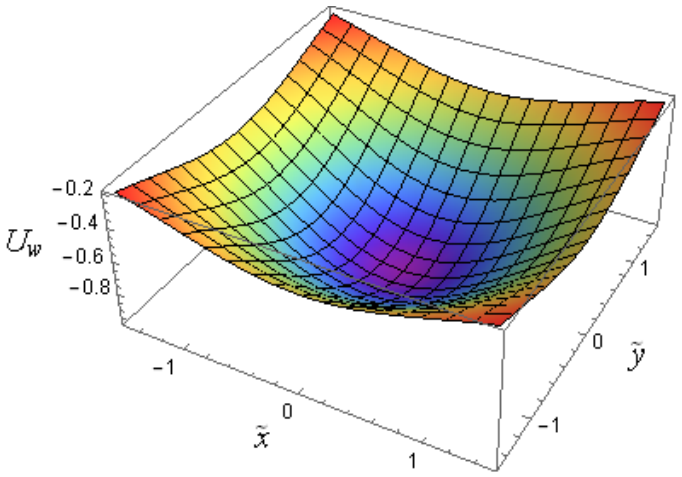

Figure 4.14: 3D plot of plasma wake potential, $U_w(\tilde{r})$ for the parabola-square profile where $\tilde{r} = \sqrt{\tilde{x}^2 + \tilde{y}^2}$. The plot is scaled here by a factor 10^6.

where $\tilde{K} = K/k_s^2$. We multiply the latter by $d\tilde{\sigma}^2/d\tilde{\tau}$. Then, we integrate one time with respcet to $\tilde{\tau}$, obtaining:

$$2\left(\frac{d\tilde{\sigma}}{d\tilde{\tau}}\right)^2 + 2\tilde{K}\tilde{\sigma}^2 = 4\mathcal{A} + \frac{2}{\tilde{\sigma}^2}\int G(\tilde{\tilde{\sigma}})\,\tilde{\sigma}\,d\tilde{\sigma} + \frac{\mathcal{E}_0}{\tilde{\sigma}^2}\,, \tag{4.7.13}$$

where

$$G(\tilde{\sigma}) = \frac{4\pi}{k_s^2\lambda_0}\int_0^\infty \left|\frac{\partial U_w(\tilde{r},\tilde{\sigma})}{\partial\tilde{r}}\right|^2 \tilde{r}d\tilde{r}\,, \tag{4.7.14}$$

and $\mathcal{E}_0$ is an integration constant, which can be evaluated by using the initial conditions, i.e.,

$$\mathcal{E}_0 = 2\tilde{\sigma}_0^2\tilde{\sigma}_0'^2 + 2\tilde{K}\tilde{\sigma}_0^4 - 4\mathcal{A}\tilde{\sigma}_0^2 - 2\left[\int G(\tilde{\sigma})\,\tilde{\sigma}\,d\tilde{\sigma}\right]_{\tilde{\sigma}=\tilde{\sigma}_0}. \tag{4.7.15}$$

Now, we expand $d^2\tilde{\sigma}^2/d\tilde{\sigma}^2$ in Eq. (4.7.12), i.e., $d^2\tilde{\sigma}^2/d\tilde{\sigma}^2 = 2\,(d\tilde{\sigma}/d\tilde{\tau})^2 + 2\tilde{\sigma}d^2\tilde{\sigma}/d\tilde{\tau}^2$, then combine this with Eq. (4.7.13). We finally obtain the following envelope equation:

$$\frac{d^2\tilde{\sigma}}{d\tilde{\tau}^2} + \tilde{K}\tilde{\sigma} + \frac{\mathcal{E}_0}{2\tilde{\sigma}^3} + \frac{1}{\tilde{\sigma}^3}\int G(\tilde{\sigma})\,\tilde{\sigma}\,d\tilde{\sigma} - \frac{G(\tilde{\sigma})}{2\tilde{\sigma}} = 0\,. \tag{4.7.16}$$

In a way fully similar to the one shown in the previous sections, we introduce also here the definition of Sagdeev potential, i.e.,

$$\frac{d^2\tilde{\sigma}}{d\tilde{\tau}^2} = -\frac{\partial V_s}{\partial\tilde{\sigma}}\,.$$

Then, unless an arbitrary constant, we get:

$$V_s(\tilde{\sigma}) = \frac{1}{2}\tilde{K}\tilde{\sigma}^2 - \frac{\mathcal{E}_0}{4\tilde{\sigma}^2} - \frac{1}{2\tilde{\sigma}^2}\int_{\tilde{\sigma}} G(\tilde{\sigma}')\,\tilde{\sigma}'\,d\tilde{\sigma}'\,. \tag{4.7.17}$$

Note that in Eqs. (4.7.15) - (4.7.17) the integration in $d\tilde{\sigma}$ is indefinite. Furthermore, the last two terms at left-hand side of Eq. (4.7.16) and at right-hand side of Eq. (4.7.17) have to be evaluated explicitly by substituting the explicit form of $n_b(\tilde{r},\tilde{\sigma})$ in Eq. (4.7.6), as we do in the next section.

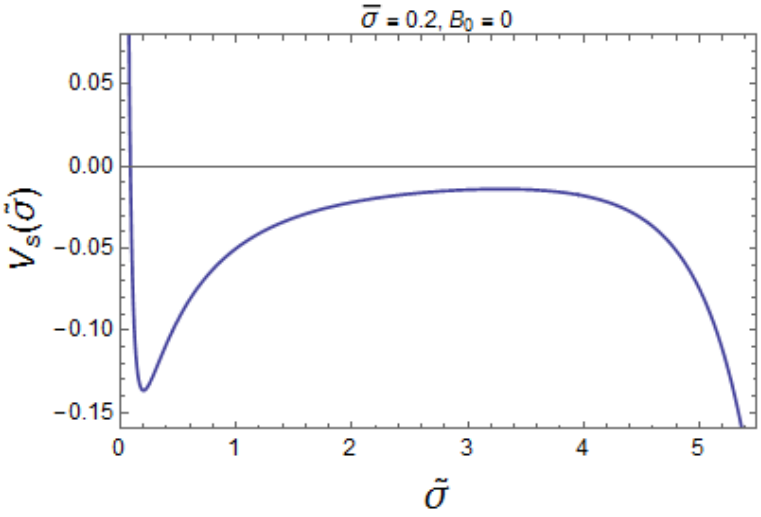

Figure 4.15: V_s as function of $\tilde{\sigma}$ for the entire range of values and for a relatively small point of minimum, i.e., $\bar{\sigma} = 0.2$.

4.7.3 Analysis of the envelope self-modulation in the general case

Once we have replaced the explicit form of the beam density in Eq. (4.7.6), we have evaluated numercally $U_w(\tilde{r},\tilde{\sigma})$. The latter, in turn has been used to evaluate numerically the function $G(\tilde{\sigma})$, as defined by Eq. (4.7.14). Therefore, the numerical knowledge of $G(\tilde{\sigma})$ has allowed us to determine numerically the Sagdeev potential defined by Eq. (4.7.17) and to integrate numerically the envelope equation (4.7.16) for given initial conditions. As we already pointed out in the previous sections, we have performed this analysis by considering only the beam profile defined by Eq. (4.7.8), since the features of the other profiles (Eqs.

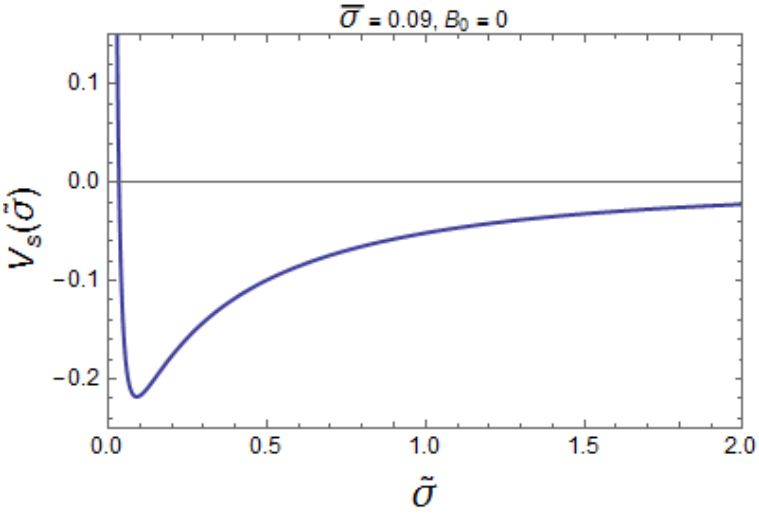

Figure 4.16: V_s as function of $\tilde{\sigma}$ ranging in the nonlocal region, for a very small point of minimum, i.e., $\bar{\sigma} = 0.09$.

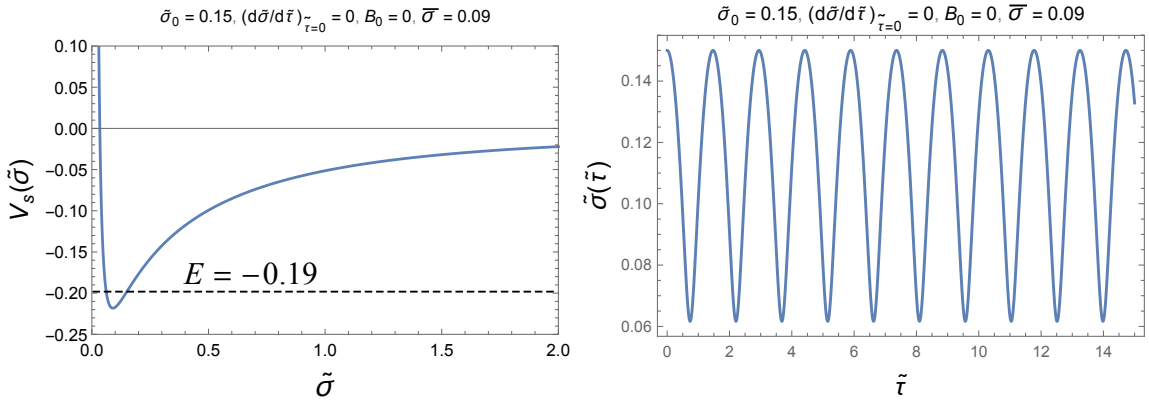

Figure 4.17: Left: V_s as function of $\tilde{\sigma}$, for a very small point of minimum, i.e., $\bar{\sigma} = 0.09$. Right: envelope oscillations corresponding to initial conditions that fix $E < 0$ (see left) above the minimum, but below the plateau, i.e., $E = -0.19$.

(4.7.9) - (4.7.11)) are very similar. Due to this similarity, the analysis permits us extrapolate considerations and write that are the same for all cylindrically symmetric bell-like shaped density profiles. We restrict our discussion to the case of $B_0 = 0$.

Figures 4.15 and 4.16 display the structure of $V_s(\tilde{\sigma})$ in two different scales of $\tilde{\sigma}$. Figure 4.15 shows almost entire shape of $V_s(\tilde{\sigma})$, whereas Figure 4.16 shows s similar structure on a smaller scale of $\tilde{\sigma}$. In all profiles obtained (including a number is not displayed here),

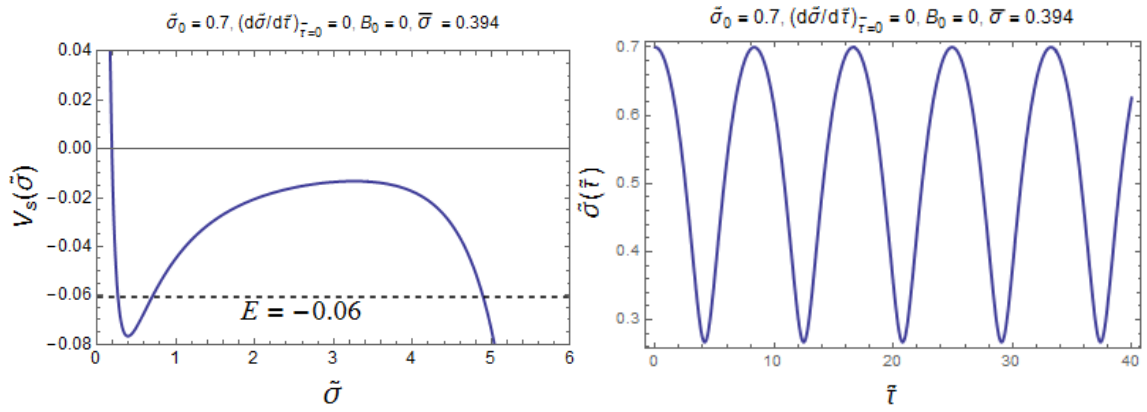

Figure 4.18: Left: V_s as function of $\tilde{\sigma}$, for a relatively small point of minimum, i.e., $\bar{\sigma} = 0.394$. Right: envelope oscillations corresponding to initial conditions that fix $E < 0$ (see left) above the minimum, but below the plateau, i.e., $E = -0.06$.

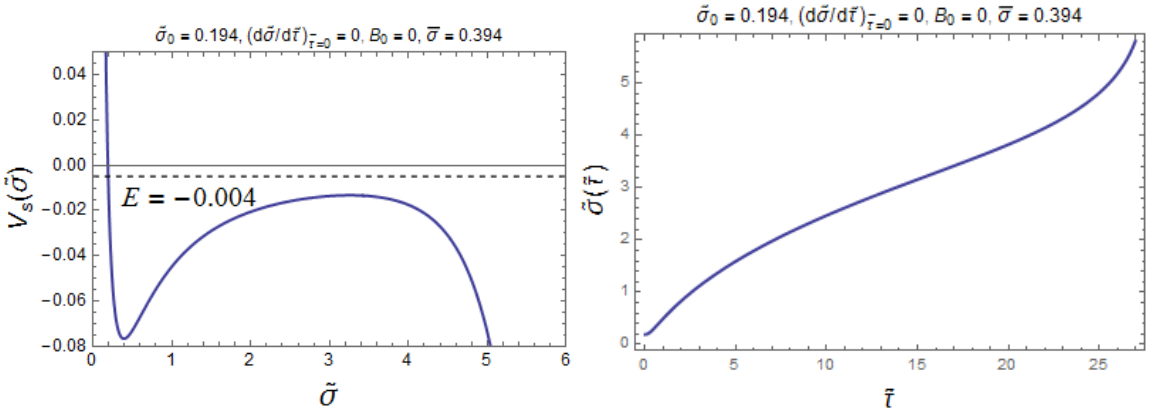

Figure 4.19: Left: V_s as function of $\tilde{\sigma}$, for a relatively small point of minimum, i.e., $\bar{\sigma} = 0.394$. Right: envelope oscillations corresponding to initial conditions that fix $E < 0$ (see left) above the minimum, but below the plateau (i.e., $E = -0.004$), and therefore leading to an unstable evolution of the beam envelope, starting from of values of $\tilde{\sigma}_0$ sufficiently small between the asymptote around zero and $\bar{\sigma}$.

$V_s(\tilde{\sigma})$ has a relative minimum in the region of relatively small or very small $\tilde{\sigma}$ (i.e., $\tilde{\sigma} \ll 1$). Approaching the adjacent region of larger $\tilde{\sigma}$ ($\gtrsim 1$), $V_s(\tilde{\sigma})$ grows slowly reaching a region of a *plateau*, with a relatively long extent compared to the one where the relative minimum is located. Further larger values of $\tilde{\sigma}$ lead to a region where $V_s(\tilde{\sigma})$ decrease very fast showing the existence of a vertical asymptote. Another asymptote exists for $\tilde{\sigma} \to 0$. Figures 4.15 and 4.16 are plotted for different values of $\tilde{\sigma}$, say $\bar{\sigma}$, corresponding to the minimum of V_s,

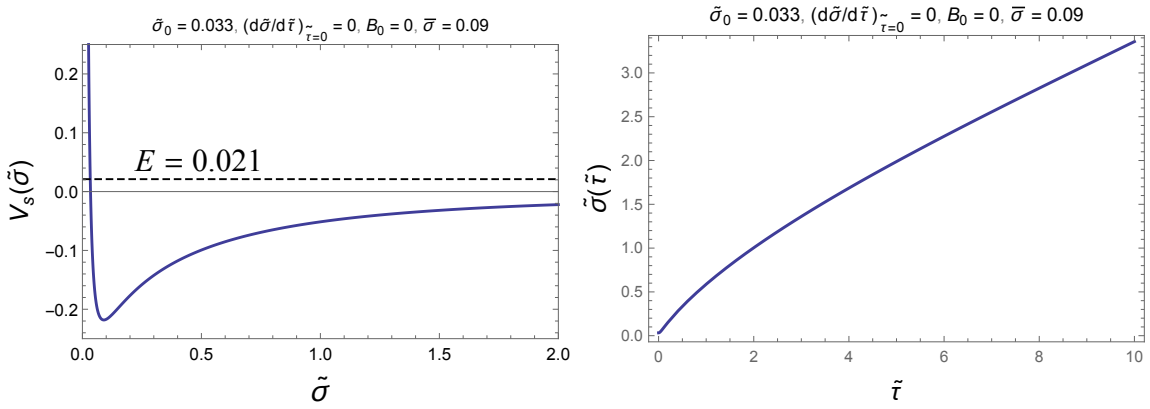

Figure 4.20: Left: V_s as function of $\tilde{\sigma}$, for a very small point of minimum, i.e., $\bar{\sigma} = 0.09$. Right: envelope oscillations corresponding to initial conditions that fix $E > 0$ (see left) above the plateau (i.e., $E = 0.021$), and therefore leading to an unstable evolution of the beam envelope, starting from of values of $\tilde{\sigma}_0$ sufficiently small between the asymptote around zero and $\bar{\sigma}$.

i.e., $(\partial V_s/\partial\tilde{\sigma})_{\bar{\sigma}} = 0$. The small values of $\bar{\sigma}$ indicate the character of strong nonlocality of the beam envelope dynamics of this region, in agreement with both qualitative and quantitative descriptions presented in the previous sections. Finally, Figures 4.15 and 4.16 show in particular the same structure of V_s predicted for the general case by means of the qualitative analysis carried out in section 4.6, except for the asymptotic behaviour for very large $\tilde{\sigma}$.

On the other hand, the discrepancy in this asymptotic region is anyway expected, because as $\tilde{\sigma}$ becomes larger and larger, the limit of applicability of the numerical comutation method used starts to fail as well as our model starts to be no longer applicable. In fact, the larger flatness of the beam transverse profile produced by the increase of $\tilde{\sigma}$, makes such significant the transverse dynamics. Therefore, in agreement with the previous analysis, we can conclude that the region around the minimum corresponds to the strongly nonlocal region, the adjacent are between the former and the plateau corresponds to the moderately nonlocal region and, finally, the plateau, which is the most extended one corresponds to the local region. If we overcome this region, i.e., we exclude from the analysis the asymptotic region, the qualitative prediction presented in section 4.6 is fully recovered.

Figures 4.17 and 4.18 show (left) the existence of periodic time evolutions of $\tilde{\sigma}$ with

different values of the initial conditions and $\bar{\sigma}$, respectively. This, in fact, corresponds to the values of the conserved quantity

$$E = \frac{1}{2}\tilde{\sigma'}_0^2 + V_s(\tilde{\sigma}_0) \tag{4.7.18}$$

that are below the plateau (and therefore, $E < 0$), where for simplicity $\tilde{\sigma'}_0 = 0$ for all cases. The plots on the right, confirm such a prediction.

Figures 4.19 and 4.20 display a different behaviour. Plots on the left regards value of $\tilde{\sigma}_0$ and $\bar{\sigma}$ corresponding two values of E (negative of positive) that are above the plateau. From there, it is evident that we predict motion that are not periodic with unstable evolution. This is confirmed by the plots on he right. In particular, such unstable evolution correspond to initial conditions belonging to the strongly nonlocal region between the asymptote and the minimum of V_s. This is the clear evidence of the envelope self-modulation instability occurrence.

4.8 Conclusions

We have carried out an analysis of the transverse self-modulation experienced by a cylindrically symmetric ultra-relativistic and nonlaminar driving beam while interacting with the surrounding plasma. This has been accomplished by using the pair of 3D Vlasov-Poisson equations found in Chapter 3, that here has been specialized to the purely 2D transverse case in cylindrical symmetry. The plasma has been supposed to be overdense, cold, and magnetized. Due to the conditions of very long beam, the self-consistent PWF mechanism works very efficiently to sensitively characterize the self-modulated dynamics.

We have implemented the Vlasov-Poisson-type system of equation with the virial equations. Their coupling have provided a suitable description of the beam envelope self-modulation. Remarkably, we have shown the importance of the constants of motion involved in such a description, that have allowed us to obtain suitable beam envelope equations, i.e., ordinary differential equations for the beam spot size that are easily integrated analytically and/or numerically. To approach also our problem qualitatively, we have used the method of the

pseudo potential (or Sagdeev potential) that is associated with these envelope equations.
We have first carried out an analysis in two different limiting cases, i.e., the local case (the beam spot size is much greater than the plasma wavelength) and the strongly nonlocal case (the beam spot size is much smaller than the plasma wavelength) where several types of self-modulation, in terms of focusing, defocusing and betatron-like oscillations, have been obtained and the criteria for instability, such as collapse and self-modulation instability, have been formulated. To this ends, within the context of the envelope description, we have found suitable envelope equations, i.e., ordinary differential equations for the beam spot size, that have been easily integrated analytically and physically described in terms of the Sagdeev potential method.
Then, the analysis has been extended to the general case where the beam spot size and the plasma wavelength are not necessarily constrained as in the local or strongly nonlocal cases. In these conditions, we have performed a semi-analytical and numerical analysis by means of the virial equations, where the above methods of the envelope equations and Sagdeev potential have been used, as well. To this end, criteria for predicting stability and self-modulation instability have been suitably provided.

Chapter 5

Longitudinal instability analysis of beam-plasma system

We carry out an analysis of the beam modes that are originated by perturbing the 'beam-plasma' system in the purely longitudinal case. This is done by considering the pair of 3D Vlasov-Poisson-type equation, presented in Chapter 3 that are specialized to the case in which the transverse driving beam dynamics is disregarded and only the longitudinal dynamics becomes effective. To this end, we perturb the Vlasov-Poisson-type system up to the first order, then take the Fourier transform to reduce the Vlasov-Poisson system to a set of algebraic equations in the frequency and wavenumber domain, from which we easily get a Landau-type dispersion relation for the beam modes, that is fully similar to the one holding for plasma modes. First, we consider the case of a monochromatic beam (i.e., cold beam, that is described by a distribution function in the form of delta-function in p space) for which the existence of a purely growing mode is shown and a simple stability criterion formulated. Then, by taking into account a unperturbed distribution function with finite, relatively small width (small thermal correction), the Landau approach, widely used in other physics area, leads to obtain both the dispersion relation for the real part (showing all the possible beam modes in the diverse regions of the wavenumber) and an expression for the imaginary part of the frequency (showing the stable or unstable character of the beam modes), which suggests a simple stability criterion.

5.1 Introduction

As we have shown in the previous chapters, the interaction of a relativistic beam with the plasma involves self-consistent collective and nonlinear mechanisms that lead to the beam self-modulation. In particular, in Chapter 4, we have presented the envelope self-modulation that has shown the occurrence of several self-consistent transverse electromechanical effects and investigated the conditions for the occurrence of the self-modulation instability. Analogous effects occur also in the longitudinal dynamics. In particular, a high-intensity electron beam of finite extent can be subjected to longitudinal instabilities. The nonlinear collective effects that take place in the longitudinal dynamics of charged-particle beams while travelling in a plasma constitute a large-body of phenomena in the plasma-based accelerators. The standard theory of collective longitudinal relativistic beam dynamics in accelerators is based on kinetic theory described by the Vlasov equation, which in general is coupled with a Poisson-type equation describing the plasma wake field excitations.

In this chapter, we carry out an instability analysis within the linearized kinetic theory of the self-consistent beam-plasma interaction, where the Landau damping plays a role. This is done by assuming that the beam-plasma system is governed by the self-consistent Vlasov-Poisson-type pair of equation. We take into account a cold, unmagnetized plasma, constituted by immobile ions (forming a backgroud of positive charge) and mobile electrons, and a nonlaminar, relativistic charged particle beam travelling therein, along the longitudinal direction ($\hat{z}$). According to the concepts described in Chapter 2, in the purely longitudinal case, the wake field and the wake potential reduce to the longitudinal electric field and the scalar potential, respectively. Correspondingly, in absence of significant magnetic effects (the vector potential can be fixed to zero), Eq. (2.1.14) reduces to:

$$F(\xi,\tau) = q\,\frac{\partial\Omega(\xi,\tau)}{\partial\xi}\,. \tag{5.1.1}$$

In case of free evolution, the plasma oscillations are governed by the differential equation

$$\frac{\partial^2\Omega}{\partial\xi^2} + k_p^2\,\Omega = 0\,, \tag{5.1.2}$$

whereas in the presence of the charged particle beam this equation contains, additionally, a forcing term, i.e.,

$$\frac{\partial^2 \Omega}{\partial \xi^2} + k_p^2 \, \Omega = 4\pi q n_b \,, \tag{5.1.3}$$

where $n_b = n_b(\xi, \tau)$ is the volumic beam number density. It is related to the single-particle distribution function $f(\xi, p, \tau)$ which is defined in the longitudinal 2D (ξ, p) phase space (p being the longitudinal single-particle linear momentum conjugate of ξ). In fact, by denoting with $\lambda(\xi, \tau)$ the longitudinal $1D$ number density (i.e., number of particles per unitary longitudinal length), we have:

$$\lambda(\xi, \tau) = n_b(\xi, \tau) \, \pi \sigma_\perp^2 \,,$$

where $\sigma_\perp$ is the effective beam transverse size (i.e., spot size). Thus, the following relationship holds:

$$n_b(\xi, \tau) \, \pi \sigma_\perp^2 = \int f(\xi, p, \tau) \, dp \,. \tag{5.1.4}$$

In addition, $f(\xi, p, \tau)$ obeys to the following purely longitudinal Vlasov equation (for details, see Chapter 3):

$$\frac{\partial f}{\partial \tau} + p \frac{\partial f}{\partial \xi} + \frac{q}{m_{b0} \gamma_0 c^2} \frac{\partial \Omega}{\partial \xi} \frac{\partial f}{\partial p} = 0 \,. \tag{5.1.5}$$

We start from the equilibrium state that is described by the quantities:

$$n_p = n_0 \,, \quad n_b = n_{b0} \,, \quad \Omega = \Omega_0 \,, \quad \text{and} \quad f = f_0(p) \,,$$

where n_p is the plasma electron density. Then, we perturb this state with small (i.e., first-order) deviations, i.e.,

$$n_p(\xi, \tau) = n_0 + n_1(\xi, \tau) \,, \quad n_b(\xi, \tau) = n_{b0} + n_{b1}(\xi, \tau) \,, \quad \Omega(\xi, \tau) = \Omega_0 + \Omega_1(\xi, \tau) \,,$$

and

$$f(\xi, p, \tau) = f_0(p) + f_1(\xi, p, \tau) \,.$$

Here, n_0, n_{b0}, and Ω_0 are constant quantities. Consequently, up to the first order, the system of equations (5.1.3) - (5.1.5) reduces to:

$$k_p^2 \, \Omega_0 = 4\pi \, q \, n_{b0} \,, \tag{5.1.6}$$

which defines the unperturbed wake potential in terms of the unperturbed beam density, where

$$n_{b0}\,\pi\sigma_\perp^2 = \int f_0(p)\,dp\,, \tag{5.1.7}$$

and

$$\frac{\partial^2\Omega_1}{\partial\xi^2} + k_p^2\,\Omega_1 = 4\pi q\,n_{b1}\,, \tag{5.1.8}$$

$$\frac{\partial f_1}{\partial\tau} + p\frac{\partial f_1}{\partial\xi} + \frac{q}{m_{b0}\gamma_0 c^2}\frac{\partial\Omega_1}{\partial\xi}\frac{\partial f_0}{\partial p} = 0\,, \tag{5.1.9}$$

where

$$n_{b1} = \frac{1}{\pi\sigma_\perp^2}\int f_1\,dp\,. \tag{5.1.10}$$

The linearized system of equations (5.1.8) - (5.1.10) governs the self-consistent spatiotemporal evolution of the PWF interaction in the case of purely longitudinal dynamics. Note the full similarity between Eq. (5.1.8) and Eq. (2.7.5), which holds in the overdense regime (i.e., $n_b \ll n_0$). Here, n_{b1} ($\ll n_{b0} \sim n_0$) plays the role that in Eq. (2.7.5) is played by n_b as first order quantity. This means that, in the case under discussion, the perturbation n_{b1} is actually the source of the plasma wake field.

The linearization of the Vlasov-Poisson-type system of equations, offers the advantage, by means of the Fourier transform, to reduce such system to a set of algebraic equations, leading to the dispersion relations, i.e., a relation between the frequency and the wave number of each mode. This procedure is carried out in the next section.

5.2 Dispersion relation

The Fourier transformation transforms the system of equations (5.1.8) - (5.1.10) into the following algebraic system of equations ($\partial/\partial\tau \to -i\omega/c$ and $\partial/\partial\xi \to ik$), i.e.,

$$\left(k_p^2 - k^2\right)\tilde{\Omega}_1 = 4\pi q\,\tilde{n}_{b1}\,, \tag{5.2.1}$$

$$i\left(pk - \frac{\omega}{c}\right)\tilde{f}_1 + \frac{ikq\tilde{\Omega}_1}{m_{b0}\gamma_0 c^2}f_0' = 0\,, \tag{5.2.2}$$

where $f_0' = df_0/dp$ and the quantities $\tilde{\Omega}_1 = \tilde{\Omega}_1(k,\omega)$, $\tilde{n}_{b1} = \tilde{n}_{b1}(k,\omega)$ and $\tilde{f}_1 = \tilde{f}_1(k,p,\omega)$ stand for the Fourier transforms of Ω_1, n_{b1} and f_1, respectively.

Then, by combining Eqs. (5.2.1) to (5.2.2), we easily get,

$$1 = \frac{\omega_b^2}{\gamma_0 c^2}\,\frac{1}{k^2 - k_p^2}\int \frac{\hat{f}_0'\,dp}{p - \frac{\omega}{ck}}\,. \tag{5.2.3}$$

where $\omega_b = \left(4\pi q^2 n_{b0}/m_{b0}\right)^{1/2}$ is the plasma frequency of the beam and

$$\hat{f}_0 = f_0/(n_{b0}\pi\sigma_\perp^2).$$

Therefore, Eq. (5.2.3) can be written as:

$$1 = \frac{\eta}{\bar{k}^2 - 1}\int \frac{\hat{f}_0'\,dp}{p - \frac{\bar{\omega}}{\bar{k}}}\,, \tag{5.2.4}$$

where $\eta = (n_{b0}/\gamma_0 n_0)\,(q^2/e^2)(m_{e0}/m_{b0})$ is a positive constant, $k_b^2 = \omega_b^2/c^2$, and we have introduces the following normalized quantities

$$\bar{\omega} = \omega/\omega_p,\;\; \bar{k} = k/k_p.$$

We assume, for simplicity, that the beam under consideration is an electron beam, i.e., $m_{b0} = m_{e0}$ and $q = e$. Hence the constant η becomes

$$\eta = \frac{1}{\gamma_0}\,\frac{n_{b0}}{n_0}.$$

Once the profile of $\hat{f}_0$ is given, dispersion relation (5.2.4) can be suitably used to carry out an analysis of the beam modes. Then, taking into account both the Landau damping phenomenon and the instability occurrence, we try to formulate the instability criteria.

5.3 Monochromatic profile

We start to analyse the case when the beam is monochromatic (or cold), i.e., $\hat{f}_0 \propto \delta(p)$. By integrating by part the term at the right-hand side of Eq. (5.2.4) we obtain,

$$\bar{\omega}^2 = \frac{\eta\,\bar{k}^2}{\bar{k}^2 - 1}\,. \tag{5.3.1}$$

Then, after writing $\bar{\omega} = \bar{\omega}_R + i\bar{\omega}_I$, and assuming that $\bar{k}$ is real, we can divide the real from the imaginary part. So that we finally find

$$\bar{\omega}_R\,\bar{\omega}_I = 0\,, \tag{5.3.2}$$

$$\bar{\omega}_R^2 - \bar{\omega}_I^2 = \frac{\eta\,\bar{k}^2}{\bar{k}^2 - 1}\,. \tag{5.3.3}$$

- If $\bar{\omega}_I = 0$, from Eq. (5.3.3) we get,

$$\bar{\omega}_R = \pm\frac{\sqrt{\eta}\,|\bar{k}|}{\sqrt{\bar{k}^2 - 1}}\,. \tag{5.3.4}$$

  Then, since $\bar{\omega}_R$ is real, $\bar{k}^2 > 1$. In addition, since $\bar{\omega}_I = 0$, the modes $(\bar{k}, \bar{\omega}_R\left(\bar{k}\right))$ described by dispersion relation (5.3.4) are stable.

- If $\bar{\omega}_R = 0$, from Eq. (5.3.3) we get,

$$\bar{\omega}_I = \pm\frac{\sqrt{\eta}\,|\bar{k}|}{\sqrt{1 - \bar{k}^2}}\,. \tag{5.3.5}$$

  Then, since $\bar{\omega}_I$ is real, $\bar{k}^2 < 1$.

According to Eq. (5.3.5), at fixed $\bar{k}$, for any negative solution of $\bar{\omega}_I$ there is a positive solution of $\bar{\omega}_I$. This indicates instability of the corresponding beam mode which appears as a purely growing mode.

Figure 5.1 and 5.2 show the plots of the dispersion relation i.e., $\bar{\omega}_R\left(\bar{k}\right)$ and $\bar{\omega}_I\left(\bar{k}\right)$, for an initial monochromatic beam profile and for a given ratio n_{b0}/n_0. The former displays the stable modes that possess cut-off for both $\bar{k}$ and $\bar{\omega}_R$. The latter, shows the purely growing mode, whose growth rate, i.e., $\bar{\omega}_I$, does not possess any cuf-off, but is limited in the range, $-1 < \bar{k} < 1$.

Note that for a plasma density $n_0 = 5 \times 10^{17} cm^{-3}$, the plasma frequency is $\omega_p \simeq 4 \times 10^{13}$ rad/s. Then, from the definition of $\bar{\omega}_R$ and $\bar{\omega}_I$, we find that in Figures 5.1 and 5.2, $|\omega_R|$ and $|\omega_I|$ range (from 0.4 to 2.4) $\times 10^{13}$ rad/s and (from 0 to 1.6) $\times 10^{13}$ rad/s, respectively.

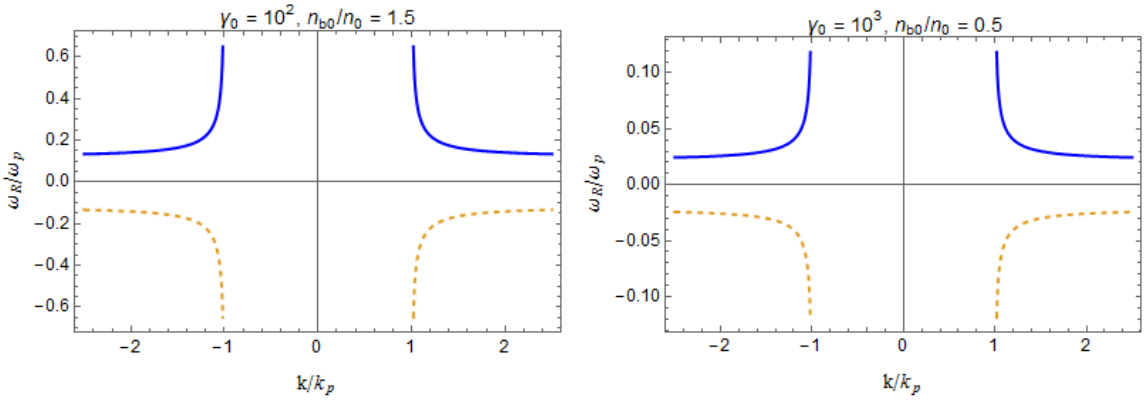

Figure 5.1: Variations of $\bar{\omega}_R$ with $\bar{k}$ for a monochromatic beam profile at fixed ratio n_{b0}/n_0. Here the solid lines indicate positive $\bar{\omega}_R$ and the dashed lines indicate negative $\bar{\omega}_R$ according to Eq. (5.3.4).

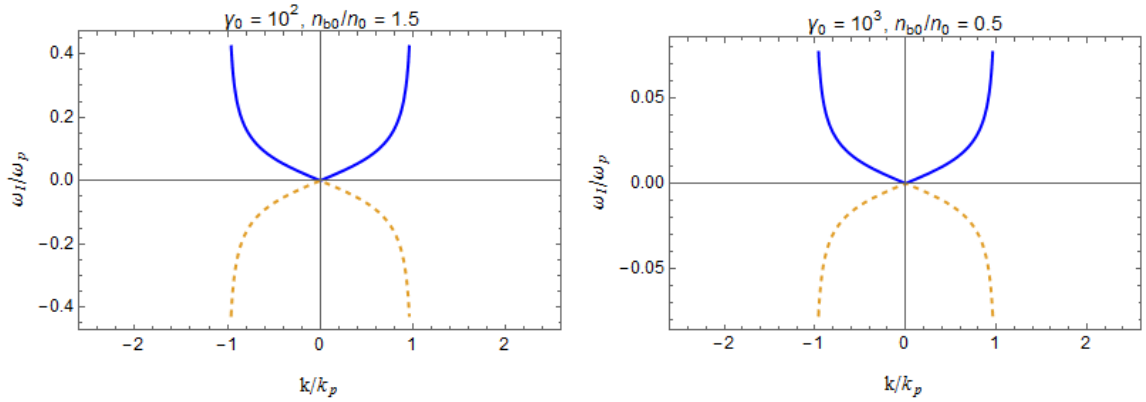

Figure 5.2: Variations of $\bar{\omega}_I$ with $\bar{k}$ for a monochromatic beam profile at fixed ratio n_{b0}/n_0. Here the solid lines indicate positive $\bar{\omega}_I$ and the dashed lines indicate negative $\bar{\omega}_I$ according to Eq. (5.3.5).

5.4 Non-monochromatic case: weak Landau damping and instability

The beam is called *non-monochromatic* or *warm* when the distribution function $\hat{f}_0(p)$ has a finite width due to the presence of the random character of the particle motion. We assume that $\hat{f}_0(p)$ is a bell-like shaped function such that $\hat{f}_0(-p) = \hat{f}_0(p)$, such as in the case of

normalized *parabola-square* profile, i.e.,

$$\hat{f}_0(p) = \frac{15}{16}\frac{1}{\sqrt{7}\sigma_p}\left(1 - \frac{p^2}{7\sigma_p^2}\right)^2, \; -\sqrt{7}\sigma_p \leq p \leq \sqrt{7}\sigma_p\,, \tag{5.4.1}$$

and the case of normalized *Gaussian* profile, i.e.,

$$\hat{f}_0(p) = \frac{1}{\sqrt{2\pi\sigma_p^2}}\exp\left[-\frac{p^2}{2\sigma_p^2}\right], \; -\infty < p < \infty\,, \tag{5.4.2}$$

where $\sigma_p = \langle p^2 \rangle^{1/2}$. Furthermore, one can introduce reasonably the definition of temperature T, i.e., $\sigma_p \equiv v_T \equiv \left(k_B T / m_{b0}\gamma_0 c^2\right)^{1/2}$, where v_T is the dimensionless thermal velocity.

We assume that v_T is very small compared to the dimensionless phase velocity, i.e., $\bar{\omega}/\bar{k}$, of the beam perturbation: $\bar{k}v_T/\bar{\omega} \ll 1$. Therefore, compared to the case of Eq. (5.3.4) of the monochromatic beam (where $\bar{\omega}_I = 0$), this condition represents a small deviation from the delta function distribution. Then, the integral in Eq. (5.2.4) has to be solved according to the Landau prescription [66, 67], i.e.,

$$1 = \frac{\eta}{\bar{k}^2 - 1}\left[\int_{PV}\frac{\hat{f}_0' dp}{p - \frac{\bar{\omega}}{\bar{k}}} + i\pi\hat{f}_0'\left(\frac{\bar{\omega}}{\bar{k}}\right)\right], \tag{5.4.3}$$

where $\int_{PV}\hat{f}_0'/(p - \bar{\omega}/\bar{k})\,dp$ stands for the Cauchy principal value and the second term in the square bracket accounts for the residue. By performing the integration by parts in the integral of Eq. (5.4.3), expanding the term $(p - \bar{\omega}/\bar{k})^{-1}$ in powers of p, and taking into account the assumptions of both symmetry and small deviation from the monochromatic case, one can easily get,

$$\int_{PV}\frac{\hat{f}_0' dp}{p - \frac{\bar{\omega}}{\bar{k}}} = \frac{\bar{k}^2}{\bar{\omega}^2}\left(1 + \frac{3\bar{k}^2 v_T^2}{\bar{\omega}^2}\right), \tag{5.4.4}$$

where, consistently with the above assumptions, we have truncated the expansion in p up to the second power. The small deviation from the monochromatic case is therefore related to the smallness of the quantity $\bar{k}v_T/\bar{\omega}$. For a given v_T, it implies that $\hat{f}_0'\left(\bar{\omega}_R/\bar{k}\right)$ is a small quantity compared to the principal value. In turn, the smallness of the residue implies the smallness of $\bar{\omega}_I$, compared to $\bar{\omega}_R$. Therefore, in Eqs. (5.4.3) and (5.4.4), we assume that

$\bar{\omega} = \bar{\omega}_R + i\,\bar{\omega}_I$ with the condition $|\bar{\omega}_I| \ll |\bar{\omega}_R|$. Then, separating the real from the imaginary parts, we obtain

$$\bar{\omega}_R^2 = \frac{\eta\,\bar{k}^2}{\bar{k}^2 - 1}\left(1 + \frac{3\bar{k}^2\,v_T^2}{\bar{\omega}_R^2}\right),\ \bar{k}^2 > 1\,, \tag{5.4.5}$$

which can be cast as,

$$\bar{\omega}_R = \pm\frac{\sqrt{\eta}\,|\bar{k}|}{\sqrt{\bar{k}^2 - 1}}\left(1 + \frac{3\bar{k}^2\,v_T^2}{\bar{\omega}_R^2}\right)^{1/2},\ \bar{k}^2 > 1\,. \tag{5.4.6}$$

However, since $\bar{k}v_T/\bar{\omega}_R \ll 1$, in second term of right-hand side of the above mentioned equation we can replace $\bar{\omega}_R$ by using Eq. (5.3.4). Therefore, Eq. (5.4.6) can be approximated as:

$$\bar{\omega}_R = \pm\frac{\sqrt{\eta}\,|\bar{k}|}{\sqrt{\bar{k}^2 - 1}}\left(1 + \frac{3}{2}\frac{v_T^2}{\eta}(\bar{k}^2 - 1)\right),\ \bar{k}^2 > 1\,, \tag{5.4.7}$$

On the other hand, the imaginary part of the combination of Eqs. (5.4.3) and (5.4.4) gives

$$\bar{\omega}_I = \frac{\pi}{2}\frac{\eta\,\bar{\omega}_R}{\bar{k}^2 - 1}\hat{f}_0'\left(\frac{\bar{\omega}_R}{\bar{k}}\right),\ \bar{k}^2 > 1\,. \tag{5.4.8}$$

Equation (5.4.8) shows that, for positive (negative) sign of the product $\bar{\omega}_R\hat{f}_0'\left(\frac{\bar{\omega}_R}{\bar{k}}\right)$, $\bar{\omega}_I$ is positive (negative). If $\bar{\omega}_I$ is negative, the wave associated with the beam perturbation experiences the damping effect. This is the phenomenon of Landau damping which is well known in plasmas [67] and in a number of other physics areas [68]. However, if $\bar{\omega}_I$ is positive the wave amplitude grows and this circumstance indicates the instability of the beam perturbation.

As in the ordinary Landau damping occurring in plasmas, here we can provide the physical explanation in terms of wave-particle interaction. In fact, the beam is non-monochromatic, i.e., its phase space distribution $f_0(p)$ is bell-like shaped [see the examples given by Eqs. (5.4.1) and (5.4.2)]. Then for a given phase velocity of the beam density perturbation or of the PWF perturbations (i.e., ω/ck), there are more particles with $p < \omega/ck$ (that are taking energy from the wave) than the ones with $p > \omega/ck$ (that are giving energy to the wave). Therefore, statistically, the wave experiences the phenomenon of damping (i.e., Landau damping). This effect, being in competition with the instability, contributes to the system

stabilization. It is worthy noting that Landau damping disappears as the temperature of the system goes to zero (cold beam or the monochromatic beam). The absence of such an effect leads to instability that is, therefore, the analog of the two stream instability and represents a purely growing mode.

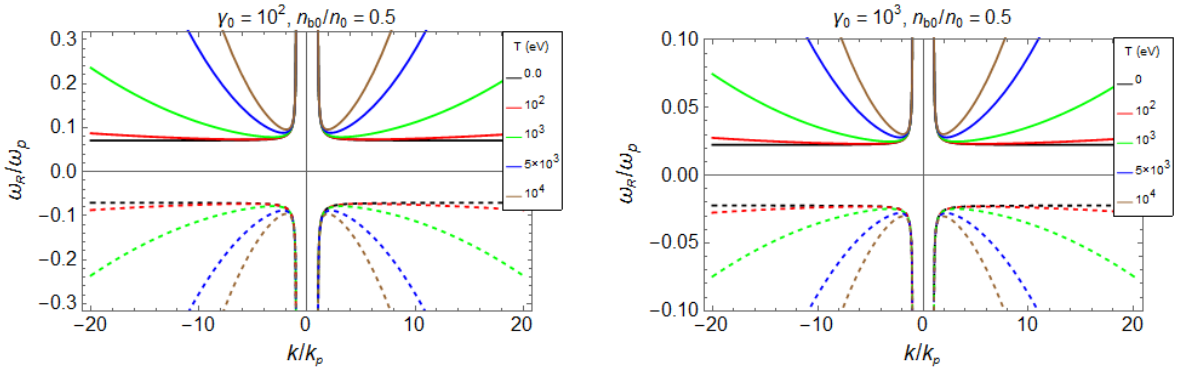

Figure 5.3: Variation of $\bar{\omega}_R$ with $\bar{k}$ for bell-like shaped non-monochromatic beams for different beam temperatures at fixed energy and ratio $n_{b0}/n_0 = 0.5$.

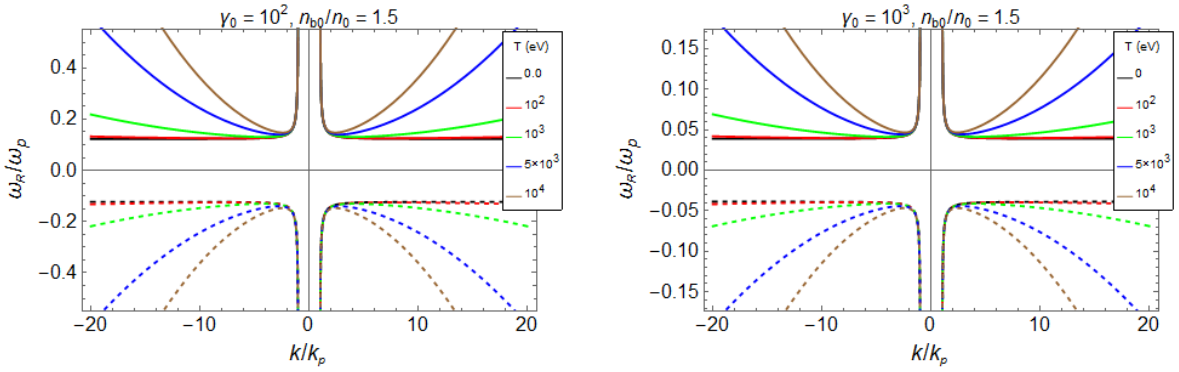

Figure 5.4: Variation of $\bar{\omega}_R$ with $\bar{k}$ for bell-like shaped non-monochromatic beams for different beam temperatures at fixed energy and ratio $n_{b0}/n_0 = 1.5$.

In Figures 5.3 and 5.4, the solid lines indicate positive $\bar{\omega}_R$ and the dashed lines indicate negative $\bar{\omega}_R$, according to Eq. (5.4.7). These figures show $\bar{\omega}_R$ as function of $\bar{k}$ when the distribution function is a bell-like shaped non-monochromatic, but exhibits a small width due to the finite temperature. The different plots are given for different temperatures with fixed γ_0 and n_{b0}/n_0. Compared to the corresponding plot of the monochromatic case (Figure

5.1), the case of $T = 0$ is recovered. As T increases, the horizontal asymptotes changes into oblique axes, increasing gradually the cut-off frequency of each of the four sectors of the plot. This produces a progressive enlargement of the gap between the domain of the positive frequency and the one of the negative frequency, showing also a more "acute" shapes of each plot. An important consequence of this deformation is the increasing of the absolute value of both phase velocity and group velocity in all the permitted domains of $\bar{k}$. In addition, the deformation is stronger in the case of smaller energy of the beam (γ_0).

5.5 Conclusions

We have carreid out an analysis of the beam modes that are originated by perturbing the 'beam-plasma system' in the purely longitudinal dynamics of a relativistic driving beam. This has been accomplished by specializing to the 1D longitudinal case the pair of 3D Vlasov-Poisson-type equation, presented in Chapter 3. To this end, we have perturbed the 1D Vlasov-Poisson-type system up to the first order, then used the Fourier transform to reduce the Vlasov-Poisson system to a set of algebraic equations in the frequency and wavenumber domain. From the latter we have easily found the Landau-type dispersion relation for the beam modes that is fully similar to the one holding for plasma modes. As a first case, we have studied the dispersion relation in the case of monochromatic beam that is described by a distribution function in the form of delta-function in p space). The analysis has shown the existence of a purely growing mode and a simple stability criterion. Then, by taking into account a non-monochromatic (i.e., a distribution function with a relatively small width due to the finite temperature), the Landau approach has lead to obtain both the dispersion relation for the real part (showing all the possible beam modes in the diverse regions of the wave number) and an expression for the imaginary part of the frequency, which has suggested a simple stability criterion.

Chapter 6

The coupling impedance concept for PWF self-interaction

Starting from the collisionless Vlasov-Poisson-type system of equation for longitudinal beam dynamics, that has been presented in Chapter 5, we formulate a novel approach in which we put forward the concept of longitudinal coupling impedance associated with the beam-plasma interaction, in a way fully similar to the one in use in conventional particle accelerator physics. As in the conventional theory, the concept of coupling impedance seems to be very fruitful in a plasma-based accelerator to schematize the self-interaction of the relativistic driving beam with the surrounding plasma. In particular, it allows us to develop a simple instability analysis in the plane of the real and imaginary parts of the impedance that is based on the Nyquist approach widely used in the control system theory. Furthermore, we extend the Vlasov-Poisson-type system to the collision context with a simple model of collisions between the plasma particles (actually plasma electrons) and the beam particles. Under these assumptions, the role and the features of the coupling impedance defined here are compared to the ones of the coupling impedance in conventional theory. Examples of specific physical situations are finally illustrated.

6.1 Introduction

In a conventional particle accelerator, the coupling impedance schematizes the interaction of a (relativistic) charged particle beam with the surrounding medium. This interaction involves

the *wake fields* that are produced by each charged particle of the beam [69]. Therefore, such an interaction is a macroscopic (collective) manifestation of the beam in the surroundings. A very effective way to describe such an interaction makes use of the concept of both image charges and image currents [70, 71]. They are produced, for instance, on the metallic walls of the vacuum chamber, by the charged particles of the beam. Therefore, they are the sources of electric and magnetic fields which are moving behind the beam at the same its speed (wake fields). However, there are some other sources of wake fields, such as the variations of the vacuum chamber geometric features, which produce scattered electromagnetic fields. In general, one can distinguish *short range wake fields* influencing the single bunch beam dynamics from the *long range wake fields*, influencing the multi-bunch beam dynamics. However, restricting to the wake fields associated with the space charge effects, one can see that sufficiently short bunches affect mainly the particle of another bunch moving behind. However, as the beam becomes longer and longer, those fields affect more and more the particles of the beam itself. As we discuss later for plasma wake field (PWF) accelerators, in analogy with the conventional accelerators, the dynamics of long enough single bunches is sensitively affected by the wake fields. Then, the beam particles experience the effects of the fields that they have themselves produced in the surroundings (self-interaction). Due to the nature of the interaction between the beam and the surroundings, some reactive (capacitive as well as inductive) energy related to the beam space charge and current is involved in the system. In addition, the possible resistive character of the metallic walls experienced by the image currents and the geometric variation of the pipe (leading to beam losses), involves some resistive energy, as well. Therefore, in the domain of frequency and wave number, the interaction of the beam with the surroundings can be effectively represented by a sequence of elements of an electric transmission line. Each of these elements accounts for an equivalent impedance per unitary length which is constituted by an equivalent capacitance, inductance and resistance per unitary length. This is usually referred to as the *coupling impedance*, since it schematizes the self-consistent interaction between the beam and the surrounding medium.

In 1959, Andrew M. Sessler, in collaboration with Carl Nielsen and Keith Symon, took

up the study of collective instabilities of a relativistic charged-particle beam that take place in an accelerating machine, the so-called *coherent beam instabilities* (a special case of them is the well known *negative-mass instability*) [72]. The approach of these researchers lead soon to conclude that coherent instabilities are due to the beam space charge through the mechanism of the self interaction that the same space charge experiences with the surroundings via the image charges distributed on the wall of the vacuum chamber. It was the first exploration, based on the Vlasov kinetic theory, that allowed them to realize the important role of the Landau damping [66] as a stabilizing effect acting to cure the coherent instabilities. The Landau damping is, in fact, a phenomenon resulting from the interaction of space charge waves (the so-called electrostatic waves arising in plasmas or in generic charged-particle systems, such as beams) with the single particles. Namely, this is the interaction of a *collective mode* of the system with a *single individual* (single-particle). In the single process of wave-particle interaction, the energy can be transferred from the wave to the particle or from the particle to the wave, provided that the phase velocity of the wave is slightly greater or slightly smaller than the particle velocity, respectively. The *resonance condition* is established when these velocities are the same. This means that wave and particles are actually interacting around the resonance. Lev D. Landau demonstrated that, for single-humped thermal particle distributions, the statistical energy balance coming from all the wave-particle interactions shows that the space charge wave is damped and, therefore, it provides to contrast the wave growth due to the instability. Then, the way in which the interplay between coherent instability and Landau damping takes place works leading to stable or unstable evolution of the system. The stability or the instability depends on precise conditions that are related to the coupling impedance.

In subsequent studies with L. Jackson Laslett and V. Kelvin Neil [73] and Ernest Courant [74], Sessler became interested in single bunches rather than a continuous beam, and he realized that wall resistance is only one aspect of the general concept of impedance. The latter was later developed in collaboration with Vittorio G. Vaccaro [75], who suggested to

formulate a more general definition of the coupling impedance that they applied to the collective longitudinal dynamics of an azimuthally uniform beam. Although Sessler had a high opinion of Vaccaro, this formulation was not soon accepted at CERN. Meanwhile, Vaccaro was producing a subsequent work in collaboration with Alessandro G. Ruggiero [76], where the previous approach to the longitudinal instability was improved and formalized in terms of a stability criterion *a la Nyquist*, later sometimes referred to as *Sessler-Ruggero-Vaccaro criterion*. After a few years, the concept of coupling impedance became more and more popular in particle accelerator physics. ≪ Nowadays everyone uses their work to calculate, measure, and control impedance in order to limit instabilities.≫ [77].

6.2 Phenomenological platform of the beam-plasma interaction

The interaction between charged-particle beams with plasmas touches a large variety of phenomena, ranging from laboratory to space and astrophysical plasmas.

Part of these phenomena concern types of beam-plasma interactions in which the plasma can be thought as a collection of streams. Each of them is constituted by different particle species in terms of mass and charge. Such a system satisfies the global charge neutrality condition. In linear theory, the multi-stream instability theory is the simplest approach to the plasma instability that can be provided by both fluid and kinetic models. In particular, it is very useful to approach the beam-plasma instability, such as Buneman instability [78, 79]. Note that here, the beam is not an object external to the plasma. It actually represents one of its own components. Therefore, the self-consistent spatiotemporal evolution of the beam takes place while contributing to satisfy the global neutrality conditions.

A different scenario appears when a charged-particle beam enters the plasma. In fact, while the plasma components satisfy all together the global neutrality condition, the external beam introduces an additional charge that cannot be balanced in the beam-plasma system.

The beam introduces a local charge density perturbation which the plasma tends to neutralize locally. Contextually, a current density perturbation is introduced, as well. The resulting electric and magnetic fields act locally on the particles of the system and, therefore, both plasma and beam evolve in space and time self-consistently, according to the pair of Vlasov-Poisson-type equations for the beam-plasma system. Then, the concept of the coupling impedance in the beam-plasma interaction ruled by the PWF excitation can be introduced after linearizing the Vlasov-Poisson-type system (around an unperturbed state) and taking the Fourier transform of the resulting equations.

6.3 Vlasov-Poisson-type pair of equations

To perform an analysis of the linearized beam-plasma system dynamics by means of the concept of coupling impedance, for simplicity, we confine our description to the case of an *electron beam*. We take into account the case of a collisionless beam-plasma dynamics, where a nonlaminar, relativistic, electron beam travelling through a cold, unmagnetized plasma in the longitudinal direction. In general, this analysis can be easily applied to the transverse case or extended to the 3D case. Then, the linearized pair of Vlasov-Poisson-type equations governing the spatiotemporal longitudinal dynamics of our system (similar to the system of equations given in Section 5.1) is

$$\left(\frac{\partial^2}{\partial\xi^2} + k_p^2\right)\Omega_1 = k_p^2 \frac{m_{e0}c}{e^2 n_0}\frac{I_{b1}}{\beta\pi\sigma_\perp^2}, \tag{6.3.1}$$

$$\frac{\partial f_1}{\partial\tau} + p\frac{\partial f_1}{\partial\xi} + \frac{(-e)}{m_{e0}\gamma_0 c^2}\frac{\partial\Omega_1}{\partial\xi}\frac{\partial f_0}{\partial p} = 0\,, \tag{6.3.2}$$

where $\Omega_1 = \Omega_1(\xi,\tau)$, $f_0 = f_0(p)$ is the unperturbed distribution function, $f_1 = f_1(\xi,p,\tau)$ is the first-order correction of this distribution and

$$I_{b1}(\xi,\tau) = (-e)\beta c\int f_1(\xi,p,\tau)\,dp = -e)\beta c\pi\sigma_\perp^2 n_{b1} \tag{6.3.3}$$

is the perturbed beam-current. Here e and $\sigma_\perp$ are the absolute value of the electron charge and the transverse beam spot size, respectively.

Equation (6.3.1) is a linear equation relating $n_{b1}(\xi,\tau)$ to $\Omega_1(\xi,\tau)$. Equation (6.3.2) accounts for the slower evolution of the beam beyond the stationary state and it is coupled with the former, therefore it is in principle a nonlinear equation. Then, the pair of equations (6.3.1) - (6.3.2) governs the self-consistent spatio-temporal evolution of the PWF interaction.

6.4 Heuristic definition of coupling impedance

Here, we put forward the following heuristic definition of *longitudinal coupling impedance per unity length*, say Z, which is fully similar to the heuristic definition given in conventional accelerators [71]. Then, by denoting with $\tilde{\Omega}_1(k,\omega)$ and $\tilde{I}_{b1}(k,\omega)$ the Fourier transform of $\Omega_1(\xi,\tau)$ and $I_{b1}(\xi,\tau)$, respectively, we define $Z(k,\omega)$ as

$$Z(k,\omega) = -i\,k\,\frac{\tilde{\Omega}_1(k,\omega)}{\tilde{I}_{b1}(k,\omega)}\,. \tag{6.4.1}$$

In principle, $Z(k,\omega)$ is a complex quantity. Then, in general, we can cast it as the sum of real and imaginary part, i.e., $Z(k,\omega) = Z_R(k,\omega) + i\,Z_I(k,\omega)$. By combining the Fourier transform of both Eqs. (6.3.1) and (6.3.2), where ($\partial/\partial\tau \to -i\omega/c$ and $\partial/\partial\xi \to ik$), we get the following dispersion relation of the beam-plasma system, viz.,

$$1 = -i\eta_c \frac{Z(k,\omega)}{k}\int \frac{\hat{f}_0'(p)dp}{p-\omega/ck}, \tag{6.4.2}$$

where $\eta_c = \omega_b^2/(\gamma_0 c^2)\,\beta c\sigma_\perp^2/4$, is a positive constant, $\hat{f}_0$ denotes the normalized equilibrium distribution function and $\hat{f}_0^{'}(p) \equiv d\hat{f}_0/dp$. This is the Landau-type dispersion relation. Each possible mode (k,ω) of the system must satisfy it. For each mode (k,ω), if $Z_R \neq 0$, the coupling between beam and plasma involves some resistive energy that must be represented by losses; whilst if $Z_I \neq 0$, some reactive energy is involved in such a coupling, which means that the energy is stored in the electric and magnetic parts of the PWFs.

6.5 Stability analysis

The spectrum of the possible modes is different for different explicit expression of $Z(k,\omega)$ provided by Eq. (6.4.1) and the Fourier tranform of Eq. (6.3.1). For the specific case under

consideration here, the latter is:

$$(-k^2 + k_p^2)\tilde{\Omega}_1 = k_p^2 \frac{m_{e0}c}{e^2 n_0} \frac{\tilde{I}_{b1}}{\beta\pi\sigma_\perp^2} \,. \tag{6.5.1}$$

Then, by combining it with Eq. (6.4.1), we easily get the following conditions of compatibility

$$Z_R = 0\,, \; \frac{Z(k)}{k} = \frac{i\,Z_I(k)}{k} \;\Rightarrow\; \frac{Z_I(k)}{k} = \frac{K_0 k_p^2}{(k^2 - k_p^2)}\,, \tag{6.5.2}$$

where $K_0 = m_{e0}c/n_0 e^2 \beta\pi\sigma_\perp^2$, and here we have assumed that k is a real quantity. These conditions show that in the case under discussion the impedance is purely imaginary (i.e., purely reactive). In fact, we have assumed that the beam-plasma system is collisionless, and this implies that there is no dissipation in the system. Consequently, dispersion relation (6.4.2) becomes:

$$1 = \eta_c \frac{Z_I\,(k)}{k} \int \frac{\hat{f}_0'(p)dp}{p - \omega/ck} \,. \tag{6.5.3}$$

6.5.1 Monochromatic beam

We first consider the case of monochromatic beam, i.e., a beam with the particle distribution function which is represented by a *delta function*, viz.,

$$\hat{f}_0 = \delta(p)\,. \tag{6.5.4}$$

Consequently, the dispersion relation (6.5.3) reduces to:

$$\omega^2 = \eta_c\, k\, Z_I(k)\,. \tag{6.5.5}$$

For $kZ_I > 0$ ($kZ_I < 0$), ω is real (imaginary). On the other hand, $Z_I > 0$ ($Z_I < 0$) when k is such that $-k_p < k < 0$ or $k > k_p$ ($k < -k_p$ or $0 < k < k_p$). Then conditions of stability or instability can be summarized as in Table 6.1. We conclude that in the plane (Z_R, Z_I) of the impedance (see Figure 6.1), the system can be represented with a point that falls on the imaginary axis only. If this point falls on the positive (negative) semi-axis of Z_I, then the system is stable (unstable) against a small perturbation.

	$\mathbf{Z_I > 0}$	$\mathbf{Z_I < 0}$
$\mathbf{k > 0}$	Stable ($k > k_p$)	Unstable ($0 < k < k_p$)
$\mathbf{k < 0}$	Unstable ($-k_p < k < 0$)	Stable ($k < -k_p$)

Table 6.1: Possible cases of stability/instability occurrence.

6.5.2 Non-monochromatic beam

If the beam has a finite spread in the thermal distribution, then the situation changes. We have to expect a stabilizing effect produced by the Landau damping which does work with a finite spread but does not in the monochromatic case. To show qualitatively this effect we refer to the following distribution function:

$$\hat{f}_0(p) = (1 - p^2/d^2)^2, \ -d \leq p \leq d\,, \tag{6.5.6}$$

where d is a positive constant. By inserting (6.5.6) in (6.4.2), we can plot the possible contours relating Z_R to Z_I in the plane of impedance by means of the mapping

$$Z_R + iZ_I = \frac{k}{\eta_c}\left[-i\int_{PV}\frac{\hat{f}_0'(p)dp}{p - (\omega_R/ck + i\omega_I/ck)} + \pi\hat{f}_0'\left(\frac{\omega_R}{ck}\right)\right]^{-1}\,, \tag{6.5.7}$$

where ω has been split into real and imaginary parts ($\omega = \omega_R + i\omega_I$) and, according to Landau prescription, the integral at the r.h.s. of Eq. (6.4.2) has been split into Cauchy principal value and residue. Figure 6.2 qualitatively displays the contours in the plane of the impedance by running ω_R/k at fixed values of ω_I/k (growth rate). We can see that the inner contour for $\omega_I = 0$ limits the stable region which prolongs along the positive part of the Z_I. The presence of the closed region is due to the stabilizing effect of Landau damping. Outside of this stable region, the growth rate is positive and therefore would correspond to unstable region. However, since in the case under discussion the impedance is purely imaginary, we

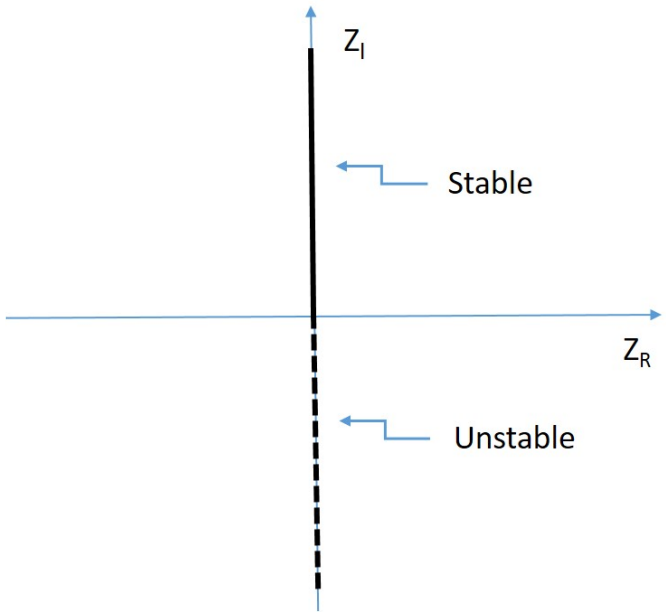

Figure 6.1: Stability analysis in the plane of the impedance for a monochromatic beam.

need to intersect contours of Figure 6.2 with the condition $Z_R = 0$. This is what we can see in Figure 6.3, from which we can conclude that, compared to the monochromatic case (see Figure 6.1), the stable region is increased by extending with a segment along the negative part of Z_I. This simply comes from the intersection of the closed region of Figure 6.2 and the Z_I axis.

6.6 Collisional beam-plasma system

Let us take here the same assumptions of section 6.3 except that now the beam-plasma system is collisional, i.e., the rate of collision between the beam particles and the plasma particles is not negligible. This way, a dissipation is introduced in the system and therefore a real part of the coupling impedance of the beam-plasma system is expected to be non-zero. In fact, we take the set of Lorentz-Maxwell system governing the spatiotemporal evolution of the plasma in the presence of beam's charge and current, that is written in the presence of a viscous force term to model the collisions between beam's and plasma's particles. Then, the

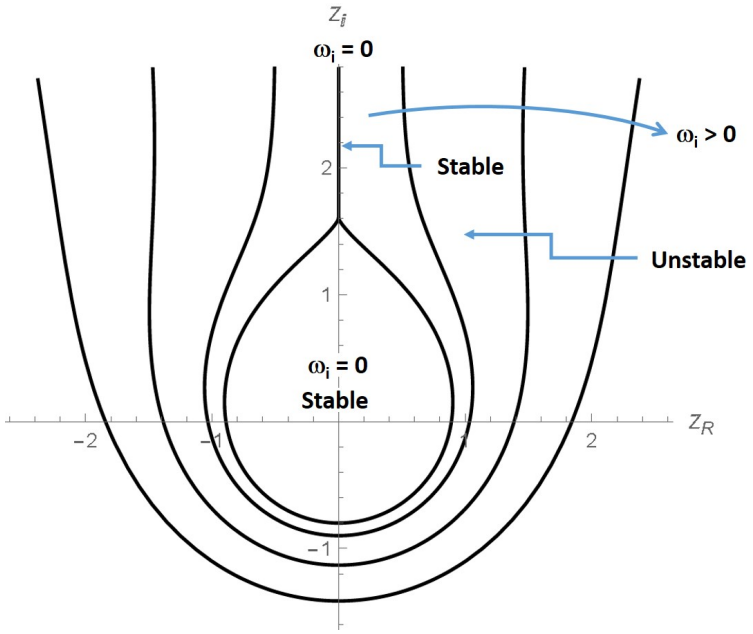

Figure 6.2: Qualitative plot of the contours in the plane (Z_R, Z_I), generated by the mapping (6.5.7) for different constant instability growth rates ω_I, for a thermal distribution given by (6.5.6). The stability region is surrounded by the curve $\omega_I = 0$.

linearized Poisson-like equation in Fourier space is affected by this collision term and can be cast as

$$\frac{\tilde{\Omega}_1}{\tilde{I}_{b1}} = \frac{K_0 k_p^2 \left(1 + i\nu_c/ck\right)}{k_p^2 - \left(1 + i\nu_c/ck\right) k^2}\,, \tag{6.6.1}$$

where ν_c stands for collision frequency. Regarding the beam spatiotemporal evolution, a collisional Boltzmann-Vlasov equation is adopted, where the collisional term is simply modelled by $\nu_c(f_0 - f)$. Consequently, the linearized kinetic equation is

$$\frac{\partial f_1}{\partial \tau} + p\frac{\partial f_1}{\partial \xi} + \frac{(-e)}{m_{e0}\gamma_0 c^2}\frac{\partial \Omega_1}{\partial \xi}\frac{\partial f_0}{\partial p} = -\nu_c \frac{f_1}{c}. \tag{6.6.2}$$

Taking the Fourier transform of the latter and combining it with Eq. (6.6.1), we finally get the following *collisional* Landau-type dispersion relation

$$1 = -i\eta_c \frac{Z\left(k,\omega\right)}{k} \int \frac{\hat{f}_0'(p)dp}{p - \omega/ck - i\nu_c/ck}\,. \tag{6.6.3}$$

Note that Eq. (6.6.3) is formally similar to the one of collisionless case, except for the presence of the collisional frequency, which represents a shift for the imaginary part of the

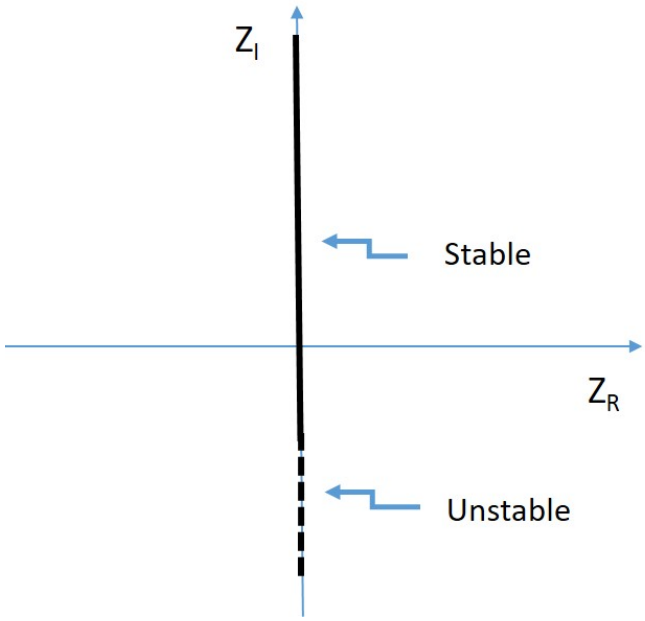

Figure 6.3: Qualitative stability diagram in the plane of the impedance for a non-monochromatic beam whose thermal distribution is given by (6.5.6), as a result of the intersection between the contours of Figure 6.2 and the Z_I axis.

frequency. The presence of ν_c is not found in the dispersion relation for a conventional accelerator. The reason is related to the fact that in a conventional accelerator the beam does not travel through a plasma but through a vacuum chamber where the collisional effects due to the interaction with the residual gas are sensitively reduced (by the way, not in case of millions or billions of turns as in the circular machines). Collisional effects in conventional accelerators are encountered in the resistive effects that the image charge experience on the vacuum chamber walls. In this case the effect is strictly related to the electric resistance of the walls. On the other hand, in the beam-plasma interaction ruled by the PWF mechanism the dissipation is encountered only in the collisional processes, provided that the collision rate is not negligible.

For the case, under discussion, we can calculate Z_R and Z_I by expressing the ratio $\tilde{\Omega}_1/\tilde{I}_{b1}$

with Eq. (6.4.1) and separating real and imaginary parts. This way, we get

$$Z_R = \frac{\nu_c}{c} \frac{K_0 k_p^4}{(-k^2 + k_p^2)^2 + \nu_c^2 k^2/c^2}\,, \tag{6.6.4}$$

$$Z_I = -\frac{K_0 k_p^2 \left[(-k^2 + k_p^2) - \nu_c^2/c^2\right]}{(-k^2 + k_p^2)^2 + \nu_c^2 k^2/c^2} k\,. \tag{6.6.5}$$

Therefore, the collisions introduce a resistance which now plays a role in the beam-plasma dynamics. Note that in the limit $\nu_c \to 0$, Eqs. (6.6.4) and (6.6.5) recover Eqs. (6.5.2). In addition, it should be emphasised that the collisions affect also the imaginary part of the impedance and this is another important difference with respect to the conventional accelerators. For brevity, we do not present here the stability analysis for the collisional case, but the approach is fully similar to the one presented in section 6.5, except for the additional role played by ν_c.

6.7 Conclusions

We have put forward the concept of coupling impedance that schematizes the self consistent beam-plasma interaction ruled by the PWF excitation. We have emphasised similarity and differences in comparison to the concept of coupling impedance in conventional accelerators. We have illustrated with simple examples the role of the coupling impedance in the approach to coherent beam-plasma instabilities. We have also outlined the interplay between Landau damping and instability. An exhaustive and more rigorous approach which opens up to important physical aspects, both energetic and collisional, is under way.

We would like to point out that the conditions of stability/instability discussed in section 6.5.1 and summarized in Table 6.1, have some similarities with the ones of monochromatic coasting beam in the conventional accelerators. In particular, the possibility to combine the sign of Z_I with the sign of k fixes two symmetric conditions of instability that resemble the ones of positive and negative mass instability, respectively. In conventional accelerators, $Z_I > 0$ and $Z_I < 0$ correspond to impedances dominated by inductive and capacitive characters, respectively. The interplay between these impedance characters and the sign of the slip

factor [64] leads to the coherent instability conditions. Compare to the latter, the stability conditions obtained in this work carry a little different meaning. In fact, the analog of the negative mass instability seems to be associated with the case of $k < 0$ and $Z_I > 0$, displayed in Table 6.1. But here, the unstable evolution of a beam density/current perturbation appears when the latter is propagating backward (and therefore, associated to some negative momentum/energy). This and several other aspects of the beam-plasma instability, resulting from the self-consistent PWF excitation, such as the physical condition of positive and negative coupling impedance in connection with their inductive or capacitive character, and the extension of the coupling impedance in PWF accelerators to the transverse case, will be deepen in a forthcoming work.

As a final remark we point out that a sensitive momentum (and thus energy) spread, typical of beams accelerated injected in plasmas [80], could in principle stabilize the beam itself by Landau damping, as described in this Section; such stabilization can only occur provided that the growth rate of the instability that is inducing the momentum spread is lower than the damping rate. Further work is necessary to study the interaction between such kind of instabilities and Landau damping in the beam.

Conclusions and Remarks

We have carried out a theoretical investigation on the self-modulated dynamics that takes place when a nonlaminar, relativistic, charged particle beam is travelling through a magnetized plasma while experiencing a strong interaction with the latter. This has been accomplished by developing the kinetic theory of the plasma wake field excitation. While travelling, the beam experiences the strong electromechanical actions of the self consistent EM fields of beam-plasma system that affect the beam envelope evolution. In this framework, the pair of the 3D Vlasov-Poisson-type equations has been derived in the unperturbed particle reference system. These equations governs the spatiotemporal evolution of the beam. We have specialized this system of equations to a 2D purely transverse system and to a 1D purely longitudinal system to describe the transverse and the longitudinal dynamics, respectively.

In the transverse dynamics, we have implemented the 2D Vlasov-Poisson-type equations for a cylindrically symmetric driving beam with the related virial equations. This has allowed us to find some constant of motions and to obtain ordinary differential equations for the time evolution of the beam spot size (envelope equations), that have been easily integrated analytically and/or numerically. The use of the method of pseudo potential or Sagdeev potential has been very helpful to carry out a qualitative analysis of the beam envelope self-modulation. On the basis of such method, we have first carried out our analysis in the two limiting cases of local (the beam spot size is much greater than the plasma wavelength) and strongly non-local regimes (the beam spot size is much smaller than the plasma wavelength). We have described several types of self-modulations, in terms of focusing, defocusing and betatron-like oscillations, and have obtained the criteria for instability, such as collapse and self-modulation instability. The analysis has been, then, extended to the general case where

the beam spot size and the plasma wavelength are not necessarily constrained as in the local or strongly nonlocal regimes. In these conditions, we have performed a semi-analytical and numerical analysis of the envelope self-modulated dynamics and criteria for predicting stability and self-modulation instability have been suitably provided.

In the longitudinal dynamics, we have used the Landau approach to the longitudinal Vlasov-Poisson-type pair of equations. In fact, after linearizing this system around an unperturbed state, and taking the Fourier transformation of the resulting equation, we have obtained a set of algebraic equation in frequency and wave number domain. From the latter, we have easily found the Landau-type dispersion relation. By using the latter, in the monochromatic beam case, we have shown the existence of a purely growing mode and a simple stability criterion. Then, by taking into account a non-monochromatic beam (describing a slightly warm beam), the Landau approach has lead to obtain both the dispersion relation for the real part (showing all the possible beam modes in the diverse regions of the wave number) and an expression for the imaginary part of the frequency, which has suggested a simple stability criterion.

Within the context of the longitudinal beam dynamics, we have also introduced the novel concept of coulpling impedance in plasma wake field accelerators in a way that is fully similar to the one introduced in conventional particle accelerators. Based on the Landau-type dispersion relation and the methods of Nyquist control theory, we have put forward an alternative way to describe the coherent instabilities in the beam-plasma interaction.

In conclusion, the results we have obtained can be summarized as follows:

- We have developed the kinetic theory of the PWF excitation that provides the generalized Vlasov-Poisson-type pair of equations for the diverse conditions of plasma and beam;

- We have provided the self-modulated beam dynamics analysis in both purely transverse and purely longitudinal cases;

- We have provided a satisfactory model for the self-modulation instability in the transverse case, by implementing the Vlasov-Poisson-type equations with the related virial

description (envelope equations);

- We have carried out an instability analysis within the linearized kinetic theory of the self-consistent beam-plasma interaction, in the purely longitudinal case within two approaches based on Landau theory.

Appendix A

Virial descriptions

Virial description is a method to integrate the single particle motion equation (i.e., Vlasov equation) of a statistical system of charged particle beam, where the beam optics is described in terms of root mean square (rms) beam moments and their respective equations of motion. This method leads to find a set of equations, usually referred to as the *virial equations* for the system of N particles bounded by a potential. Virial equations relate the average of the total kinetic energy which comes from the kinetic description once the average of certain physical quantities are taken by means of the distribution function.

Let us consider the transverse dynamics of a relativistic charged particle electron/positron beam into a cold, Magnetized plasma. The beam is travelling along the $z-$ axis with velocity βc ($\beta \simeq 1$) in the presence of an external magnetic field ($\mathbf{B}_0 = \hat{z}B_0$). The motion of each single particle is associated with an unperturbed total energy $m_{b0}\gamma_0 c^2$ (m_{b0} and γ_0 being the particle rest mass and the unperturbed relativistic factor, respectively). In the unperturbed-particle frame, the transverse motion of each single-particle is associated with an effective Hamiltonian, i.e., $H(\mathbf{r}_\perp, \mathbf{p}_\perp, \tau)$, i.e.,

$$H(\mathbf{r}_\perp, \mathbf{p}_\perp, \tau) = \frac{1}{2}p_\perp^2 + \frac{1}{2}k_c\,\hat{z}\cdot(\mathbf{r}_\perp \times \mathbf{p}_\perp) + \frac{1}{2}Kr_\perp^2 + U_w(\mathbf{r}_\perp, \tau)\,, \tag{A.0.1}$$

where U_w is the normalized plasma wake potential, $K = \left(qB_0/2m_{b0}\gamma_0 c^2\right)^2 = (k_c/2)^2$, $k_c = -qB_0/m_{b0}\gamma_0 c^2$, $\mathbf{r}_\perp$ and $\mathbf{p}_\perp$ are the transverse component of position vector $\mathbf{r}$ and corresponding conjugate momentum $\mathbf{p}$. We can cast the above mentioned equation as:

$$H(\mathbf{r}_\perp, \mathbf{p}_\perp, \tau) = T(\mathbf{p}_\perp) + U(\mathbf{r}_\perp, \mathbf{p}_\perp, \tau)\,, \tag{A.0.2}$$

where

$$T\left(\mathbf{p}_{\perp}\right)=\frac{1}{2}p_{\perp}^{2}\,, \tag{A.0.3}$$

$$U(\mathbf{r}_{\perp},\mathbf{p}_{\perp},\tau)=\frac{1}{2}k_{c}\,\hat{z}\cdot(\mathbf{r}_{\perp}\times\mathbf{p}_{\perp})+\frac{1}{2}Kr_{\perp}^{2}+U_{w}\left(\mathbf{r}_{\perp},\tau\right)\,. \tag{A.0.4}$$

The spatiotemporal evolution of the beam can be provided by the following Vlasov equation in phase space:

$$\frac{\partial f}{\partial\tau}+\frac{\partial H}{\partial\mathbf{p}_{\perp}}\cdot\frac{\partial f}{\partial\mathbf{r}_{\perp}}-\frac{\partial H}{\partial\mathbf{r}_{\perp}}\cdot\frac{\partial f}{\partial\mathbf{p}_{\perp}}=0\,, \tag{A.0.5}$$

where $f=f\left(\mathbf{r}_{\perp},\mathbf{p}_{\perp},\tau\right)$ is the single-particle distribution function in 4D $(\mathbf{r}_{\perp},\mathbf{p}_{\perp})$-phase space which is normalized to unity, i.e.,

$$\int f(\mathbf{r}_{\perp},\mathbf{p}_{\perp},\tau)d^{2}r_{\perp},d^{2}p_{\perp}=1\,. \tag{A.0.6}$$

If $F(\mathbf{r}_{\perp},\mathbf{p}_{\perp},\tau)$ is a generic physical quantity defined in the 4D-phase space. Then, according to Eq. (A.0.6), the average of F is defined as:

$$\langle F\rangle=\int F(\mathbf{r}_{\perp},\mathbf{p}_{\perp},\tau)f(\mathbf{r}_{\perp},\mathbf{p}_{\perp},\tau)d^{2}r_{\perp},d^{2}p_{\perp}\,. \tag{A.0.7}$$

Using this definition of F, we introduce the following averaged quantities:

- the beam spot size (effective transverse beam size), i.e.,

$$\sigma_{\perp}(\tau)=\langle r_{\perp}^{2}\rangle^{1/2}=\left[\int r_{\perp}^{2}\,f\,d^{2}r_{\perp}\,d^{2}p_{\perp}\right]^{1/2}\,; \tag{A.0.8}$$

- the momentum spread, i.e.,

$$\sigma_{p_{\perp}}(\tau)=\langle p_{\perp}^{2}\rangle^{1/2}=\left[\int p_{\perp}^{2}\,f\,d^{2}r_{\perp}\,d^{2}p_{\perp}\right]^{1/2}\,; \tag{A.0.9}$$

-the average of the total energy, i.e.,

$$\mathcal{E}(\tau)=\langle H\rangle=\int Hf\,d^{2}r_{\perp}\,d^{2}p_{\perp}=\langle T\rangle+\langle U\rangle\,, \tag{A.0.10}$$

where

$$\langle T\rangle=\int\frac{1}{2}p_{\perp}^{2}f\left(\mathbf{r}_{\perp},\mathbf{p}_{\perp},\tau\right)\,d^{2}r_{\perp}\,d^{2}p_{\perp}=\frac{1}{2}\sigma_{p_{\perp}}^{2}(\tau) \tag{A.0.11}$$

and

$$\langle U\rangle=\int U\left(\mathbf{r}_{\perp},\mathbf{p}_{\perp},\tau\right)f\left(\mathbf{r}_{\perp},\mathbf{p}_{\perp},\tau\right)\,d^{2}r_{\perp}d^{2}r_{\perp}\,. \tag{A.0.12}$$

Note that to define $\sigma_{\perp}$ and $\sigma_{\mathbf{p}_{\perp}}$, we have assumed that $\langle\mathbf{r}_{\perp}\rangle=\langle\mathbf{p}_{\perp}\rangle=0$, since in the unperturbed particle frame, the beam centroid is moving always along $\hat{z}$.

First virial equation

We are going to derive an evolution equation for $\sigma_\perp^2(\tau)$. Therefore, we first differentiate the square of Eq. (A.0.8) with respect to τ, i.e.,

$$\frac{d\sigma_\perp^2}{d\tau} = \int r_\perp^2 \frac{\partial f}{\partial \tau}\, d^2r_\perp\, d^2p_\perp\,. \tag{A.0.13}$$

Using Eq. (A.0.5), we substitute $\partial f/\partial \mathbf{r}_\perp$ in Eq. (A.0.13), and get,

$$\frac{d\sigma_\perp^2}{d\tau} = -\int r_\perp^2 \left[\frac{\partial \mathcal{H}}{\partial \mathbf{p}_\perp}\cdot\frac{\partial f}{\partial \mathbf{r}_\perp} - \frac{\partial \mathcal{H}}{\partial \mathbf{r}_\perp}\cdot\frac{\partial f}{\partial \mathbf{p}_\perp}\right] d^2r_\perp\, d^2p_\perp\,. \tag{A.0.14}$$

This equation can be written as,

$$\frac{d\sigma_\perp^2}{d\xi} = -\int r_\perp^2 \frac{\partial \mathcal{H}}{\partial \mathbf{p}_\perp}\cdot\frac{\partial f}{\partial \mathbf{r}_\perp} d^2r_\perp\, d^2p_\perp + \int r_\perp^2 \frac{\partial \mathcal{H}}{\partial \mathbf{r}_\perp}\cdot\frac{\partial f}{\partial \mathbf{p}_\perp}\, d^2r_\perp\, d^2p_\perp\,. \tag{A.0.15}$$

To evaluate the first integral in the left-hand side of Eq. (A.0.15), at first we take the divergence of the quantity $r_\perp^2\,(\nabla_{p_\perp} H)\, f$,

$$\nabla_\perp \cdot \left[r_\perp^2(\nabla_{p_\perp}H)f\right] = 2r_\perp\cdot(\nabla_{p_\perp}H)f + r_\perp^2\nabla_\perp\cdot(\nabla_{p_\perp}H)f + r_\perp^2(\nabla_{p_\perp}H)\cdot(\nabla_\perp f) \tag{A.0.16}$$

or,

$$r_\perp^2\frac{\partial \mathcal{H}}{\partial \mathbf{p}_\perp}\cdot\frac{\partial f}{\partial \mathbf{r}_\perp} = \nabla_\perp\cdot\left[r_\perp^2\frac{\partial \mathcal{H}}{\partial \mathbf{p}_\perp}f\right] - 2r_\perp\cdot\frac{\partial \mathcal{H}}{\partial \mathbf{p}_\perp}f - r_\perp^2\nabla_\perp\cdot(\nabla_{p_\perp}H)f\,. \tag{A.0.17}$$

Taking integration of (A.0.17), we get,

$$\begin{aligned}\int r_\perp^2\frac{\partial \mathcal{H}}{\partial \mathbf{p}_\perp}\cdot\frac{\partial f}{\partial \mathbf{r}_\perp}\, d^2r_\perp\, d^2p_\perp = \int \nabla_\perp\cdot\left[r_\perp^2\frac{\partial \mathcal{H}}{\partial \mathbf{p}_\perp}f\right] d^2r_\perp\, d^2p_\perp - 2\int \mathbf{r}_\perp\cdot\frac{\partial \mathcal{H}}{\partial \mathbf{p}_\perp} f\, d^2r_\perp\, d^2p_\perp \\ - \int r_\perp^2\nabla_\perp\cdot(\nabla_{p_\perp}H)f\, d^2r_\perp\, d^2p_\perp\,.\end{aligned} \tag{A.0.18}$$

At the infinity the first integration of the right-hand side of Eq. (A.0.18) goes to zero and after using Eq. (A.0.18) into (A.0.15), we get

$$-\int r_\perp^2\frac{\partial \mathcal{H}}{\partial \mathbf{p}_\perp}\cdot\frac{\partial f}{\partial \mathbf{r}_\perp}\, d^2r_\perp\, d^2p_\perp = 2\left\langle \mathbf{r}_\perp\cdot\nabla_{p_\perp}H\right\rangle + \left\langle r_\perp^2\nabla_\perp\cdot(\nabla_{p_\perp}H)\right\rangle\,. \tag{A.0.19}$$

The second integral in the right-hand side of Eq. (A.0.15) can be written as,

$$\int r_\perp^2\frac{\partial \mathcal{H}}{\partial \mathbf{r}_\perp}\cdot\frac{\partial f}{\partial \mathbf{p}_\perp}\, d^2r_\perp\, d^2p_\perp = -\left\langle r_\perp^2\nabla_{p_\perp}\cdot(\nabla_\perp H)\right\rangle\,. \tag{A.0.20}$$

Using Eqs. (A.0.19) and (A.0.20) into Eq. (A.0.15), we get:

$$\frac{d\sigma_\perp^2}{d\tau} = 2\left\langle \mathbf{r}_\perp \cdot \nabla_{p_\perp} H \right\rangle + \left\langle r_\perp^2 \left[\nabla_\perp \cdot (\nabla_{p_\perp} H) - \nabla_{p_\perp} \cdot (\nabla_\perp H) \right] \right\rangle . \tag{A.0.21}$$

By taking the derivatives of Hamiltonian given in Eq. (A.0.1) with respect to $\mathbf{p}_\perp$ and $\mathbf{r}_\perp$, we get,

$$\nabla_{\mathbf{p}_\perp} H = \frac{\partial H}{\partial p_\perp} = \mathbf{p}_\perp + \frac{1}{2} k_c (\hat{z} \times \mathbf{r}_\perp) \tag{A.0.22}$$

and

$$\nabla_\perp H = \frac{\partial H}{\partial \mathbf{r}_\perp} = K\mathbf{r}_\perp + \nabla_\perp U_w - \frac{1}{2} k_c (\hat{z} \times \mathbf{p}_\perp) . \tag{A.0.23}$$

Taking the scalar products of Eq. (A.0.22) with respect to $\nabla_\perp$ and of Eq. (A.0.23) with respect to $\nabla_{\mathbf{p}_\perp}$, respectively, we get,

$$\nabla_\perp \cdot (\nabla_{p_\perp} H) = \nabla_\perp \cdot \left[\mathbf{p}_\perp + \frac{1}{2} k_c (\hat{z} \times \mathbf{r}_\perp) \right] = 0 \tag{A.0.24}$$

and

$$\nabla_{\mathbf{p}_\perp} \cdot (\nabla_\perp H) = \nabla_{\mathbf{p}_\perp} \cdot \left[K\mathbf{r}_\perp + \frac{\partial U_w}{\partial \mathbf{r}_\perp} - \frac{1}{2} k_c (\hat{z} \times \mathbf{p}_\perp) \right] = 0 . \tag{A.0.25}$$

Using Eqs. (A.0.24) and (A.0.25), we see that the second term at the right-hand side of Eq. (A.0.21) vanishes; therefore this equation becomes

$$\frac{d\sigma_\perp^2}{d\tau} = 2\langle \mathbf{r}_\perp \cdot \mathbf{p}_\perp \rangle = 2 \int (\mathbf{r}_\perp \cdot \mathbf{p}_\perp) f \, d^2 r_\perp \, d^2 p_\perp , \tag{A.0.26}$$

which can be also cast as

$$\sigma_\perp \frac{d\sigma_\perp}{d\tau} = \langle \mathbf{r}_\perp \cdot \mathbf{p}_\perp \rangle . \tag{A.0.27}$$

We take the derivative of Eq. (A.0.26),

$$\frac{d^2\sigma_\perp^2}{d\tau^2} = 2 \int (\mathbf{r}_\perp \cdot \mathbf{p}_\perp) \frac{\partial f}{\partial \tau} \, d^2 r_\perp \, d^2 p_\perp . \tag{A.0.28}$$

Then, we obtain $\partial f / \partial \tau$ from Eq. (A.0.5) and substitute into (A.0.28),

$$\frac{d^2\sigma_\perp^2}{d\tau^2} = -2 \int (\mathbf{r}_\perp \cdot \mathbf{p}_\perp) \left[\frac{\partial \mathcal{H}}{\partial \mathbf{p}_\perp} \cdot \frac{\partial f}{\partial \mathbf{r}_\perp} - \frac{\partial \mathcal{H}}{\partial \mathbf{r}_\perp} \cdot \frac{\partial f}{\partial \mathbf{p}_\perp} \right] d^2 r_\perp \, d^2 p_\perp \tag{A.0.29}$$

or,

$$\frac{d^2\sigma_\perp^2}{d\tau^2} = -2 \int (\mathbf{r}_\perp \cdot \mathbf{p}_\perp) \frac{\partial \mathcal{H}}{\partial \mathbf{p}_\perp} \cdot \frac{\partial f}{\partial \mathbf{r}_\perp} \, d^2 r_\perp \, d^2 p_\perp + 2 \int (\mathbf{r}_\perp \cdot \mathbf{p}_\perp) \frac{\partial \mathcal{H}}{\partial \mathbf{r}_\perp} \cdot \frac{\partial f}{\partial \mathbf{p}_\perp} \, d^2 r_\perp \, d^2 p_\perp . \tag{A.0.30}$$

Following the similar procedure to reach Eqs. (A.0.19) and (A.0.20), the integrals in the right-hand side of (A.0.30) can be expressed as,

$$-2\int(\mathbf{r}_\perp\cdot\mathbf{p}_\perp)\frac{\partial\mathcal{H}}{\partial\mathbf{p}_\perp}\cdot\frac{\partial f}{\partial\mathbf{r}_\perp}\,d^2r_\perp\,d^2p_\perp = 2\left\langle\mathbf{p}_\perp\cdot\nabla_{\mathbf{p}_\perp}H\right\rangle + 2\left\langle(\mathbf{r}_\perp\cdot\mathbf{p}_\perp)\,\nabla_\perp\cdot(\nabla_{\mathbf{p}_\perp}H)\right\rangle \quad \text{(A.0.31)}$$

and

$$2\int(\mathbf{r}_\perp\cdot\mathbf{p}_\perp)\frac{\partial\mathcal{H}}{\partial\mathbf{r}_\perp}\cdot\frac{\partial f}{\partial\mathbf{p}_\perp}\,d^2r_\perp\,d^2p_\perp = -2\,\langle\mathbf{r}_\perp\cdot\nabla_\perp H\rangle\ . \quad \text{(A.0.32)}$$

Using Eqs. (A.0.31) and (A.0.32) into (A.0.30), we get

$$\frac{d^2\sigma_\perp^2}{d\tau^2} = 2\left\langle\mathbf{p}_\perp\cdot\nabla_{p_\perp}H\right\rangle + 2\left\langle(\mathbf{r}_\perp\cdot\mathbf{p}_\perp)\nabla_\perp\cdot(\nabla_{p_\perp}H)\right\rangle - 2\,\langle\mathbf{r}_\perp\cdot(\nabla_\perp H)\rangle\ . \quad \text{(A.0.33)}$$

Then, taking dot product of $\mathbf{p}_\perp$ and $\mathbf{r}_\perp$ with Eqs. (A.0.24) and (A.0.25), respectively, we get

$$\mathbf{p}_\perp\cdot\nabla_{p_\perp}H = p_\perp^2 + \frac{1}{2}k_c\mathbf{p}_\perp\cdot(\hat{z}\times\mathbf{r}_\perp)\,, \quad \text{(A.0.34)}$$

$$\mathbf{r}_\perp\cdot\nabla_\perp H = Kr_\perp^2 + \mathbf{r}_\perp\cdot\nabla_\perp U_w - \frac{1}{2}k_c\mathbf{r}_\perp\cdot(\hat{z}\times\mathbf{p}_\perp)\,. \quad \text{(A.0.35)}$$

Furthermore, we observe that,

$$\nabla_\perp\cdot(\nabla_{p_\perp}H) = \nabla_\perp\cdot\left[\mathbf{p}_\perp + \frac{1}{2}k_c(\hat{z}\times\mathbf{r}_\perp)\right] = 0\,. \quad \text{(A.0.36)}$$

Using Eqs. (A.0.34) - (A.0.36) into (A.0.33), we finally obtain:

$$\frac{d^2\sigma_\perp^2}{d\tau^2} = 2\left\langle\mathbf{p}_\perp^2\right\rangle + k_c\langle\mathbf{p}_\perp\cdot(\hat{z}\times\mathbf{r}_\perp)\rangle - 2K\langle r_\perp^2\rangle - 2\langle\mathbf{r}_\perp\cdot\nabla_\perp U_w\rangle + k_c\langle\mathbf{r}_\perp\cdot(\hat{z}\times\mathbf{p}_\perp)\rangle\,,$$

which can be expressed as

$$\frac{d^2\sigma_\perp^2}{d\tau^2} = 2\sigma_{p_\perp}^2 - 2K\sigma_{p_\perp}^2 - 2\langle\mathbf{r}_\perp\cdot\nabla_\perp U_w\rangle + k_c\langle\hat{z}\cdot(\mathbf{r}_\perp\times\mathbf{p}_\perp) + \hat{z}\cdot(\mathbf{p}_\perp\times\mathbf{r}_\perp)\rangle\,. \quad \text{(A.0.37)}$$

We observe that the sum of the last two terms of Eq. (A.0.37) is zero, i.e., $\hat{z}\cdot(\mathbf{r}_\perp\times\mathbf{p}_\perp) + \hat{z}\cdot(\mathbf{p}_\perp\times\mathbf{r}_\perp) = 0$, hence, we get,

$$\frac{d^2\sigma_\perp^2}{d\tau^2} = 2\sigma_{p_\perp}^2 - 2K\sigma_{p_\perp}^2 - 2\langle\mathbf{r}_\perp\cdot\nabla_\perp U_w\rangle\,. \quad \text{(A.0.38)}$$

In terms of T and V, Eq. (A.0.38) can be written as,

$$\frac{d^2\sigma_\perp^2}{d\tau^2} = 4\langle T\rangle - 2\langle\mathbf{r}_\perp\cdot\nabla_\perp V\rangle\,, \quad \text{(A.0.39)}$$

where,

$$V(\mathbf{r}_\perp, \tau) = \frac{1}{2} K r_\perp^2 + U_w(\mathbf{r}_\perp, \tau)\,. \tag{A.0.40}$$

Equation (A.0.39) is referred to be the *first virial equation*. It can be consequently cast in the following form,

$$\frac{d^2\sigma_\perp^2}{d\tau^2} = 2\sigma_{p_\perp}^2 - 2K\sigma_\perp^2 - 2\langle \mathbf{r}_\perp \cdot \nabla_\perp U_w \rangle \tag{A.0.41}$$

or,

$$\frac{d^2\sigma_\perp^2}{d\tau^2} = 4(\mathcal{E} - \langle U \rangle) - 2\langle \mathbf{r}_\perp \cdot \nabla_{r_\perp} U \rangle + k_c \mathcal{L}_z\,, \tag{A.0.42}$$

where $\mathcal{L}_z = \langle L_z \rangle$, $L_z = \hat{z} \cdot (\mathbf{r}_\perp \times \mathbf{p}_\perp)$, and U is given in Eq. (A.0.4). In case of unmagnetized plasma, the first virial equation becomes ($k_c = K = 0$):

$$\frac{d^2\sigma_\perp^2}{d\tau^2} = 4(\mathcal{E} - \langle U_w \rangle) - 2\langle \mathbf{r}_\perp \cdot \nabla_{r_\perp} U_w \rangle\,, \tag{A.0.43}$$

where $\mathcal{E} = \frac{1}{2}\langle p_\perp^2 \rangle + \langle U_w \rangle$. In order to close the virial description, we need the second virial equation which will relate $\mathcal{E}$ with U_w.

Second virial equation

Now we are going to find an equation for the time evolution of the averaged total energy $\mathcal{E}(\tau) = \langle H \rangle$ which is defined in Eq. (A.0.10). To do this, we differentiate Eq. (A.0.10) with respect to τ, obtaining

$$\frac{d\mathcal{E}}{d\tau} = \int \frac{\partial H}{\partial \tau} f d^2 p_\perp d^2 r_\perp + \int H \frac{\partial f}{\partial \tau} d^2 p_\perp d^2 r_\perp\,, \tag{A.0.44}$$

which, by using Eq. (A.0.5) can be cast as:

$$\frac{d\mathcal{E}}{d\tau} = \left\langle \frac{\partial H}{\partial \tau} \right\rangle - \int H \left[\frac{\partial H}{\partial \mathbf{p}_\perp} \cdot \frac{\partial f}{\partial \mathbf{r}_\perp} - \frac{\partial H}{\partial \mathbf{r}_\perp} \cdot \frac{\partial f}{\partial \mathbf{p}_\perp} \right] d^2 p_\perp d^2 r_\perp\,. \tag{A.0.45}$$

The last term of Eq. (A.0.45) can be written as,

$$H \left[\frac{\partial H}{\partial \mathbf{p}_\perp} \cdot \frac{\partial f}{\partial \mathbf{r}_\perp} - \frac{\partial H}{\partial \mathbf{r}_\perp} \cdot \frac{\partial f}{\partial \mathbf{p}_\perp} \right] = \frac{H}{2} \left(\frac{\partial H^2}{\partial \mathbf{p}_\perp} \cdot \frac{\partial f}{\partial \mathbf{r}_\perp} - \frac{\partial H^2}{\partial \mathbf{r}_\perp} \cdot \frac{\partial f}{\partial \mathbf{p}_\perp} \right). \tag{A.0.46}$$

We can write the following derivatives as,

$$\nabla_\perp \left[\frac{\partial H^2}{\partial \mathbf{p}_\perp} f \right] = \frac{\partial H^2}{\partial \mathbf{p}_\perp^2} \frac{\partial f}{\partial \mathbf{r}_\perp} + f \nabla_\perp (\nabla_{p\perp} H^2) \tag{A.0.47}$$

and

$$\nabla_{p\perp}\left[\frac{\partial H^2}{\partial \mathbf{r}_\perp} f\right] = \frac{\partial H^2}{\partial \mathbf{r}_\perp}\frac{\partial f}{\partial \mathbf{p}_\perp} + f\nabla_{p\perp}(\nabla_{r\perp} H^2)\,. \tag{A.0.48}$$

Using Eqs. (A.0.47) and (A.0.48) into Eq. (A.0.46) while using the boundary condition at infinity, the last integral of Eq. (A.0.45) becomes,

$$\int H\left[\frac{\partial H}{\partial \mathbf{p}_\perp}\cdot\frac{\partial f}{\partial \mathbf{r}_\perp} - \frac{\partial H}{\partial \mathbf{r}_\perp}\cdot\frac{\partial f}{\partial \mathbf{p}_\perp}\right] d^2p_\perp d^2r_\perp = \int f\left[\nabla_\perp\cdot(H\nabla_{p\perp}H) - \nabla_{p_\perp}\cdot(H\nabla_\perp H)\right] d^2p_\perp d^2r_\perp\,,$$

or,

$$\int H\left[\frac{\partial H}{\partial \mathbf{p}_\perp}\cdot\frac{\partial f}{\partial \mathbf{r}_\perp} - \frac{\partial H}{\partial \mathbf{r}_\perp}\cdot\frac{\partial f}{\partial \mathbf{p}_\perp}\right] d^2p_\perp d^2r_\perp = \int f\left[H\frac{\partial}{\partial x_i}\left(\frac{\partial H}{\partial p_i}\right) - H\frac{\partial}{\partial p_j}\left(\frac{\partial H}{\partial x_j}\right)\right] d^2p_\perp d^2r_\perp\,,$$

or,

$$\int H\left[\frac{\partial H}{\partial \mathbf{p}_\perp}\cdot\frac{\partial f}{\partial \mathbf{r}_\perp} - \frac{\partial H}{\partial \mathbf{r}_\perp}\cdot\frac{\partial f}{\partial \mathbf{p}_\perp}\right] d^2p_\perp d^2r_\perp = \int f\left[H\left[\frac{\partial^2 H}{\partial x_i\partial p_i} - \frac{\partial^2 H}{\partial p_j\partial x_j}\right]\right] d^2p_\perp d^2r_\perp = 0\,. \tag{A.0.49}$$

Using Eq. (A.0.49) into Eq. (A.0.45), we get

$$\frac{d\mathcal{E}}{d\tau} = \left\langle\frac{\partial U_w}{\partial \tau}\right\rangle = \int \frac{\partial U_W}{\partial \tau} f d^2r_\perp d^2p_\perp\,, \tag{A.0.50}$$

where we have used the explicit form of H given by Eq. (A.0.1) and observed that $U_w(\mathbf{r}_\perp, \tau)$ is the only term of the Hamiltonian that depends explicitly on τ.

We refer Eq. (A.0.50) to be the *second virial equation*, which describes the time evolution of the averaged energy $\mathcal{E}$. Equations (A.0.39) and (A.0.50) constitute a pair of coupled equations governing the time evolution of the beam envelope.

Appendix B

Envelope descriptions

To give a complete self-consistent description of the beam plasma system, along with the two virial equations (A.0.39) and (A.0.50) described in the Appendix A, the knowledge of f and U_w is required. Therefore, equations (A.0.39) and (A.0.50) do not comprise a complete set of equations. To satisfy the self-consistency, we have to couple the Vlasov-Poisson-type system of equations with equations with (A.0.39) and (A.0.50). Imposing suitable initial and boundary conditions, we have to solve the Vlasov-Poisson-type pair of equations. Once $f(\mathbf{r}_\perp, \mathbf{p}_\perp, \tau)$ and $U_w(\mathbf{r}_\perp, \tau)$ are known, we can use the virial equations to describe the time evolution of the beam envelope.

We take into account the following Vlasov-Poisson-type pair of equations,

$$\frac{\partial f}{\partial \tau} + \left[\mathbf{p}_\perp + \frac{1}{2}k_c\,(\hat{z}\times\mathbf{r}_\perp)\right]\cdot\nabla_\perp f - \left[K\mathbf{r}_\perp - \frac{1}{2}k_c\,(\hat{z}\times\mathbf{p}_\perp) + \nabla_\perp U_w\right]\cdot\nabla_{p_\perp} f = 0\,, \tag{B.0.1}$$

$$\left(\nabla_\perp^2 - k_s^2\right)U_w = k_s^2\lambda_0\int f\,d^2p_\perp\,, \tag{B.0.2}$$

where $\lambda_0 = N/n_0\gamma_0\sigma_z$ (N being the total number of electrons or positrons of the driving beam) and $k_s = k_p^2/k_{uh}$. Since U_w is independent of $\mathbf{p}_\perp$, from Eq. (A.0.50) we get,

$$\frac{d\mathcal{E}}{d\tau} = \int\frac{\partial U_W}{\partial\tau}d^2r_\perp\int f d^2p_\perp\,. \tag{B.0.3}$$

Using Eqs. (B.0.2) and (B.0.3), we get:

$$\frac{d\mathcal{E}}{d\tau} = \frac{1}{k_s^2\lambda_0}\left[\int\frac{\partial U_w}{\partial\tau}\nabla_\perp^2 U_w\,d^2r_\perp - k_s^2\int U_w\,\frac{\partial U_w}{\partial\tau}\,d^2r_\perp\right]. \tag{B.0.4}$$

To evaluate the first integral in the left-hand side of Eq. (B.0.4), at first we take the divergence of the $(\partial U_w)/(\partial\tau)\,\nabla_\perp U_w$,

$$\nabla_\perp \cdot \left[\frac{\partial U_w}{\partial \tau}\nabla_\perp U_w\right] = \left(\nabla_\perp \frac{\partial U_w}{\partial \tau}\right)\cdot \nabla_\perp U_w + \frac{\partial U_w}{\partial \tau}\nabla_\perp^2 U_w\,,$$

which in turn gives,

$$\frac{\partial U_w}{\partial \tau}\nabla_\perp^2 U_w = \nabla_\perp \cdot \left[\frac{\partial U_w}{\partial \tau}\nabla_\perp U_w\right] - \frac{1}{2}\frac{\partial}{\partial \tau}\left|\nabla_\perp U_w\right|^2 . \tag{B.0.5}$$

Using Eq. (B.0.5) into Eq. (B.0.4), we get

$$\frac{d\mathcal{E}}{d\tau} = \frac{1}{k_s^2\lambda_0}\left[\int \nabla_\perp \cdot \left(\frac{\partial U_w}{\partial \tau}\nabla_\perp U_w\right) d^2 r_\perp - \frac{1}{2}\int \frac{\partial}{\partial \tau}\left|\nabla_\perp U_w\right|^2 d^2 r_\perp - k_s^2 \int \frac{1}{2}\frac{\partial U_w^2}{\partial \tau}\, d^2 r_\perp\right]. \tag{B.0.6}$$

At the infinity the first integration of the right-hand side of Eq. (B.0.6) goes to zero. Therefore, we get,

$$\frac{d\mathcal{E}}{d\tau} = -\frac{1}{2k_s^2\lambda_0}\frac{d}{d\tau}\int \left(\left|\nabla_\perp U_w\right|^2 + k_s^2 U_w^2\right) d^2 r_\perp\,, \tag{B.0.7}$$

or,

$$\frac{d}{d\tau}\left[\mathcal{E} + \frac{1}{2k_s^2\lambda_0}\int \left(\left|\nabla_\perp U_w\right|^2 + k_s^2 U_w^2\right) d^2 r_\perp\right] = 0\,. \tag{B.0.8}$$

Consequently, from this equation we can define the following constant of motion:

$$C = \mathcal{E} + \frac{1}{2k_s^2\lambda_0}\int \left(\left|\nabla_\perp U_w\right|^2 + k_s^2 U_w^2\right) d^2 r_\perp\,. \tag{B.0.9}$$

By expressing explicitly $\mathcal{E} = \langle H\rangle$ along with Eqs. (A.0.2) - (A.0.4) in the above equation, we easily get:

$$C = \frac{1}{2}\sigma_{p\perp}^2 + \frac{1}{2}K\sigma_\perp^2 + \frac{1}{2k_s^2\lambda_0}\int \left(\left|\nabla_\perp U_w\right|^2 + k_s^2 U_w^2\right) d^2 r_\perp + \langle U_w\rangle + \frac{1}{2}k_c\mathcal{L}_z\,. \tag{B.0.10}$$

Then, using $\langle U_w\rangle$, i.e.,

$$\langle U_w\rangle = -\frac{1}{k_s^2\lambda_0}\int \left(\left|\nabla_\perp U_w\right|^2 + k_s^2 U_w^2\right) d^2 r_\perp\,, \tag{B.0.11}$$

into Eq. (B.0.10), we get

$$C = \frac{1}{2}\sigma_{p\perp}^2 + \frac{1}{2}K\sigma_\perp^2 - \frac{1}{2k_s^2\lambda_0}\int \left(\left|\nabla_\perp U_w\right|^2 + k_s^2 U_w^2\right) d^2 r_\perp + \frac{1}{2}k_c\mathcal{L}_z\,. \tag{B.0.12}$$

By means of Eq. (B.0.12), we express $\mathcal{E}$ in terms of C and substitute it in the first virial equation. Then, using Eqs. (B.0.12) and (A.0.4) into Eq. (A.0.42) we easily get:

$$\frac{d^2\sigma_\perp^2}{d\tau^2} + 4\,K\sigma_\perp^2 \;=\; 4C - \frac{2}{k_s^2\lambda_0}\int \left(|\nabla_\perp U_w|^2 + k_s^2 U_w^2\right) d^2r_\perp - 4\langle U_w\rangle - 2\langle \mathbf{r}_\perp\cdot\nabla_\perp U_w\rangle - 2k_c\mathcal{L}_z\,. \tag{B.0.13}$$

After performing the integrations by parts, contained in the terms at the right-hand side of Eq. (B.0.13), we finally obtain the following envelope equation, i.e.,

$$\frac{d^2\sigma_\perp^2}{d\tau^2} + 4\,K\sigma_\perp^2 \;=\; 4C + \frac{2}{k_s^2\lambda_0}\int |\nabla_\perp U_w|^2\; d^2r_\perp - 2k_c\mathcal{L}_z\,. \tag{B.0.14}$$

Note that, for the case of unmagnetized plasma ($\mathbf{B}_0 = 0$), we easily get:

$$\frac{d^2\sigma_\perp^2}{d\tau^2} \;=\; 4C + \frac{2}{k_p^2\lambda_0}\int |\nabla_\perp U_w|^2\; d^2r_\perp\,. \tag{B.0.15}$$

List of Publications/Communications

International publications

R. Fedele, **T. Akhter**, D. Jovanović, S. De Nicola, and A. Mannan, *Transverse evolution of a long relativistic electron beam governed by the Vlasov-Poisson-type pair of equations within the plasma wake field dynamics in the local regime*, Eur. Phys. J. D **68**, 210 (2014). DOI: 10.1140/epjd/e2014-50219-y

R. Fedele, A. Mannan, S. De Nicola, D. Jovanović, and **T. Akhter**, *Vlasov's kinetic theory of the collective charged particle beam transport through a magnetized plasma in the strongly nonlocal regime*, Eur. Phys. J. D, **68**, 271 (2014). DOI: 10.1140/epjd/e2014-50220-6

R. Fedele, **T. Akhter**, S. De Nicola, M. Migliorati, A. Marocchino, F. Massimo, and L. Palumbo, *The concept of coupling impedance in the self-consistent plasma wake field excitation*, Nucl. Instr. Meth. A, Accepted, (2015).

T. Akhter, R. Fedele, S. De Nicola, F. Tanjia, D. Jovanović, and A. Mannan, *Self-modulated dynamics of a relativistic charged particle beam in plasma wake field excitation*, Nucl. Instr. Meth. A, Submitted (2015).

F. Tanjia, R. Fedele, S. De Nicola, **T. Akhter**, and D. Jovanovic, *Formation and stability of a hollow electron beam in the presence of a plasma wake field driven by an ultra-short electron bunch*, Nucl. Instr. Meth. A, Revised, (2015).

F. Tanjia, R. Fedele, S. De Nicola, **T. Akhter**, D. Jovanovic, *Formation of stable hollow electron beam by external injection in a plasma wake field accelerator*, Phys. Rev. A. B., Submitted, (2015).

Poster Presentations

1. **T. Akhter**, R. Fedele, S. De Nicola, F. Tanjia, D. Jovanović, *Study of the self-modulated propagation of relativistic charged particle beam in warm-magnetized plasmas within the kinetic description*, FISMAT 2015, 28 September - 02 October, 2015, Plalermo, Italy

2. **T. Akhter**, R. Fedele, A. Mannan, S. De Nicola and F. Tanjia, *Dynamics of a Self-Modulated Relativistic Charged Particle Beam in a Plasma*, International Congress On Plasma Physics ICPP 2014, 15 - 19 September 2014, Lisbon, Portugal.

3. **T. Akhter**, R. Fedele, A. Mannan, S. De Nicola and F. Tanjia, *Dynamics of a Self-Modulated Relativistic Charged Particle Beam in a Plasma*, Joint ICTP-IAEA College on Advanced Plasma Physics, 18 - 29 August 2014, ICTP, Trieste, Italy.

4. R. Fedele, S. De Nicola, **T. Akhter**, A. Mannan, F. Tanjia and D. Jovanović, *Quantum-like aspects of the charged-particle beam self-modulation in the presence of a laser wake field excitation*, School on Non-linear Dynamics, Dynamical Transitions and Instabilities in Classical and Quantum Systems, ICTP, 14 July - 1 August 2014, Trieste, Italy.

5. A. Mannan, R. Fedele, S. De Nicola, D. Jovanović, and **T. Akhter**, *Collective transport of a charged particle beam through an unmagnetized plasma within the framework of the Vlasovs kinetic theory in strongly nonlocal regime*, VLASOVIA 2013, International workshop on the theory and applications of Vlasov equation, 25 - 28 November 2013, Nancy, France.

6. **T. Akhter**, R. Fedele, S. De Nicola, D. Jovanović, and A. Mannan, *Analysis of the transverse plasma wake field dynamics of a long relativistic electron beam governed by the Vlasov-Poisson-like pair of equations in purely local regime*, VLASOVIA 2013, International workshop on the theory and applications of Vlasov equation, 25 - 28 November 2013, Nancy, France.

Oral Presentations

1. T. Akhter, R. Fedele, A. Mannan, S. De Nicola, and F. Tanjia *Self-Modulated Relativistic Charged Particle Beam dynamics in a Plasma*, 100° Congresso Nazionale SIF, 22 - 26 September 2014, Pisa, Italy.

2. T. Akhter, R. Fedele, S. De Nicola, D. Jovanović, and A. Mannan *Stabilizing Effects in a Self-Modulated Long Relativistic Charged Particle Beam Travelling in a Plasma*, Trieste, Italy.

3. T. Akhter, R. Fedele, S. De Nicola, F. Tanjia, D. Jovanović, *Self modulated dynamics of relativistic charged particle beam in plasma wake field excitation*, La Biodola, Isola dElba, Italy, 13-19 September, 2015.

4. T. Akhter, R. Fedele, S. De Nicola, F. Tanjia, D. Jovanović, *Kinetic theory of the generalized self-consistent 3D plasma wake field excitation in overdense regime*, Roma, Italy, 21-25 September, 2015.

International conferences & visits

1. 2nd European Advanced Accelerator Concepts Workshop, La Biodola, Isola dElba, Italy, 13-19 September, 2015.

2. 101° Congresso Nazionale, Societa Italiana di Fisica, Roma, Italy, 21-25 September, 2015.

3. 100° Congresso Nazionale SIF, 22 - 26 September 2014, Pisa, Italy.

4. International Congress On Plasma Physics ICPP 2014, 15 - 19 September 2014, Lisbon, Portugal.

5. Joint ICTP-IAEA College on Advanced Plasma Physics, 18 - 29 August 2014, ICTP, Trieste, Italy.

6. VLASOVIA 2013, International workshop on the theory and applications of Vlasov equation, 25 - 28 November 2013, Nancy, France.

Bibliography

[1] T. Tajima and J. M. Dawson. Laser electron accelerator. *Phys. Rev. Lett.*, 43:267–270, 1979.

[2] L. M. Gorbunov and V. I. Kirsanov. Excitation of plasma waves by an electromagnetic wave packet. *Sov. Phys. JETP*, 66:290–294, 1987.

[3] P. Sprangle, E. Esarey, A. Ting, and G. Joyce. *Appl. Phys. Lett.*, 53:2146–2148, 1988.

[4] P. Chen, J. M. Dawson, R. W. Huff, and T. Katsouleas. Acceleration of electrons by the interaction of a bunched electron beam with a plasma. *Phys. Rev. Lett.*, 54:693–696, 1985.

[5] R. D. Ruth, A. W. Chao, P. L. Morton, and P. B. Wilson. *Part. Accel.*, 17:171, 1985.

[6] P. Chen, J. J. Su, J. M. Dawson, K. L. F. Bane, and P. B. Wilson. *Phys. Rev. Lett.*, 56:1252, 1986.

[7] J. Rosenzweig. *IEEE Trans. Plasma Science*, PS-15:186, 1987.

[8] T. Katsouleas. *Phys. Rev. A*, 33:2056, 1986.

[9] R. Fedele, U. de Angelis, and T. Katsouleas. Generation of radial fields in the beat-wave accelerator for gaussian pump profiles. *Phys. Rev. A*, 33:4412–4414, 1986.

[10] U. De Angelis, R. Fedele, G. Miano, and C. Nappi. *Plasma Phys. Control. Fusion*, 29:789, 1987.

[11] C. Joshi, T. Katsouleas, J. M. Dawson, Y. T. Yan, and J. M. Slater. *IEEE Trans. J. Quantum Electronics*, QE-23:1571, 1987.

[12] R. Fedele, G. Miano, and V. G. Vaccaro. *Physica Scripta*, T30:192, 1990.

[13] A. O. Benz. *Astrophys. J.*, 211:270, 1977.

[14] J. Kuijpers. *'Particle acceleration' in Plasma Astrophysics*, Springer:Berlin, 1996.

[15] M. E. Dieckmann, P. Ljung, A. Ynnerman, and K. G. McClements. *Phys. Plasmas*, 7:5171, 2000.

[16] K. G. McClements, R. O. Dendy, M. E. Dieckmann, A. Ynnerman, and S. C. Cha Pma. *J. Plasma Physics*, 71:127, 2005.

[17] P. Chen, T. Tajima, and Y. Takahashi. *Phys. Rev. Lett.*, 89:161101, 2002.

[18] A. M. Sessler and D. Vaughan. *Free-Electron Lasers*. University of California, Berkeley, 1987.

[19] H. Winick et al. Wiggler and undulator magnets. *Phys. Today*, 34N5:50–63, 1981.

[20] H. Winick. Synchrotron radiation. *Scientific American*, 255:88–89, 1987.

[21] J. M. Dawson. *From Particles to Plasmas*, page 131. Addison Wesley, Reading, MA, 1959.

[22] J. M. Dawson. Nonlinear electron oscillations in a cold plasma. *Phys. Rev.*, 113:383387, 1959.

[23] J. Faure, Y. Glinec, A. Pukhov, S. Kiselev, S. Gordienko, E. Lefebvre, J. P. Rousseau, F. Burgy, and V. Malka. *Nature*, 431:541, 2004.

[24] C. G. R. Geddes, Cs. Toth, J. Van Tilborg, E. Esarey, C. B. Schroeder, D. Bruh-wiler, C. Nieter, J. Cary, and W. P. Leemans. *Nature*, 431:538, 2004.

[25] S. P. D. Mangles et al. Monoenergetic beams of relativistic electrons from intense laserplasma interactions. *Nature*, 431:535–538, 2004.

[26] J. Faure, C. Rechatin, A. Norlin, A. Lifschitz, Y. Glinec, and V. Malka. *Nature*, 444:737, 2006.

[27] W. Leemans, B. Nagler, A. J. Gonsalves, Cs. Toth, K. Nakamura, C. G. R. Geddes, E. Esarey, C. B. Schroeder, and S. M. Hooker. *Nat. Phys.*, 2:696, 2006.

[28] C. E. Clayton, J. E. Ralph, F. Albert, R. A. Fonseca, S. H. Glenzer, C. Joshi, W.Lu, K. A. Marsh, S. F. Martins, W. B. Mori, A. Pak, F.S. Tsung, B. B. Pollock, J. S. Ross, L. O. Silva, and D. H. Froula. *Phys. Rev. Lett.*, 105:105003, 2010.

[29] K.A. Marsh, C. E. Clayton, C. Joshi, W. Lu, W. B. Mori, A. Pak, L. O. Silva, N. Lemos, R. A. Fonseca, S. de Freitas Martins, F. Albert, T. Doeppner, C. Filip, D. Froula, S. H. Glenzer, D. Price, J. Ralph, and B. B. Pollock. *LLNLPROC*, 476791, 2011.

[30] R. Bingham, J.T. Mendonça, and P.K. Shukla. Plasma based charged-particle accelerators. *Plasma Phys. Control. Fusion*, 46:R1–R23, 2004.

[31] D. Jovanović, R. Fedele, F. Tanjia, S. De Nicola, and L. A. Gizzi. *Eur. Phys. J. D*, 66:328, 2012.

[32] D. Jovanović, R. Fedele, and M. Belić. *Euro. phys. Let.*, 107:44004, 2014.

[33] A.V. Korzhimanov, A. Gonoskov, E. A Khazanov, and A. M Sergeev. *Phys. Usp.*, 54:9, 2011.

[34] X. Wang, R. Zgadzaj, N. Fazel, Z. Li, S. A. Yi, X. Zhang, W. Henderson, Y.-Y. Chang, R. Korzekwa, H.-E. Tsai, C.-H. Pai, H. Quevedo, G. Dyer, E. Gaul, M. Martinez, A. C. Bernstein, T. Borger, M. Spinks, M. Donovan, V. Khudik, G. Shvets, T. Ditmire, and M. C. Downer. *Nature Communications*, 4:1988, 2013.

[35] W. Lu nad C. Huang and M. Zhou et al. *Phys. Plasmas*, 13:056709, 2006.

[36] I. Kostyukov, A. Pukhov, and S. Kiselev. *Phys. Plasmas*, 11:5256, 2004.

[37] R. Bingham. *Nature*, 445:721, 2007.

[38] V. Malka, J. Faure, Y. A. Gauduel, E. Lefebvre, A. Rousse, and K.T. Phuoc. *Nature Physics*, 4:447, 2008.

[39] P. Muggli and M. J. Hogan. Review of high-energy plasma wakefield experiments. *C. R. Phys.*, 10:116–129, 2009.

[40] J.B. Rozenzweig, D.B. Cline, B. Cole, H. Figueroa, W. Gai, R. Konecny, J. Norem, P. Schoessow, and J. Simpson. *Phys. Rev. Lett.*, 61:98–101, 1988.

[41] J. B. Rosenzweig, B. Breizman, T. Katsouleas, and J. J. Su. Acceleration and focusing of electrons in two-dimensional nonlinear plasma wake fields. *Phys. Rev. A*, 44:R6189–R6192, 1991.

[42] G. Xia, O. Mete, A. Aimidula, C. P. Welsch, S. Chattopadhay, S. Mandry, and M. Wing. *Nucl. Instrum. Meth. A*, 740:173, 2014.

[43] E. Öz and P. Muggli. *Nucl. Instrum. Meth. A*, 740:197, 2014.

[44] M. J. Hogan et al. *New J. Phys.*, 12:055030, 2010.

[45] B. Marchetti, A. Bacci, E. Chiadroni, A. Cianchi, M. Ferrario, A. Mostacci, R. Pompili, C. Ronsivalle, B. Spataro, and I. Zagorodnov. *Rev. Sci. Instrum.*, 7(10.1063/1.4922882):073301, 2015.

[46] A. B. Mikhailovskii. *Plasma Phys.*, 22:133, 1980.

[47] V. N. Tsytovich. *Sov. Phys. Doklady*, 7:31, 1962.

[48] A. I. Akhiezer, I. A. Akhiezer, R. V. Polovin, A. G. Sitenko, and K. N. Stepanov. *Plasma Electrodynamics*, 2, 1975.

[49] A. A. Vlasov. On vibration properties of electron gas. *J. Exp. Theor. Phys. (in Russian)*, 8:3, 1938.

[50] D. R. Hartree. *The calculation of Atomic Structures*. John Wiley & Sons Ltd., New York, 1957.

[51] K. Huang. *Statistical Mechanics*. John Wiley & Sons Ltd., New York, 2 edition, 1987.

[52] A. I. Akhiezer, I. A. Akhiezer, R. V. Polovin, A. G. Sitenko, and K. N. Stepanov. *Plasma Electrodynamics*, 1, 1975.

[53] C. Castaldo, R. Fedele, U. de Angelis, and R. Bingham. Thermal effects in relativistic plasmas. First Course Int. School of Particle Accelerators of the 'Ettore Majorana' Centre for Scientific Culture. RAL-90-082 November 1990; Proc. 10th European Plasma Physics Summer School, Tbilisi, 2-15 September, 2015. N.L. Tsintzadze (Ed.) (World scientific, Singapore, 1990) p. 371.

[54] Gerhard Rein. *Comm. Math. Phys.*, 135:41, 1990.

[55] W. K. H. Panofsky and W. A. Wenzel. Some considerations concerning the transverse deflection of charged particles in radio-frequency fields. *Rev. Sci. Instrum.*, 27:967, 1956.

[56] R. Fedele, F. Tanjia, S. De Nicola, D. Jovanović, and P.K. Shukla. *Phys. Plasmas*, 19:102106, 2012.

[57] F. Tanjia, R. Fedele, S. De Nicola, T. Akhter, and D. Jovanovi. *Phys. Rev. A. B. (Revised)*, 2015.

[58] R. Fedele, T. Akhter, D. Jovanovi, S. De Nicola, and A. Mannan. *Eur. Phys. J. D*, 68:210, 2014.

[59] R. Fedele, A. Mannan, S. De Nicola, D. Jovanovi, and T. Akhter. *Eur. Phys. J. D*, 68:271, 2014.

[60] T. Akhter, R. Fedele, S. De Nicola, F. Tanjia, and D. Jovanovi. *Nucl. Instr. Meth. A (Revised)*, 2015.

[61] R. Fedele, D. Jovanovi, S. De Nicola, A. Mannan, and F. Tanjia. *Journal of Physics: Conference Series*, 482:012014, 2014.

[62] R. Fedele, D. Jovanovi, F. Tanjia, and S. De Nicola. *Nuclear Instruments and Methods in Physics Research A*, 740:180, 2014.

[63] J. D. Jackson. *Classical Electrodynamics, Second Edition*. John Wiley and Sons, 1975.

[64] J. D. Lawson. *The Physics of Charged-Particle Beams*. Clarendon Press, Oxford, 2nd edition, 1988.

[65] S. Humphies. *Principles of Charged Particle Acceleration*. John Wiley and Sons, 1999.

[66] L. D. Landau. *J. Phys. USSR 10*, 25, 1946.

[67] F. F.Chen. *Introduction to plasma physics and controlled fusion*. Plenum Press, New York, 2 edition, 1984.

[68] R. Fedele and D. Anderson. A quantum-like landau damping of an electromagnetic wavepacket. *J- Opt. B: Quantum Semiclass. Opt.*, 2:207–213, 2000.

[69] L. Palumbo, V. G. Vaccaro, and M. Zobov. *Wake Fields and Impedance*. INFN Rep. LNF-94/041(P), 5 September 1994; CAS Advanced School on Accelerator Physics, Rhodes Greece 20 Sept. 1 Oct. (1994).

[70] V. G. Vaccaro. *Nuclear Instruments and Methods in Physics Research A (NIMA)*, 239:65, 1985.

[71] A. Hofmann. Single-beam collective phenomena - longitudinal. page 139. First Course Int. School of Particle Accelerators of the 'Ettore Majorana' Centre for Scientific Culture, 1977. Erice, 10-22 November 1976, CERN 77-13, 19 July 1977.

[72] A. M. Sessler, C. E. Nielsen, and K. R. Symon. Longitudinal instabilities in intense relativistic beams. page 239. Proc. Int. Conf. High-Energy Accelerators and Instruments, 1959. Geneva, CERN.

[73] L. J. Laslett, V. K. Neil, and A. M. Sessler. *Rev. Sci. Instrum.*, 36:436, 1965.

[74] E. D. Courant and A. M. Sessler. *Rev. Sci. Instrum.*, 37:1579, 1966.

[75] A. M. Sessler and V. G. Vaccaro. *Longitudinal instabilities of azimuthally uniform beams in circular electrical properties*. Rep. No. ISR 67-2, CERN, Geneva, 1967.

[76] A. C. Ruggiero and V. G. Vaccaro. *Solution of the dipsersion relation for longitudinal stability of an intense coasting beam in a circular accelerator (application to the ISR)*. Rep. No. ISR-TH/68-33, CERN, Geneva, 1968.

[77] E. J. N. Wilson. *Andrew M. Sessler 1928-2014. Biographycal Memoirs*. National Academy of Sciences, USA, 2014.

[78] O. Bunemann. *Physical Review*, 115:503, 1959.

[79] P. Sturrock. *Plasma Physics: An Introduction to the Theory of Astrophysical, Geophysical, and Laboratory Plasmas*. Cambridge University Press, New York, 1994.

[80] M. Migliorati, A. Bacci, C. Benedetti, E. Chiadroni, M. Ferrario, A. Mostacci, L. Palumbo, A. R. Rossi, L. Serafini, and P. Antici. *Phys. Rev. ST Accel. Beams*, 16:011302, 2013.